

University of California Santa Cruz

The Mori-Zwanzig Approach to Dimension Reduction and Uncertainty Quantification

Daniele Venturi

Department of Applied Mathematics University of California, Santa Cruz

**AFOSR Program on Computational Mathematics
Contract Number FA9550-16-1-0092**

FINAL PROJECT REPORT

Table of Contents

1	Abstract	1
2	The Mori-Zwanzig formulation for deterministic dynamical systems	2
2.1	Projection operators	3
2.1.1	Chorin’s Projection	3
2.1.2	Mori’s projection	3
2.1.3	Berne’s projection	5
3	Analysis of the MZ memory integral	5
3.1	Memory growth	6
3.2	Short memory approximation and the t -model	7
3.3	Hierarchical memory approximation methods	8
3.3.1	The H -model	10
3.3.2	The H_t -model	13
3.4	Linear dynamical systems	15
3.5	Memory estimates for finite-rank projections and Hamiltonian systems	17
3.6	Hamiltonian dynamical systems with finite-rank projections	19
3.6.1	Harmonic chains of oscillators	19
3.6.2	Chorin-Hald system	20
3.7	Non-Hamiltonian systems with infinite-rank projections	22
3.7.1	Linear Dynamical Systems	22
3.7.2	Nonlinear dynamical systems	24
4	Mori-Zwanzig formulation for stochastic dynamical systems	27
4.1	Effective Mori-Zwanzig (EMZ) equation	29
4.1.1	An example: EMZ for the Ornstein-Uhlenbeck process	31
4.2	Analysis of the EMZ equation	32
4.2.1	The Kolmogorov operator \mathcal{K}	32
4.2.2	Projected Kolmogorov operator $\mathcal{Q}\mathcal{K}\mathcal{Q}$	37
4.3	Application to Langevin dynamics of a particle system	40
4.3.1	EMZ memory and fluctuation terms	46
5	Approximation methods for the MZ equation	46
5.1	Operator series expansions	47
5.1.1	MZ-Dyson expansion	48
5.2	MZ-Faber expansion	49
5.3	Other series expansions of the MZ-memory integral	50
5.3.1	MZ-Lagrange expansion	50
5.3.2	MZ-Newton expansion	51
5.4	The generalized Langevin equation (GLE)	52
5.4.1	Application to linear dynamical systems	52
5.4.2	Evolution equation for the conditional expectation	52
5.4.3	Evolution equation for the autocorrelation function	53
5.4.4	Exact solution to the MZ equation	53
5.5	GLEs for nonlinear systems	54
5.6	Convergence analysis	55

5.7	Numerical examples	60
5.7.1	Random wave propagation	60
5.7.2	Harmonic oscillator chains on the Bethe lattice	63
6	Systems with local polynomial interactions	68
6.1	Calculation of the MZ memory kernel from first principles	68
6.2	Systems with polynomial nonlinearities	70
6.3	Mapping the index set $\mathcal{I}^{(n)}$	73
6.4	An example: the Fermi-Pasta-Ulam (FPU) model	74
6.5	Modeling the MZ fluctuation term	76
6.5.1	Building MZ-KL stochastic models from first principles	79
6.6	Application to random wave propagation	79
6.6.1	Linear waves	80
6.6.2	Nonlinear waves	84
7	Publications during reporting period	88

List of Figures

1	Harmonic chain of oscillators. (a) Velocity auto-correlation function $C_{p_1}(t)$ and (b) memory kernel $K(t)$ of the corresponding MZ equation. It is seen that our theoretical estimate (78) (dashed line) correctly bounds the MZ memory kernel. Note that the upper bound we obtain is of the same order of magnitude as the memory kernel.	21
2	Hald Hamiltonian system (80). (a) Autocorrelation function of the displacement $q_1(t)$ and (b) memory kernel of the governing MZ equation. Here $C_{q_1}(t)$ is computed by Markov chain Monte-Carlo (MCMC) while $K(t)$ is determined by inverting numerically the Laplace transform in (85) with the Talbot algorithm. It is seen that the theoretical upper bound (84) (dashed line) is of the same order of magnitude as the memory kernel.	22
3	Convergence of the H -model for the linear dynamical system with matrix (86). The benchmark solution is computed with Monte-Carlo (MC) simulation. Also, the zero-order H -model represents the Markovian approximation to the MZ equation, i.e. the MZ equation without the memory term.	24
4	Linear dynamical system with matrix (86). In (a) we plot the memory term $w_0(t)$ we obtain from Monte Carlo simulation together with the estimated upper bound (87). In (b) and (c) we plot H -model approximation error $ w_0(T) - w_0^n(T) $ together with the upper bound (88) for different differentiation orders n and at different times t	24
5	Linear dynamical system with matrix A (90). Convergence of the H -model to the conditional mean path solution $\mathbb{E}[x_1(t) x_1(0)]$. The initial condition is set as $x_1(0) = 3$, while $\{x_2(0), \dots, x_{100}(0)\}$ are i.i.d. Normals.	25
6	Accuracy of the H_t model in representing the conditional mean path in the Lorenz-63 system (91). It is seen that if $r = 0.5$ (first row), then the zeroth-order H_t -model, i.e., the t -model, is accurate for long integration times. On the other hand, if we consider the chaotic regime at $r = 28$ (second row) then we see that the t -model and its high-order extension (H_t -model) are accurate only for relatively short time.	26
7	Accuracy of the H_t -model in representing the conditional mean path in the Lorenz-96 system (91). Here we set $F = 5$ and $N = 100$. It is seen that the H_t -model converges only for short time and provides results that are more accurate than the classical t -model.	27
8	Sketch of the cusp-shaped region of the complex plane enclosing the spectrum of the operators \mathcal{K} and \mathcal{QKQ}	34
9	Mean solution of the random wave equation in the annulus. We consider two random initial conditions in the form (267), with different number of modes: $M = 25$ (first row), $M = 50$ (second row).	62
10	Dyson and Faber expansions of the Mori-Zwanzig memory kernel $g(t - s)$ in equation (278). Shown are results for different polynomial orders n . It is seen that the MZ-Faber series converges faster than the MZ-Dyson series.	63
11	MZ-Dyson and MZ-Faber approximation errors of the mean wave amplitude at $(r, \theta) = (1.1, 0.1)$ as a function of the polynomial order n . It is seen that the MZ-Faber expansion converges faster than the MZ-Dyson series.	64
12	Bethe lattices with coordination numbers 2 (left), and 3 (right).	65
13	Velocity auto-correlation functions (286) (left) and (289) (right) of a tagged oscillator in an harmonic chain interacting on a Bethe lattice with coordination number $l = 2$ and $l = 3$, respectively.	66
14	Harmonic chains of oscillators. Dyson and Faber expansions of the Mori-Zwanzig memory kernel $g(t - s)$. Shown are results for different polynomial orders n . It is seen that the MZ-Faber series converges faster than the MZ-Dyson series.	68

15	Accuracy of the MZ-Dyson and MZ-Faber expansions in representing the velocity auto-correlation function of the tagged oscillator $j = 2$ in an harmonic chain interacting on the Bethe lattice with coordination number 2. It is seen that the MZ-Dyson and the MZ-Faber expansions yield accurate predictions as we increase the polynomial order n . Moreover, the MZ-Faber expansion converges faster than the MZ-Dyson expansion.	69
16	Accuracy of the MZ-Dyson and MZ-Faber expansions in representing the velocity auto-correlation function of the oscillator at the center of a Bethe lattice with coordination number 3, 8 shells and $N = 766$ oscillators. It is seen that the MZ-Dyson and the MZ-Faber expansion yield accurate predictions as we increase the polynomial order n . Moreover, the MZ-Faber expansion converges faster than the MZ-Dyson series.	70
17	Sample solutions of the nonlinear wave equation (351) with initial conditions $u(x, 0) = e^{-\sin(2x)}(1 + \cos(x))$ (first row), $u(x, 0) = e^{-\sin(2x)}(1 + \cos(5x))$ (second row), and $u(x, 0) = e^{-\sin(2x)}(1 + \cos(9x))$ (third row). We set the group velocity α to $(2\pi/100)^2$ and consider different nonlinear interaction terms: $G = 0$ (first column – linear waves), $G = \beta u_x^4/4$ with $\beta = (2\pi/100)^4$ (second column – nonlinear waves). It is seen that as the initial condition becomes rougher, the nonlinear effects become more important.	81
18	Snapshots of the solution shown in Figure 17.	82
19	Linear wave equation (353). Temporal auto-correlation function of the wave momentum $p(x_j, t) = \partial u(x_j, t)/\partial t$ (Eq. (357), any location x_j) and MZ memory kernel $K(t)$. We compare the analytical results (358) and (360), with results we obtained by using the recursive algorithm we presented in Section 6.1 for different Faber polynomial orders n . It is seen that the MZ-Faber expansion rapidly converges to the exact MZ-kernel and auto-correlation function we increase the polynomial order.	84
20	Linear wave equation (353). Temporal auto-correlation functions (362) of the wave momentum. The MZ kernel here is approximated with a Faber polynomial series of degree $n = 10$	84
21	Nonlinear wave equation (363). Temporal auto-correlation function of the wave displacement $r_j(t)$ for different values of the nonlinear parameter β_1 . We compare results we obtained by calculating the MZ memory from first principles using n -th order Faber polynomials (Section 6.2) with results from Markov-Chain-Monte-Carlo (10^6 sample paths). The thermodynamic parameter γ is set to 1 (high-temperature) in the first row and to 40 (low-temperature) in the second row.	86
22	Nonlinear wave equation (363). Temporal auto-correlation function of polynomial observables $p_j^m(t)$ (first row) $r_j^m(t)$ (second row) with $m = 1, 2, 4$. We compare results from Markov-Chain-Monte-Carlo simulation (MC), KL expansion based on the first-principle MZ memory kernel calculation (359) (KL-FP), and KL expansion based on a data-driven estimate of the temporal auto-correlation function (KL-DD). The parameter γ appearing in (365) is set to 40, while $\alpha_1 = \beta_1 = 1$	87

List of Tables

- 1 Series expansions of the Mori-Zwanzig memory operator. Here J_j is the j th Bessel function of the first kind, c_0 and c_1 are real numbers, $f_{1,j}(t)$ are defined in (209), and λ_j are the eigenvalues of any matrix representation of \mathcal{QL} 51

1 Abstract

The Mori-Zwanzig (MZ) formulation is a technique originally developed in statistical mechanics to formally integrate out phase variables in nonlinear dynamical systems by means of a projection operator. One of the main features of such formulation is that it allows us to systematically derive exact equations of motion for quantities of interest (macroscopic observables), based on microscopic equations of motion. Such equations can be found in a variety of applications, including particle dynamics [79, 98, 55, 56, 53], partial differential equations (PDEs) [15, 83, 12, 14, 88], fluid dynamics [69, 70, 82], and solid-state physics [97, 54, 60]. Computing the solution to the MZ equation is a challenging task. One of the main difficulties is the approximation of the memory integral (convolution term), and the fluctuation term (noise), which encode the interaction between the so-called orthogonal dynamics and the dynamics of the quantity of interest. The orthogonal dynamics is essentially a high-dimensional nonlinear flow that satisfies a hard-to-solve integro-differential equation. Such flow has, in general, the same order of magnitude and dynamical properties as the quantity of interest, i.e., there is no general scale separation between the so-called resolved and the unresolved variables of the system [18, 81]. As a consequence, approximating the MZ memory integral and the fluctuation term in these cases is a daunting task, because of the strong coupling between the orthogonal dynamics and the dynamics of the macroscopic observables.

In this project, we developed an in-depth mathematical analysis of the MZ formulation for both deterministic and stochastic dynamical systems, and established an effective computational framework that allows us to perform numerical simulations of the MZ equation. This report includes a detailed description of the main research achievement we have obtained during the period of performance July 2015 - Sep 2019. Such achievements may be summarized as follows:

1. We developed rigorous error estimates and provably convergent approximations for the MZ memory integral and fluctuation terms for both deterministic and stochastic dynamical systems. In particular, we developed and studied new hierarchical approximations based on Faber operator series expansions, first-principle memory calculation methods, and data-driven approximation schemes. These contributions effectively turn the MZ formalism into a practical computational tool, which can find its way in many different application areas.
2. We derived and studied a new type of MZ equation, which we called effective Mori-Zwanzig (EMZ) equation, governing the dynamics of noise-averaged observables defined on stochastic flow. Building upon recent work on hypoelliptic operators, we rigorously proved that EMZ memory kernel and fluctuation terms converge exponentially fast in time to a computable equilibrium state. This has applications in high-dimensional particle dynamics, and swarms of autonomous agents.

The report includes extensive discussion and technical details on these major achievements, as well as many application examples ranging from random wave propagation to high-dimensional interacting particle systems.

2 The Mori-Zwanzig formulation for deterministic dynamical systems

Consider the following nonlinear dynamical system evolving on a smooth manifold $\mathcal{M} \subseteq \mathbb{R}^N$

$$\frac{d\mathbf{x}}{dt} = \mathbf{F}(\mathbf{x}), \quad \mathbf{x}(0) = \mathbf{x}_0, \quad (1)$$

where $\mathbf{x}_0 \in \mathcal{M}$ is a random initial state with probability density function $\rho_0(\mathbf{x})$. The dynamics of any vector-valued phase space function

$$\begin{aligned} \mathbf{u}: \mathcal{M} &\rightarrow \mathbb{R}^M \\ \mathbf{x} &\mapsto \mathbf{u}(\mathbf{x}) \end{aligned} \quad (2)$$

can be expressed in terms of a semi-group of linear operators acting on $\mathbf{u}(\mathbf{x}_0)$, i.e.,

$$\mathbf{u}(\mathbf{x}(t, \mathbf{x}_0)) = e^{t\mathcal{L}(\mathbf{x}_0)}\mathbf{u}(\mathbf{x}_0), \quad \mathcal{L}(\mathbf{x}_0) = \sum_{k=1}^N F_k(\mathbf{x}_0) \frac{\partial}{\partial x_{0k}}. \quad (3)$$

In this equation, $\mathbf{x}(t, \mathbf{x}_0)$ represents the flow [95] generated by the system (1), while $e^{t\mathcal{L}}$ is the composition (Koopman) operator of the system [48, 23]. The Mori-Zwanzig formulation [102, 15, 99] allows us to derive the exact evolution equation for the phase space function $\mathbf{u}(t) = \mathbf{u}(\mathbf{x}(t, \mathbf{x}_0))$. The first step is to introduce an orthogonal projection operator \mathcal{P} , and the complementary projection $\mathcal{Q} = \mathcal{I} - \mathcal{P}$, where \mathcal{I} is the identity operator. In Section (2.1) we review a few commonly used projection operators \mathcal{P} . The mathematical properties of such projections are discussed in detail in [99, 23]. By differentiating the well-known Dyson's identity

$$e^{t\mathcal{L}} = e^{t\mathcal{Q}\mathcal{L}} + \int_0^t e^{s\mathcal{L}}\mathcal{P}\mathcal{L}e^{(t-s)\mathcal{Q}\mathcal{L}} ds \quad (4)$$

with respect to time, we obtain the following evolution equation for the Koopman operator $e^{t\mathcal{L}}$

$$\frac{d}{dt}e^{t\mathcal{L}} = e^{t\mathcal{L}}\mathcal{P}\mathcal{L} + e^{t\mathcal{Q}\mathcal{L}}\mathcal{Q}\mathcal{L} + \int_0^t e^{s\mathcal{L}}\mathcal{P}\mathcal{L}e^{(t-s)\mathcal{Q}\mathcal{L}}\mathcal{Q}\mathcal{L} ds. \quad (5)$$

Applying this equation to any phase space function $\mathbf{u}(0) = \mathbf{u}(\mathbf{x}_0)$ yields the Mori-Zwanzig (MZ) equation

$$\frac{\partial}{\partial t}e^{t\mathcal{L}}\mathbf{u}(0) = e^{t\mathcal{L}}\mathcal{P}\mathcal{L}\mathbf{u}(0) + e^{t\mathcal{Q}\mathcal{L}}\mathcal{Q}\mathcal{L}\mathbf{u}(0) + \int_0^t e^{s\mathcal{L}}\mathcal{P}\mathcal{L}e^{(t-s)\mathcal{Q}\mathcal{L}}\mathcal{Q}\mathcal{L}\mathbf{u}(0) ds. \quad (6)$$

The three terms at the right hand side are called, respectively, streaming term, fluctuation (or noise) term, and memory term. It is often more convenient (and tractable) to compute the evolution of the observable $\mathbf{u}(t)$ within a closed linear space, e.g., the image of the projection operator \mathcal{P} . To this end, we apply such projection to both sides of equation (6). This yields the following exact evolution equation¹

$$\frac{\partial}{\partial t}\mathcal{P}e^{t\mathcal{L}}\mathbf{u}(0) = \mathcal{P}e^{t\mathcal{L}}\mathcal{P}\mathcal{L}\mathbf{u}(0) + \int_0^t \mathcal{P}e^{s\mathcal{L}}\mathcal{P}\mathcal{L}e^{(t-s)\mathcal{Q}\mathcal{L}}\mathcal{Q}\mathcal{L}\mathbf{u}(0) ds. \quad (7)$$

Depending on the choice of the projection operator, the MZ equation (7) can yield evolution equations for different quantities. For example, if we use Chorin's projection [15, 16, 99, 88], then (7) is an evolution equation for the conditional mean of $\mathbf{u}(t)$. Similarly, if we use Mori's projection [100, 79], then (7) is an evolution equation for the temporal auto-correlation function of $\mathbf{u}(t)$.

¹Note that the projected fluctuation term $\mathcal{P}e^{t\mathcal{Q}\mathcal{L}}\mathcal{Q}\mathcal{L}\mathbf{u}(0)$ is identically zero since $\mathcal{P}\mathcal{Q} = 0$.

2.1 Projection operators

In this Section we briefly review the most commonly used projection operators in the Mori-Zwanzig formulation. Such projection operators are conditional expectations in the sense of operator algebras [23], and they can have different forms.

2.1.1 Chorin's Projection

In a series of papers [15, 18, 17], A. J. Chorin and collaborators defined the following projection operator

$$(\mathcal{P}\mathbf{u})(\hat{\mathbf{x}}_0) = \frac{\int_{-\infty}^{+\infty} \mathbf{u}(\hat{\mathbf{x}}(t; \hat{\mathbf{x}}_0, \tilde{\mathbf{x}}_0), \tilde{\mathbf{x}}(t; \hat{\mathbf{x}}_0, \tilde{\mathbf{x}}_0)) \rho_0(\hat{\mathbf{x}}_0, \tilde{\mathbf{x}}_0) d\tilde{\mathbf{x}}_0}{\int_{-\infty}^{+\infty} \rho_0(\hat{\mathbf{x}}_0, \tilde{\mathbf{x}}_0) d\tilde{\mathbf{x}}_0}, \quad (8)$$

which represents a conditional expectation in the sense of classical probability theory. In equation (8), $\mathbf{x}(t; x_0)$ denotes the flow map generated by (1), which we can split into resolved $\hat{\mathbf{x}}(t; \hat{\mathbf{x}}_0, \tilde{\mathbf{x}}_0)$ and unresolved $\tilde{\mathbf{x}}(t; \hat{\mathbf{x}}_0, \tilde{\mathbf{x}}_0)$ maps, $\mathbf{u}(\mathbf{x}) = \mathbf{u}(\hat{\mathbf{x}}, \tilde{\mathbf{x}})$ is the quantity of interest, and $\rho_0(\hat{\mathbf{x}}_0, \tilde{\mathbf{x}}_0)$ is the probability density function of the initial state \mathbf{x}_0 . Alternatively, one can replace ρ_0 with the equilibrium distribution of the system $\rho_{eq}(\hat{\mathbf{x}}, \tilde{\mathbf{x}})$, assuming it exists. Clearly, if \mathbf{x}_0 is deterministic then $\rho_0(\hat{\mathbf{x}}_0, \tilde{\mathbf{x}}_0)$ is a product of Dirac delta functions. On the other hand, if $\hat{\mathbf{x}}_0$ and $\tilde{\mathbf{x}}_0$ are statistically independent, i.e. $\rho_0(\hat{\mathbf{x}}_0, \tilde{\mathbf{x}}_0) = \hat{\rho}_0(\hat{\mathbf{x}}_0)\tilde{\rho}_0(\tilde{\mathbf{x}}_0)$, then the conditional expectation (8) simplifies to

$$(\mathcal{P}\mathbf{u})(\hat{\mathbf{x}}_0) = \int_{-\infty}^{+\infty} \mathbf{u}(\hat{\mathbf{x}}(t; \hat{\mathbf{x}}_0, \tilde{\mathbf{x}}_0), \tilde{\mathbf{x}}(t; \hat{\mathbf{x}}_0, \tilde{\mathbf{x}}_0)) \tilde{\rho}_0(\tilde{\mathbf{x}}_0) d\tilde{\mathbf{x}}_0. \quad (9)$$

In the special case where $\mathbf{u}(\hat{\mathbf{x}}, \tilde{\mathbf{x}}) = \hat{\mathbf{x}}(t; \hat{\mathbf{x}}_0, \tilde{\mathbf{x}}_0)$ we have

$$(\mathcal{P}\hat{\mathbf{x}})(\hat{\mathbf{x}}_0) = \int_{-\infty}^{+\infty} \hat{\mathbf{x}}(t; \hat{\mathbf{x}}_0, \tilde{\mathbf{x}}_0) \tilde{\rho}_0(\tilde{\mathbf{x}}_0) d\tilde{\mathbf{x}}_0, \quad (10)$$

i.e. the conditional expectation of the resolved variables $\hat{\mathbf{x}}(t)$ given the initial condition $\hat{\mathbf{x}}_0$. This means that an integration of (10) with respect to $\hat{\rho}_0(\hat{\mathbf{x}}_0)$ yields the mean of the resolved variables

$$\langle \hat{\mathbf{x}}(t) \rangle_{\rho_0} = \int_{-\infty}^{\infty} (\mathcal{P}\hat{\mathbf{x}})(\hat{\mathbf{x}}_0) \hat{\rho}_0(\hat{\mathbf{x}}_0) d\hat{\mathbf{x}}_0 = \int_{-\infty}^{\infty} \hat{\mathbf{x}}(t, \mathbf{x}_0) \rho_0(\mathbf{x}_0) d\mathbf{x}_0. \quad (11)$$

Obviously, if the resolved variables $\hat{\mathbf{x}}(t)$ evolve from a deterministic initial state $\hat{\mathbf{x}}_0$ then the conditional expectation (10) represents the average of the reduced-order flow map $\hat{\mathbf{x}}(t; \hat{\mathbf{x}}_0, \tilde{\mathbf{x}}_0)$ with respect to the PDF of $\tilde{\mathbf{x}}_0$, i.e.,

$$\mathbf{X}_0(t; \hat{\mathbf{x}}_0) = \int_{-\infty}^{+\infty} \hat{\mathbf{x}}(t; \hat{\mathbf{x}}_0, \tilde{\mathbf{x}}_0) \tilde{\rho}_0(\tilde{\mathbf{x}}_0) d\tilde{\mathbf{x}}_0. \quad (12)$$

In this case, the MZ equation (7) is an unclosed evolution equation (PDE) for the averaged flow map (12).

2.1.2 Mori's projection

Suppose that the phase space function (2) belongs to the weighted Hilbert space $H = L^2(\mathcal{M}, \rho)$, where ρ is a positive weight function in \mathcal{M} . For instance, ρ can be the probability density function of the random initial state \mathbf{x}_0 (i.e., ρ_0 , see Eq. (1)), or the equilibrium distribution of the system ρ_{eq} (assuming it exists). Let

$$\langle f, g \rangle_{\rho} = \int_{\mathcal{M}} f(\mathbf{x})g(\mathbf{x})\rho(\mathbf{x})d\mathbf{x} \quad f, g \in H \quad (13)$$

be the inner product in H . For any closed linear subspace $V \subset H$ the Mori projection operator \mathcal{P} is defined to be the orthogonal projection onto V , relative to the inner product (13). If V is finite-dimensional with dimension M , then \mathcal{P} can be effectively constructed if we are given M linearly independent functions $u_i(0) = u_i(\mathbf{x}) \in V$ ($i = 1, \dots, M$). Clearly, if $\{u_1(0), \dots, u_M(0)\}$ are linearly independent then $V = \text{span}\{u_1(0), \dots, u_M(0)\}$. To construct Mori's projection, we first compute the positive-definite Gram matrix $G_{ij} = \langle u_i(0), u_j(0) \rangle_\rho$, i.e.,

$$G_{ij} = \int_{\mathcal{M}} u_i(\mathbf{x})u_j(\mathbf{x})\rho(\mathbf{x})d\mathbf{x}. \quad (14)$$

With G_{ij} available, we define

$$\mathcal{P}f = \sum_{i,j=1}^M G_{ij}^{-1} \langle u_i(0), f \rangle_\rho u_j(0), \quad f \in H. \quad (15)$$

In classical statistical dynamics of Hamiltonian systems, a common choice for the density ρ is the Boltzmann-Gibbs distribution

$$\rho_{eq}(\mathbf{x}) = \frac{1}{Z} e^{-\beta\mathcal{H}(\mathbf{x})}, \quad (16)$$

where $\mathcal{H}(\mathbf{x}) = \mathcal{H}(\mathbf{q}, \mathbf{p})$ is the Hamiltonian of the system, $\mathbf{x} = (\mathbf{q}, \mathbf{p})$ are generalized coordinates/momenta, and Z is the partition function. For other systems, ρ can be, e.g., the probability density function of the random initial state (see Eq. (1)). Next, suppose that each observable $u_i(\mathbf{x})$ ($i = 1, \dots, M$) belongs to the linear space $\mathcal{P}H \cap \mathcal{D}(\mathcal{L})$, where $\mathcal{P}H = V$ and $\mathcal{D}(\mathcal{L})$ denotes the domain of the Liouville operator \mathcal{L} defined in (3). The MZ equation (6), with \mathcal{P} defined in (15), reduces to

$$\frac{d\mathbf{u}(t)}{dt} = \mathbf{\Omega}\mathbf{u}(t) + \int_0^t \mathbf{K}(t-s)\mathbf{u}(s)ds + \mathbf{f}(t), \quad (17)$$

where²

$$G_{ij} = \langle u_i(0), u_j(0) \rangle_\rho \quad (\text{Gram matrix}), \quad (19a)$$

$$\Omega_{ij} = \sum_{k=1}^M G_{jk}^{-1} \langle u_k(0), \mathcal{L}u_i(0) \rangle_\rho \quad (\text{streaming matrix}), \quad (19b)$$

$$K_{ij}(t) = \sum_{k=1}^M G_{jk}^{-1} \langle u_k(0), \mathcal{L}e^{t\mathcal{Q}\mathcal{L}}\mathcal{Q}\mathcal{L}u_i(0) \rangle_\rho \quad (\text{memory kernel}), \quad (19c)$$

$$\mathbf{f}(t) = e^{t\mathcal{Q}\mathcal{L}}\mathcal{Q}\mathcal{L}\mathbf{u}(0) \quad (\text{fluctuation term}). \quad (19d)$$

Equation (17) is often referred to as generalized Langevin equation (GLE) in classical statistical physics and other disciplines [79]. By applying Mori's projection to (17) we obtain the following linear (and closed) evolution equation for the projected phase space function

$$\frac{d}{dt}\mathcal{P}\mathbf{u}(t) = \mathbf{\Omega}\mathcal{P}\mathbf{u}(t) + \int_0^t \mathbf{K}(t-s)\mathcal{P}\mathbf{u}(s)ds. \quad (20)$$

²Note that the i th component of the system (113) can be explicitly written as

$$\frac{du_i(t)}{dt} = \sum_{j=1}^M \Omega_{ij}u_j(t) + \sum_{j=1}^M \int_0^t K_{ij}(t-s)u_j(s)ds + f_i(t). \quad (18)$$

Acting with the inner product $\langle u_j(0), \cdot \rangle_\rho$ on both sides of equation (20), yields the following exact equation for the temporal auto-correlation matrix $C_{ij}(t) = \langle u_j(0), u_i(t) \rangle_\rho$

$$\frac{d}{dt} C_{ij}(t) = \sum_{k=1}^M \Omega_{ik} C_{kj}(t) + \sum_{k=1}^M \int_0^t K_{ik}(t-s) C_{kj}(s) ds. \quad (21)$$

In the particular case where the system (1) is Hamiltonian, and the random initial state \mathbf{x}_0 is distributed according to the Boltzmann-Gibbs distribution (16), i.e., $\rho_0 = \rho_{eq}$, we have that the Liouville operator \mathcal{L} is skew-adjoint relative to the inner product (13), i.e., we have

$$\langle f, \mathcal{L}g \rangle_{eq} = -\langle \mathcal{L}f, g \rangle_{eq} \quad f, g \in L^2(\mathcal{M}, \rho_{eq}) \cap \mathcal{D}(\mathcal{L}). \quad (22)$$

This allows us to simplify the expression of the memory kernel (19c) as

$$\begin{aligned} K_{ij}(t) &= - \sum_{k=1}^M G_{jk}^{-1} \langle \mathcal{Q}\mathcal{L}u_k(0), e^{t\mathcal{Q}\mathcal{L}} \mathcal{Q}\mathcal{L}u_i(0) \rangle_{eq}, \\ &= - \sum_{k=1}^M G_{jk}^{-1} \langle f_k(0), f_i(t) \rangle_{eq}, \end{aligned} \quad (23)$$

where $f_k(t)$ is the k -th component of the fluctuation term (19d). The identity (23) is known as Kubo's second fluctuation-dissipation theorem [49]. We emphasize there are several advantages in using Mori's projection (15) over other projection operators, e.g., Chorin's projection [17]. For example, both MZ equations (17) and (20) are linear and closed, which allows us perform rigorous convergence analysis [100, 99]. Secondly, the streaming matrix (19b) and the memory kernel (19c) are exactly the same for both the projected and the unprojected equations, i.e., (17) and (20)). Thirdly, we have that the second-fluctuation dissipation theorem (23) holds true, which allows us to express the MZ memory kernel in a relatively simple form in terms of averages of random forces.

2.1.3 Berne's projection

A simpler projection operator was proposed by Berne in [7] (see also [79], p. 30). The standard form for scalar observables (2) is

$$\mathcal{P}(\cdot) = \frac{\langle u_0, (\cdot) \rangle_{eq}}{\langle u_0, u_0 \rangle_{eq}} u_0. \quad (24)$$

This projection can be considered as a subcase of the Mori projection (15). Note that with Berne's projection we can easily represent the auto-correlation function the observable $u(\mathbf{x}(t))$ as

$$C_u(t) = \frac{\langle u(t), u_0 \rangle_{eq}}{\langle u_0, u_0 \rangle_{eq}} = \frac{\langle \mathcal{P}u(\mathbf{x}(t)), u_0 \rangle_{eq}}{\langle u_0, u_0 \rangle_{eq}}. \quad (25)$$

3 Analysis of the MZ memory integral

In this section we develop a thorough mathematical analysis to deduce conditions for accuracy and convergence of different approximations of the memory integral in the Mori-Zwanzig (MZ) equation, i.e.,

$$\int_0^t \mathcal{P} e^{s\mathcal{L}} \mathcal{P} \mathcal{L} e^{(t-s)\mathcal{Q}\mathcal{L}} \mathcal{Q}\mathcal{L} u_0 ds = \int_0^t \mathcal{P} e^{s\mathcal{L}} \mathcal{P} e^{(t-s)\mathcal{L}\mathcal{Q}} \mathcal{L} \mathcal{Q}\mathcal{L} u_0 ds. \quad (26)$$

In particular, we derive errors bounds and sufficient convergence conditions for short-memory approximations, the t -model, and hierarchical (finite-memory) approximations. In addition, we derive useful upper bounds for the MZ memory integral, which allow us to estimate a priori the contribution of the MZ memory to the dynamics. Such upper bounds are easily computable for systems with finite-rank projections, e.g., Mori-type projections. We begin by describing the behavior of the semigroup norms $\|e^{t\mathcal{L}}\|$, $\|e^{t\mathcal{Q}\mathcal{L}\mathcal{Q}}\|$, and $\|e^{t\mathcal{L}\mathcal{Q}}\|$ as functions of time, for different choices of projection \mathcal{P} and different norms. As we will see, the analysis will give clear computable bounds only in some circumstances, illustrating the difficulty of this problem and the need for further development and insight.

3.1 Memory growth

We begin by seeking to bound the MZ memory integral as a whole, and build our analysis from there. A key assumption of our analysis is that the semigroup $e^{t\mathcal{L}\mathcal{Q}}$ is strongly continuous, i.e., the map $t \mapsto e^{t\mathcal{L}\mathcal{Q}}g$ is continuous in the norm topology on the space of observables for each fixed g [28]. Thus, assume that there exist constants $M_{\mathcal{Q}}$ and $\omega_{\mathcal{Q}}$ such that $\|e^{t\mathcal{L}\mathcal{Q}}\| \leq M_{\mathcal{Q}}e^{t\omega_{\mathcal{Q}}}$. Throughout this section, $\|\cdot\|$ denotes a general Banach norm. We begin with the following simple estimate:

Theorem 1. (Memory growth) *Let $e^{t\mathcal{L}}$ and $e^{t\mathcal{L}\mathcal{Q}}$ be strongly continuous semigroups with upper bounds $\|e^{t\mathcal{L}}\| \leq Me^{t\omega}$ and $\|e^{t\mathcal{L}\mathcal{Q}}\| \leq M_{\mathcal{Q}}e^{t\omega_{\mathcal{Q}}}$. Then*

$$\left\| \int_0^t \mathcal{P}e^{s\mathcal{L}}\mathcal{P}\mathcal{L}e^{(t-s)\mathcal{Q}\mathcal{L}}\mathcal{Q}\mathcal{L}\mathbf{u}_0 ds \right\| \leq M_0(t), \quad (27)$$

where

$$M_0(t) = \begin{cases} C_1 t e^{t\omega_{\mathcal{Q}}}, & \omega = \omega_{\mathcal{Q}} \\ \frac{C_1}{\omega - \omega_{\mathcal{Q}}} [e^{t\omega} - e^{t\omega_{\mathcal{Q}}}], & \omega \neq \omega_{\mathcal{Q}} \end{cases} \quad (28)$$

and $C_1 = MM_{\mathcal{Q}}\|\mathcal{L}\mathcal{Q}\mathcal{L}\mathbf{u}_0\|$ is a constant. Clearly, $\lim_{t \rightarrow 0} M_0(t) = 0$.

Proof. We first rewrite the memory integral in the equivalent form

$$\int_0^t \mathcal{P}e^{s\mathcal{L}}\mathcal{P}\mathcal{L}e^{(t-s)\mathcal{Q}\mathcal{L}}\mathcal{Q}\mathcal{L}\mathbf{u}_0 ds = \int_0^t \mathcal{P}e^{s\mathcal{L}}\mathcal{P}e^{(t-s)\mathcal{L}\mathcal{Q}}\mathcal{L}\mathcal{Q}\mathcal{L}\mathbf{u}_0 ds.$$

Since $e^{t\mathcal{L}}$ and $e^{t\mathcal{L}\mathcal{Q}}$ are assumed to be strongly continuous semigroups, we have the upper bounds $\|e^{t\mathcal{L}}\| \leq Me^{t\omega}$, $\|e^{t\mathcal{L}\mathcal{Q}}\| \leq M_{\mathcal{Q}}e^{t\omega_{\mathcal{Q}}}$. Therefore

$$\begin{aligned} \left\| \int_0^t \mathcal{P}e^{s\mathcal{L}}\mathcal{P}e^{(t-s)\mathcal{L}\mathcal{Q}}\mathcal{L}\mathcal{Q}\mathcal{L}\mathbf{u}_0 ds \right\| &\leq \int_0^t \|e^{s\mathcal{L}}\mathcal{P}e^{(t-s)\mathcal{L}\mathcal{Q}}\mathcal{L}\mathcal{Q}\mathcal{L}\mathbf{u}_0\| ds \\ &\leq MM_{\mathcal{Q}}\|\mathcal{L}\mathcal{Q}\mathcal{L}\mathbf{u}_0\| \int_0^t e^{s(\omega - \omega_{\mathcal{Q}})} ds \\ &= \begin{cases} C_1 t e^{t\omega_{\mathcal{Q}}}, & \omega = \omega_{\mathcal{Q}} \\ \frac{C_1}{\omega - \omega_{\mathcal{Q}}} [e^{t\omega} - e^{t\omega_{\mathcal{Q}}}], & \omega \neq \omega_{\mathcal{Q}} \end{cases} \end{aligned}$$

where $C_1 = MM_{\mathcal{Q}}\|\mathcal{P}\|^2\|\mathcal{L}\mathcal{Q}\mathcal{L}\mathbf{u}_0\|$. □

Theorem 1 provides an upper bound for the growth of the memory integral based on the assumption that $e^{t\mathcal{L}}$ and $e^{t\mathcal{L}\mathcal{Q}}$ are strongly continuous semigroups. We emphasize that only for simple cases can such upper bounds can be computed analytically (we will compute one of the cases later in section 5.7), because of the fundamental difficulties in computing the upper bound of $e^{t\mathcal{L}\mathcal{Q}}$. However, it will be shown later that, although the specific expression for $M_0(t)$ is unknown, the *form* of it is already useful as it enables us to derive some verifiable theoretical predictions for general nonlinear systems.

3.2 Short memory approximation and the t -model

Theorem 1 can be employed to obtain upper bounds for well-known approximations of the memory integral. Let us begin with the t -model proposed in [18]. This model relies on the approximation

$$\int_0^t \mathcal{P}e^{s\mathcal{L}}\mathcal{P}\mathcal{L}e^{(t-s)\mathcal{Q}\mathcal{L}}\mathcal{Q}\mathcal{L}\mathbf{u}_0 ds \simeq te^{t\mathcal{L}}\mathcal{P}\mathcal{L}\mathcal{Q}\mathcal{L}\mathbf{u}_0 \quad (t\text{-model}). \quad (29)$$

Theorem 2. (Memory approximation via the t -model [18]) *Let $e^{t\mathcal{L}}$ and $e^{t\mathcal{L}\mathcal{Q}}$ be strongly continuous semigroups with upper bounds $\|e^{t\mathcal{L}}\| \leq Me^{t\omega}$ and $\|e^{t\mathcal{L}\mathcal{Q}}\| \leq M_{\mathcal{Q}}e^{t\omega_{\mathcal{Q}}}$. Then*

$$\left\| \int_0^t \mathcal{P}e^{s\mathcal{L}}\mathcal{P}\mathcal{L}e^{(t-s)\mathcal{L}\mathcal{Q}}\mathcal{L}\mathcal{Q}\mathcal{L}\mathbf{u}_0 ds - t\mathcal{P}e^{t\mathcal{L}}\mathcal{L}\mathcal{Q}\mathcal{L}\mathbf{u}_0 \right\| \leq M_1(t),$$

where

$$M_1(t) = \begin{cases} C_1 \left(\frac{e^{t\omega_{\mathcal{Q}}} - e^{t\omega}}{\omega_{\mathcal{Q}} - \omega} + \frac{te^{t\omega}}{M_{\mathcal{Q}}} \right) & \omega \neq \omega_{\mathcal{Q}} \\ C_1 \frac{M_{\mathcal{Q}} + 1}{M_{\mathcal{Q}}} te^{t\omega} & \omega = \omega_{\mathcal{Q}} \end{cases},$$

and $C_1 = MM_{\mathcal{Q}}\|\mathcal{P}\|^2\|\mathcal{L}\mathcal{Q}\mathcal{L}\mathbf{u}_0\|$.

Proof. By applying the triangle inequality, we obtain that

$$\begin{aligned} \left\| \int_0^t \mathcal{P}e^{s\mathcal{L}}\mathcal{P}\mathcal{L}e^{(t-s)\mathcal{L}\mathcal{Q}}\mathcal{L}\mathcal{Q}\mathcal{L}\mathbf{u}_0 ds - t\mathcal{P}e^{t\mathcal{L}}\mathcal{L}\mathcal{Q}\mathcal{L}\mathbf{u}_0 \right\| &\leq \|\mathcal{P}\|^2\|\mathcal{L}\mathcal{Q}\mathcal{L}\mathbf{u}_0\| \left(MM_{\mathcal{Q}} \int_0^t e^{s\omega} e^{(t-s)\omega_{\mathcal{Q}}} ds + tMe^{t\omega} \right) \\ &= C_1 e^{t\omega} \left(\int_0^t e^{s(\omega_{\mathcal{Q}} - \omega)} ds + \frac{t}{M_{\mathcal{Q}}} \right) \\ &= \begin{cases} C_1 \left(\frac{e^{t\omega_{\mathcal{Q}}} - e^{t\omega}}{\omega_{\mathcal{Q}} - \omega} + \frac{te^{t\omega}}{M_{\mathcal{Q}}} \right) & \omega \neq \omega_{\mathcal{Q}} \\ C_1 \frac{M_{\mathcal{Q}} + 1}{M_{\mathcal{Q}}} te^{t\omega} & \omega = \omega_{\mathcal{Q}} \end{cases} \end{aligned}$$

where $C_1 = MM_{\mathcal{Q}}\|\mathcal{P}\|^2\|\mathcal{L}\mathcal{Q}\mathcal{L}\mathbf{u}_0\|$. □

Theorem 2 provides an upper bound for the error associated with the t -model. The limit

$$\lim_{t \rightarrow 0} M_1(t) = 0, \quad (30)$$

guarantees the convergence of the t -model for short integration times. On the other hand, depending on the semigroup constants M , ω , $M_{\mathcal{Q}}$ and $\omega_{\mathcal{Q}}$ (which may be estimated numerically), the error of the t -model may remain small for longer integration times (see the numerical results in section 3.7.2) Next, we study the

short-memory approximation proposed in [80]. The main idea is to replace the integration interval $[0, t]$ in (26) by a shorter time interval $[t - \Delta t, t]$, i.e.

$$\int_0^t \mathcal{P}e^{s\mathcal{L}}\mathcal{P}\mathcal{L}e^{(t-s)\mathcal{Q}\mathcal{L}}\mathcal{Q}\mathcal{L}\mathbf{u}_0 ds \simeq \int_{t-\Delta t}^t \mathcal{P}e^{s\mathcal{L}}\mathcal{P}\mathcal{L}e^{(t-s)\mathcal{Q}\mathcal{L}}\mathcal{Q}\mathcal{L}\mathbf{u}_0 ds \quad (\text{short-memory approximation}),$$

where $\Delta t \in [0, t]$ identifies the effective *memory length*. The following result provides an upper bound to the error associated with the short-memory approximation.

Theorem 3. (Short memory approximation [80]) *Let $e^{t\mathcal{L}}$ and $e^{t\mathcal{L}\mathcal{Q}}$ be strongly continuous semigroups with upper bounds $\|e^{t\mathcal{L}}\| \leq Me^{t\omega}$ and $\|e^{t\mathcal{L}\mathcal{Q}}\| \leq M_{\mathcal{Q}}e^{t\omega_{\mathcal{Q}}}$. Then the following error estimate holds true*

$$\left\| \int_0^t \mathcal{P}e^{s\mathcal{L}}\mathcal{P}\mathcal{L}e^{(t-s)\mathcal{Q}\mathcal{L}}\mathcal{Q}\mathcal{L}\mathbf{u}_0 ds - \int_{t-\Delta t}^t \mathcal{P}e^{s\mathcal{L}}\mathcal{P}\mathcal{L}e^{(t-s)\mathcal{Q}\mathcal{L}}\mathcal{Q}\mathcal{L}\mathbf{u}_0 ds \right\| \leq M_2(t - \Delta t, t),$$

where

$$M_2(\Delta t, t) = \begin{cases} C_1(t - \Delta t)e^{t\omega_{\mathcal{Q}}} & \omega = \omega_{\mathcal{Q}} \\ C_1e^{\Delta t\omega_{\mathcal{Q}}} \frac{e^{(t-\Delta t)\omega} - e^{(t-\Delta t)\omega_{\mathcal{Q}}}}{\omega - \omega_{\mathcal{Q}}} & \omega \neq \omega_{\mathcal{Q}} \end{cases}$$

and $C_1 = MM_{\mathcal{Q}}\|\mathcal{P}\|^2\|\mathcal{L}\mathcal{Q}\mathcal{L}\mathbf{u}_0\|$.

We omit the proof due to its similarity to that of Theorem 1. Note that $\lim_{\Delta t \rightarrow t} M_2(\Delta t, t) = 0$ for all finite $t > 0$.

3.3 Hierarchical memory approximation methods

An alternative way to approximate the memory integral (26) was proposed by Stinis in [82]. The key idea is to repeatedly differentiate (26) with respect to time, and establish a hierarchy of PDEs which can eventually be truncated or approximated at some level to provide an approximation of the memory. In this section, we derive this hierarchy of memory equations and perform a thorough theoretical analysis to establish accuracy and convergence of the method. To this end, let us first define

$$\mathbf{w}_0(t) = \int_0^t \mathcal{P}e^{s\mathcal{L}}\mathcal{P}\mathcal{L}e^{(t-s)\mathcal{Q}\mathcal{L}}\mathcal{Q}\mathcal{L}\mathbf{u}_0 ds \quad (31)$$

to be the memory integral (26). By differentiating $\mathbf{w}_0(t)$ with respect to time we obtain

$$\frac{d\mathbf{w}_0(t)}{dt} = \mathcal{P}e^{t\mathcal{L}}\mathcal{P}\mathcal{L}\mathcal{Q}\mathcal{L}\mathbf{u}_0 + \mathbf{w}_1(t),$$

where

$$\mathbf{w}_1(t) = \int_0^t \mathcal{P}e^{s\mathcal{L}}\mathcal{P}\mathcal{L}e^{(t-s)\mathcal{Q}\mathcal{L}}(\mathcal{Q}\mathcal{L})^2\mathbf{u}_0 ds.$$

By iterating this procedure n times we obtain

$$\frac{d\mathbf{w}_{n-1}(t)}{dt} = \mathcal{P}e^{t\mathcal{L}}\mathcal{P}\mathcal{L}(\mathcal{Q}\mathcal{L})^{n-1}\mathbf{u}_0 + \mathbf{w}_n(t), \quad (32)$$

where

$$\mathbf{w}_n(t) = \int_0^t \mathcal{P}e^{s\mathcal{L}} \mathcal{P}\mathcal{L} e^{(t-s)\mathcal{Q}\mathcal{L}} (\mathcal{Q}\mathcal{L})^{n+1} \mathbf{u}_0 ds. \quad (33)$$

The hierarchy of equations (32)-(33) is equivalent to the following infinite-dimensional system of PDEs

$$\begin{cases} \frac{d\mathbf{w}_0(t)}{dt} &= \mathcal{P}e^{t\mathcal{L}} \mathcal{P}\mathcal{L} \mathcal{Q}\mathcal{L} \mathbf{u}_0 + \mathbf{w}_1(t) \\ \frac{d\mathbf{w}_1(t)}{dt} &= \mathcal{P}e^{t\mathcal{L}} \mathcal{P}\mathcal{L} \mathcal{Q}\mathcal{L} \mathcal{Q}\mathcal{L} \mathbf{u}_0 + \mathbf{w}_2(t) \\ &\vdots \\ \frac{d\mathbf{w}_{n-1}(t)}{dt} &= \mathcal{P}e^{t\mathcal{L}} \mathcal{P}\mathcal{L} (\mathcal{Q}\mathcal{L})^n \mathbf{u}_0 + \mathbf{w}_n(t) \\ &\vdots \end{cases} \quad (34)$$

evolving from the initial condition $\mathbf{w}_i(0) = 0, i = 1, 2, \dots$ (see equation (33)). With such initial condition available, we can solve (34) with backward substitution, i.e., from the last equation to the first one, to obtain the following (exact) *Dyson series representation* of the memory integral (31)

$$\begin{aligned} \mathbf{w}_0(t) &= \int_0^t \mathcal{P}e^{s\mathcal{L}} \mathcal{P}\mathcal{L} \mathcal{Q}\mathcal{L} \mathbf{u}_0 ds + \int_0^t \int_0^{\tau_1} \mathcal{P}e^{s\mathcal{L}} \mathcal{P}\mathcal{L} \mathcal{Q}\mathcal{L} \mathcal{Q}\mathcal{L} \mathbf{u}_0 ds d\tau_1 \\ &+ \dots + \int_0^t \int_0^{\tau_{n-1}} \dots \int_0^{\tau_1} \mathcal{P}e^{s\mathcal{L}} \mathcal{P}\mathcal{L} (\mathcal{Q}\mathcal{L})^n \mathbf{u}_0 ds d\tau_1 \dots d\tau_{n-1} + \dots \end{aligned} \quad (35)$$

So far no approximation was introduced, i.e., the infinite-dimensional system (34) and the corresponding formal solution (35) are *exact*. To make progress in developing a computational scheme to estimate the memory integral (31), it is necessary to introduce approximations. The simplest of these rely on truncating the hierarchy (34) after n equations, while simultaneously introducing an approximation of the n -th order memory integral $\mathbf{w}_n(t)$. We denote such an approximation as $\mathbf{w}_n^{e_n}(t)$. The truncated system takes the form

$$\begin{cases} \frac{d\mathbf{w}_0^n(t)}{dt} &= \mathcal{P}e^{t\mathcal{L}} \mathcal{P}\mathcal{L} \mathcal{Q}\mathcal{L} \mathbf{u}_0 + \mathbf{w}_1^n(t), \\ \frac{d\mathbf{w}_1^n(t)}{dt} &= \mathcal{P}e^{t\mathcal{L}} \mathcal{P}\mathcal{L} \mathcal{Q}\mathcal{L} \mathcal{Q}\mathcal{L} \mathbf{u}_0 + \mathbf{w}_2^n(t), \\ &\vdots \\ \frac{d\mathbf{w}_{n-1}^n(t)}{dt} &= \mathcal{P}e^{t\mathcal{L}} \mathcal{P}\mathcal{L} (\mathcal{Q}\mathcal{L})^n \mathbf{u}_0 + \mathbf{w}_n^{e_n}(t). \end{cases} \quad (36)$$

The notation $\mathbf{w}_j^n(t)$ ($j = 0, \dots, n-1$) emphasizes that the solution to (36) is, in general, different from the solution to (34). The initial condition of the system can be set as $\mathbf{w}_i^n(0) = 0$, for all $i = 0, \dots, n-1$. By using backward substitution, this yields the following formal solution

$$\begin{aligned} \mathbf{w}_0^n(t) &= \int_0^t \mathcal{P}e^{s\mathcal{L}} \mathcal{P}\mathcal{L} \mathcal{Q}\mathcal{L} \mathbf{u}_0 ds + \int_0^t \int_0^{\tau_1} \mathcal{P}e^{s\mathcal{L}} \mathcal{P}\mathcal{L} \mathcal{Q}\mathcal{L} \mathcal{Q}\mathcal{L} \mathbf{u}_0 ds d\tau_1 \\ &+ \dots + \int_0^t \int_0^{\tau_{n-1}} \dots \int_0^{\tau_1} \mathcal{P}e^{s\mathcal{L}} \mathcal{P}\mathcal{L} (\mathcal{Q}\mathcal{L})^n \mathbf{u}_0 ds d\tau_1 \dots d\tau_{n-1} \\ &+ \int_0^t \int_0^{\tau_{n-1}} \dots \int_0^{\tau_1} \mathbf{w}_n^{e_n}(s) ds d\tau_1 \dots d\tau_{n-1} \end{aligned} \quad (37)$$

representing an approximation of the memory integral (31). Note that, for a given system, such approximation depends only on the number of equations n in (36), and on the choice of approximation $\mathbf{w}_n^{e_n}(t)$. In this report, we discuss the following choices:

1. H -model

$$\mathbf{w}_n^{e_n}(t) = 0. \quad (38)$$

2. H_t -model

$$\mathbf{w}_n^{e_n}(t) = t\mathcal{P}e^{t\mathcal{L}}\mathcal{P}\mathcal{L}(\mathcal{Q}\mathcal{L})^{n+1}\mathbf{u}_0. \quad (39)$$

The first approximation, i.e., (38), is a truncation of the hierarchy obtained by assuming that $\mathbf{w}_n(t) = 0$. Such approximation was originally proposed by Stinis in [82], and we shall call it the H -model. Similarly, the H_t -model approximation is based on replacing the n -th order memory integral $\mathbf{w}_n(t)$ with a classical t -model. Note that in this setting the classical t -model approximation proposed by Chorin and Stinis [18] is equivalent to a zeroth-order H_t -model approximation.

Hereafter, we present a thorough mathematical analysis that aims at estimating the error $\|\mathbf{w}_0(t) - \mathbf{w}_0^n(t)\|$, where $\mathbf{w}_0(t)$ is full memory at time t (see (31) or (35)), while $\mathbf{w}_0^n(t)$ is the solution of the truncated hierarchy (36), with $\mathbf{w}_n^{e_n}(t)$ given by (38), or (39). With such error estimates available, we can infer whether the approximation of the full memory $\mathbf{w}_0(t)$ with $\mathbf{w}_0^n(t)$ is accurate and, more importantly, if the algorithm to approximate the memory integral converges. To the best of our knowledge, this is the first time a rigorous convergence analysis is performed on various approximations of the MZ memory integral. It turns out that the distance $\|\mathbf{w}_0(t) - \mathbf{w}_0^n(t)\|$ can be controlled through the construction of the hierarchy under some constraint on the initial condition.

3.3.1 The H -model

Setting $\mathbf{w}_n^{e_n}(t) = 0$ in (36) yields an approximation by truncation, which we will refer to as the H -model (hierarchical model). Such model was originally proposed by Stinis in [82]. Hereafter we provide error estimates and convergence results for this model. In particular, we derive an upper bound for the error $\|\mathbf{w}_0(t) - \mathbf{w}_0^n(t)\|$, and sufficient conditions for convergence of the reduced-order dynamical system. Such conditions are problem dependent, i.e., they involve the Liouvillian \mathcal{L} , the initial condition \mathbf{u}_0 , and the projection operator \mathcal{P} .

Theorem 4. (Accuracy of the H -model) *Let $e^{t\mathcal{L}}$ and $e^{t\mathcal{L}\mathcal{Q}}$ be strongly continuous semigroups with upper bounds $\|e^{t\mathcal{L}}\| \leq Me^{t\omega}$ and $\|e^{t\mathcal{L}\mathcal{Q}}\| \leq M_{\mathcal{Q}}e^{t\omega_{\mathcal{Q}}}$, and let $T > 0$ be a fixed integration time. For some fixed n , let*

$$\alpha_j = \frac{\|(\mathcal{L}\mathcal{Q})^{j+1}\mathcal{L}\mathbf{u}_0\|}{\|(\mathcal{L}\mathcal{Q})^j\mathcal{L}\mathbf{u}_0\|}, \quad 1 \leq j \leq n. \quad (40)$$

Then, for any $1 \leq p \leq n$ and all $t \in [0, T]$, we have

$$\|\mathbf{w}_0(t) - \mathbf{w}_0^p(t)\| \leq M_3^p(t) \leq M_3^p(T),$$

where

$$M_3^p(t) = C_1 A_1 A_2 \frac{t^{p+1}}{(p+1)!} \prod_{j=1}^p \alpha_j, \quad C_1 = \|\mathcal{L}\mathcal{Q}\mathcal{L}\mathbf{u}_0\| M M_{\mathcal{Q}},$$

and

$$A_1 = \max_{s \in [0, T]} e^{s(\omega - \omega_{\mathcal{Q}})} = \begin{cases} 1 & \omega \leq \omega_{\mathcal{Q}} \\ e^{T(\omega - \omega_{\mathcal{Q}})} & \omega \geq \omega_{\mathcal{Q}} \end{cases}, \quad A_2 = \max_{s \in [0, T]} e^{s\omega_{\mathcal{Q}}} = \begin{cases} 1 & \omega_{\mathcal{Q}} \leq 0 \\ e^{T\omega_{\mathcal{Q}}} & \omega_{\mathcal{Q}} \geq 0 \end{cases}. \quad (41)$$

Proof. We begin with the expression for the difference between the memory term \mathbf{w}_0 and its approximation \mathbf{w}_0^p

$$\mathbf{w}_0(t) - \mathbf{w}_0^p(t) = \int_0^t \int_0^{\tau_p} \cdots \int_0^{\tau_2} \int_0^{\tau_1} \mathcal{P} e^{s\mathcal{L}} \mathcal{P} e^{(\tau_1-s)\mathcal{L}\mathcal{Q}} (\mathcal{L}\mathcal{Q})^{n+1} \mathcal{L}\mathbf{u}_0 ds d\tau_1 \cdots d\tau_p. \quad (42)$$

Since $e^{t\mathcal{L}}$ and $e^{t\mathcal{L}\mathcal{Q}}$ are strongly continuous semigroups we have $\|e^{t\mathcal{L}}\| \leq M e^{\omega t}$ and $\|e^{t\mathcal{L}\mathcal{Q}}\| \leq M_{\mathcal{Q}} e^{\omega_{\mathcal{Q}} t}$. By using Cauchy's formula for repeated integration, we bound the norm of the error (42) as

$$\begin{aligned} \|\mathbf{w}_0(t) - \mathbf{w}_0^p(t)\| &\leq \int_0^t \frac{(t-\sigma)^{p-1}}{(p-1)!} \int_0^\sigma \|\mathcal{P} e^{s\mathcal{L}} \mathcal{P} e^{(\sigma-s)\mathcal{L}\mathcal{Q}} (\mathcal{L}\mathcal{Q})^{p+1} \mathcal{L}\mathbf{u}_0\| ds d\sigma \\ &\leq \|\mathcal{P}\|^2 M M_{\mathcal{Q}} \|(\mathcal{L}\mathcal{Q})^{p+1} \mathcal{L}\mathbf{u}_0\| \int_0^t \frac{(t-\sigma)^{p-1}}{(p-1)!} \int_0^\sigma e^{s\omega} e^{(\sigma-s)\omega_{\mathcal{Q}}} ds d\sigma \\ &\leq C_1 \left(\prod_{j=1}^p \alpha_j \right) \underbrace{\int_0^t \frac{(t-\sigma)^{p-1}}{(p-1)!} \int_0^\sigma e^{s\omega} e^{(\sigma-s)\omega_{\mathcal{Q}}} ds d\sigma}_{f_p(t, \omega, \omega_{\mathcal{Q}})} \\ &= C_1 \left(\prod_{j=1}^p \alpha_j \right) f_p(t, \omega, \omega_{\mathcal{Q}}), \end{aligned} \quad (43)$$

where $C_1 = \|\mathcal{P}\|^2 \|\mathcal{L}\mathcal{Q}\mathcal{L}\mathbf{u}_0\| M M_{\mathcal{Q}}$ as before. The function $f_p(t, \omega, \omega_{\mathcal{Q}})$, may be bounded from above as

$$\begin{aligned} f_p(t, \omega, \omega_{\mathcal{Q}}) &\leq A_1 A_2 \int_0^t \frac{(t-\sigma)^{p-1}}{(p-1)!} \int_0^\sigma ds d\sigma \\ &= A_1 A_2 \frac{t^{p+1}}{(p+1)!}. \end{aligned}$$

Hence, we have

$$\|\mathbf{w}_0(t) - \mathbf{w}_0^p(t)\| \leq C_1 A_1 A_2 \left(\prod_{j=1}^p \alpha_j \right) \frac{t^{p+1}}{(p+1)!} = M_3^p(t).$$

□

Theorem 4 states that for a given dynamical system (represented by \mathcal{L}) and quantity of interest (represented by \mathcal{P}) the error bound $M_3^p(t)$ is strongly related to $\{\alpha_j\}$ which is ultimately determined by the initial condition x_0 . It turns out that by bounding $\{\alpha_j\}$, we can control $M_3^p(t)$, and therefore the overall error $\|\mathbf{w}_0(t) - \mathbf{w}_0^p(t)\|$. The following corollaries discuss sufficient conditions such that the error $\|\mathbf{w}_0(T) - \mathbf{w}_0^n(T)\|$ decays as we increase the differentiation order n for fixed time $T > 0$.

Corollary 4.1. (Uniform convergence of the H -model) *If $\{\alpha_j\}$ in Theorem 4 satisfy*

$$\alpha_j < \frac{j+1}{T}, \quad 1 \leq j \leq n, \quad (44)$$

for any fixed time $T > 0$, then there exists a sequence of constants $\delta_1 > \delta_2 > \cdots > \delta_n$ such that

$$\|\mathbf{w}_0(T) - \mathbf{w}_0^p(T)\| \leq \delta_p \quad 1 \leq p \leq n.$$

Proof. Evaluating (43) at any fixed (finite) time $T > 0$ yields

$$\begin{aligned}\|\mathbf{w}_0(T) - \mathbf{w}_0^p(T)\| &\leq C_2 \left(\prod_{j=1}^p \alpha_j \right) f_p(T, \omega, \omega_{\mathcal{Q}}) \leq C_2 \left(\prod_{j=1}^p \alpha_j \right) \frac{T^{p+1}}{(p+1)!}, \\ \|\mathbf{w}_0(T) - \mathbf{w}_0^{p+1}(T)\| &\leq C_2 \left(\prod_{j=1}^{p+1} \alpha_j \right) \frac{T^{p+2}}{(p+2)!},\end{aligned}$$

where $C_2 = C_2(T) = C_1 A_1 A_2$. If there exists $\delta_p \geq 0$ such that

$$\|\mathbf{w}_0(T) - \mathbf{w}_0^p(T)\| \leq C_2 \left(\prod_{j=1}^p \alpha_j \right) \frac{T^{p+1}}{(p+1)!} \leq \delta_p,$$

then there exist a δ_{p+1} such that

$$\|\mathbf{w}_0(T) - \mathbf{w}_0^{p+1}(T)\| \leq C_2 \left(\prod_{j=1}^p \alpha_j \right) \frac{T^{p+1}}{(p+1)!} \frac{\alpha_{p+1} T}{p+2} \leq \delta_{p+1} < \delta_p,$$

since $\alpha_{p+1} < (p+2)/T$. Moreover, the condition $\alpha_j < (j+1)/T$ holds for all $1 \leq j \leq n$. Therefore, we conclude that for any fixed time $T > 0$, there exists a sequence of constants $\delta_1 > \delta_2 > \dots > \delta_n$ such that $\|\mathbf{w}_0(T) - \mathbf{w}_0^p(T)\| \leq \delta_p$, where $1 \leq p \leq n$. □

Corollary 4.1 provides a sufficient condition for the error $\|\mathbf{w}_0(t) - \mathbf{w}_0^p(t)\|$ to decrease monotonically as we increase p in (36). A stronger condition that yields an asymptotically decaying error bound is given by the following Corollary.

Corollary 4.2. (Asymptotic convergence of the H -model) *If α_j in Theorem 4 satisfies*

$$\alpha_j < C, \quad 1 \leq j < +\infty \tag{45}$$

for some positive constant C , then for any fixed time $T > 0$, and arbitrary $\delta > 0$, there exists a constant $1 \leq p < +\infty$ such that for all $n > p$,

$$\|\mathbf{w}_0(T) - \mathbf{w}_0^n(T)\| \leq \delta.$$

Proof. By introducing the condition $\alpha_j < C$ in the proof of Theorem 4 we obtain

$$\|\mathbf{w}_0(T) - \mathbf{w}_0^p(T)\| \leq C_2 \left(\prod_{j=1}^p \alpha_j \right) \frac{T^{p+1}}{(p+1)!} \leq C_2 T \frac{(CT)^p}{(p+1)!} \quad \text{for all } 1 < p < +\infty.$$

The limit

$$\lim_{p \rightarrow +\infty} C_2 T \frac{(CT)^p}{(p+1)!} = 0$$

allows us to conclude that there exists a constant $1 < p < +\infty$ such that for all $n > p$, $\|\mathbf{w}_0(T) - \mathbf{w}_0^n(T)\| \leq \delta$. □

An interesting consequence of Corollary 4.2 is the existence of a *convergence barrier*, i.e., a “hump” in the error plot $\|\mathbf{w}_0(T) - \mathbf{w}_0^p(T)\|$ versus p generated by the H -model. While Corollary 4.2 only shows that behavior for an upper bound of the error, not directly the error itself, the feature is often found in the actual errors associated with numerical methods based on these ideas. The following Corollary shows that the requirements on $\{\alpha_j\}$ can be dropped (we still need $\alpha_j < +\infty$) if we consider relatively short integration times T .

Corollary 4.3. (Short-time convergence of the H -model) *For any integer n for which $\alpha_j < \infty$ for $1 \leq j \leq n$, and any sequence of constants $\delta_1 > \delta_2 > \dots > \delta_n > 0$, there exists a fixed time $T > 0$ such that*

$$\|\mathbf{w}_0(T) - \mathbf{w}_0^p(T)\| \leq \delta_p$$

for $1 \leq p \leq n$.

Proof. Since $\alpha_j < +\infty$, we can choose $C = \max_{1 \leq j \leq n} \alpha_j$. By following the same steps we used in the proof of Theorem 4, we conclude that, for

$$T \leq \frac{1}{C} \min_{1 \leq p \leq n} \left[\frac{C(p+1)!}{C_2} \delta_p \right]^{\frac{1}{p+1}},$$

the errors satisfy

$$\|\mathbf{w}_0(T) - \mathbf{w}_0^p(T)\| \leq C_2 \left(\prod_{j=1}^p \alpha_j \right) \frac{T^{p+1}}{(p+1)!} \leq \frac{C_2 (CT)^{p+1}}{C (p+1)!} \leq \delta_p$$

as desired, for all $1 \leq p \leq n$. □

Corollary 4.1 and Corollary 4.2 provide sufficient conditions for the error $\|\mathbf{w}_0(T) - \mathbf{w}_0^n(T)\|$ generated by the H -model to decay as we increase the truncation order n . However, we still need to answer the important question of whether the H -model actually provides accurate results for a given nonlinear dynamics (\mathcal{L}), quantity of interest (\mathcal{P}) and initial state x_0 . Corollary 4.3 provides a partial answer to this question by showing that, at least in the short time period, condition (44) is always satisfied (assuming that $\{\alpha_j\}$ are finite). This guarantees the short-time convergence of the H -model for any reasonably smooth nonlinear dynamical system and almost any observable. However, for longer integration times T , convergence of the H -model for arbitrary nonlinear dynamical systems cannot be established in general, which means that we need to proceed on a case-by-case basis by applying Theorem 4 or by checking whether the hypotheses of Corollary 4.1 or Corollary 4.2 are satisfied. On the other hand, convergence of the H -model can be established for any finite integration time in the case of linear dynamical systems [100]. From a practical viewpoint, the implementation of the H -model requires computing $(\mathcal{LQ})^n \mathcal{L}x_0$ to high-order in n . This is not straightforward if the dynamical systems is nonlinear. However, for linear systems such terms can be easily computed (see section 3.4).

3.3.2 The H_t -model

The H_t -model is obtained by solving the system (36) with $\mathbf{w}_n^{en}(t)$ approximated using Chorin’s t -model [18] (see equation (39)). Convergence analysis can be performed by using the mathematical methods we employed for the proofs of the H -model. Note that the classical t -model is equivalent to a zeroth-order H_t -model.

Theorem 5. (Accuracy of the H_t -model) Let $e^{t\mathcal{L}}$ and $e^{t\mathcal{L}\mathcal{Q}}$ be strongly continuous semigroups with upper bounds $\|e^{t\mathcal{L}}\| \leq M e^{t\omega}$ and $\|e^{t\mathcal{L}\mathcal{Q}}\| \leq M_{\mathcal{Q}} e^{t\omega_{\mathcal{Q}}}$, and let $T > 0$ be a fixed integration time. For some fixed n , let

$$\alpha_j = \frac{\|(\mathcal{L}\mathcal{Q})^{j+1}\mathcal{L}\mathbf{u}_0\|}{\|(\mathcal{L}\mathcal{Q})^j\mathcal{L}\mathbf{u}_0\|}, \quad 1 \leq j \leq n. \quad (46)$$

Then, for any $1 \leq p \leq n$ and all $t \in [0, T]$, we have

$$\|\mathbf{w}_0(t) - \mathbf{w}_0^p(t)\| \leq M_6^p(t) \leq M_6^p(T),$$

where

$$M_6^p(t) = C_4 \left(\prod_j^p \alpha_j \right) \frac{t^{p+1}}{(p+1)!}, \quad C_4 = \left[C_1 A_1 A_2 + \frac{C_1}{M_{\mathcal{Q}} A_3} \right], \quad A_3 = \max_{s \in [0, T]} s e^{s\omega} = \begin{cases} 1 & \omega \leq 0, \\ e^{T\omega} & \omega > 0 \end{cases},$$

and C_1, A_1, A_2 are as before.

Proof. For p -th order H_t -model, the difference between the memory term w_0 and its approximation w_0^p is

$$\begin{aligned} \mathbf{w}_0(t) - \mathbf{w}_0^p(t) &= \int_0^t \int_0^{\tau_p} \cdots \int_0^{\tau_2} \left[\int_0^{\tau_1} \mathcal{P} e^{s\mathcal{L}} \mathcal{P} e^{(\tau_1-s)\mathcal{L}\mathcal{Q}} (\mathcal{L}\mathcal{Q})^{p+1} \mathcal{L}\mathbf{u}_0 ds - \right. \\ &\quad \left. \tau_1 \mathcal{P} e^{\tau_1 \mathcal{L}} \mathcal{P} (\mathcal{L}\mathcal{Q})^{p+1} \mathcal{L}\mathbf{u}_0 \right] d\tau_1 \cdots d\tau_p. \end{aligned} \quad (47)$$

Using Cauchy's formula for repeated integration, we can bound the norm of the second term in (47) as

$$\begin{aligned} \left\| \int_0^t \frac{(t-\sigma)^{p-1}}{(p-1)!} \sigma \mathcal{P} e^{\sigma \mathcal{L}} \mathcal{P} (\mathcal{L}\mathcal{Q})^{p+1} \mathcal{L}\mathbf{u}_0 d\sigma \right\| &\leq \int_0^t \frac{(t-\sigma)^{p-1}}{(p-1)!} \|\sigma \mathcal{P} e^{\sigma \mathcal{L}} \mathcal{P} (\mathcal{L}\mathcal{Q})^{p+1} \mathcal{L}\mathbf{u}_0\| d\sigma \\ &\leq \|\mathcal{P}\|^2 M \|(\mathcal{L}\mathcal{Q})^{p+1} \mathcal{L}\mathbf{u}_0\| \underbrace{\int_0^t \frac{(t-\sigma)^{p-1}}{(p-1)!} \sigma e^{\sigma\omega} d\sigma}_{g_p(t, \omega)} \\ &= \frac{C_1}{M_{\mathcal{Q}}} \left(\prod_{j=1}^p \alpha_j \right) g_p(t, \omega), \end{aligned} \quad (48)$$

where $C_1 = \|\mathcal{P}\|^2 \|\mathcal{L}\mathcal{Q}\mathcal{L}\mathbf{u}_0\| M M_{\mathcal{Q}}$ as before. The function $g_p(t, \omega)$, may be bounded from above as

$$g_p(t, \omega) \leq A_3 \int_0^t \frac{(t-\sigma)^{p-1}}{(p-1)!} \sigma d\sigma = A_3 \frac{t^{p+1}}{(p+1)!}, \quad A_3 = \max_{s \in [0, T]} e^{s\omega} = \begin{cases} 1 & \omega \leq 0 \\ e^{T\omega} & \omega > 0 \end{cases}.$$

By applying the triangle inequality to (47), and taking (48) into account, we obtain

$$\|\mathbf{w}_0(t) - \mathbf{w}_0^p(t)\| \leq C_1 A_1 A_2 \left(\prod_{j=1}^p \alpha_j \right) \frac{t^{p+1}}{(p+1)!} + \frac{C_1}{M_{\mathcal{Q}}} A_3 \left(\prod_{j=1}^p \alpha_j \right) \frac{t^{p+1}}{(p+1)!} = M_6^p(t).$$

□

One can see that the upper bounds $M_6^p(t)$ and $M_3^p(t)$ (see Theorem 4) share the same structure, the only difference being the constant out front. Hence by changing C_2 to C_4 , we can prove of a series of corollaries similar to 4.1, 4.2, and 4.3. In summary, what holds for the H -model also holds for the H_t -model. For the sake of brevity, we omit the statement and proofs of those corollaries.

3.4 Linear dynamical systems

The upper bounds we obtained above are not easily computable for general nonlinear systems and infinite-rank projections, e.g., Chorin's projection (8). However, if the dynamical system is linear, then such upper bounds are explicitly computable and convergence of the H -model can be established for linear phase space functions in any finite integration time T . To this end, consider the linear system $\dot{\mathbf{x}} = \mathbf{A}\mathbf{x}$ with random initial condition $x(0)$ sampled from the joint probability density function

$$\rho_0(\mathbf{x}_0) = \delta(x_{01} - x_1(0)) \prod_{j=2}^N \rho_{0j}(x_{0j}). \quad (49)$$

In other words, the initial condition for the quantity of interest $u(\mathbf{x}) = x_1(t)$ is set to be deterministic, while all other variables x_2, \dots, x_N are zero-mean and statistically independent at $t = 0$. Here we also assume for simplicity that ρ_{0j} ($j = 2, \dots, N$) are i.i.d. standard normal distributions. Observe that the Liouville operator associated with the linear system $\dot{\mathbf{x}} = \mathbf{A}\mathbf{x}$ is

$$\mathcal{L} = \sum_{i=1}^N \sum_{j=1}^N A_{ij} x_j \frac{\partial}{\partial x_i}, \quad (50)$$

where A_{ij} are the entries of the matrix A . If we choose observable $u(t) = x_1(t)$, then Chorin's projection operator (10) yields the evolution equation for the conditional expectation $\mathbb{E}[x_1(t)|x_1(0)]$, i.e., the *conditional mean path* (12), which can be explicitly written as

$$\frac{d}{dt} \mathbb{E}[x_1|x_1(0)] = A_{11} \mathbb{E}[x_1|x_1(0)] + w_0(t), \quad (51)$$

where $A_{11} = \mathcal{P}\mathcal{L}x_1(0)$ is the first entry of the matrix A , w_0 represents the memory integral (31). Next, we explicitly compute the upper bounds for the memory growth and the error in the H -model for this system. To this end, we first notice that the domain of the Liouville operator can be restricted to the linear space

$$V = \text{span}\{x_1, \dots, x_N\}. \quad (52)$$

In fact, V is invariant under \mathcal{L} , \mathcal{P} and \mathcal{Q} , i.e., $\mathcal{L}V \subseteq V$, $\mathcal{P}V \subseteq V$ and $\mathcal{Q}V \subseteq V$. These operators have the following matrix representations

$$\mathcal{L} \simeq \mathbf{A}^T \simeq \begin{bmatrix} a_{11} & \mathbf{b}^T \\ \mathbf{a} & \mathbf{M}_{11}^T \end{bmatrix}, \quad \mathcal{P} \simeq \begin{bmatrix} 1 & 0 & \dots & 0 \\ 0 & 0 & \dots & 0 \\ \vdots & \vdots & \ddots & \vdots \\ 0 & 0 & \dots & 0 \end{bmatrix}, \quad \mathcal{Q} \simeq \begin{bmatrix} 0 & 0 & \dots & 0 \\ 0 & 1 & \dots & 0 \\ \vdots & \vdots & \ddots & \vdots \\ 0 & 0 & \dots & 1 \end{bmatrix},$$

where \mathbf{M}_{11} is the minor of the matrix of A obtained by removing the first column and the first row, while

$$\mathbf{a} = [A_{12} \dots A_{1N}]^T, \quad \mathbf{b}^T = [A_{21} \dots A_{N1}]. \quad (53)$$

Therefore,

$$\mathcal{L}\mathcal{Q} \simeq \begin{bmatrix} 0 & \mathbf{b}^T \\ 0 & \mathbf{M}_{11}^T \end{bmatrix}, \quad \mathcal{L}(\mathcal{Q}\mathcal{L})^n x_1(0) \simeq \begin{bmatrix} \mathbf{b}^T (\mathbf{M}_{11}^T)^{n-1} \mathbf{a} \\ (\mathbf{M}_{11}^T)^n \mathbf{a} \end{bmatrix}. \quad (54)$$

At this point, we set $x_{01} = x_1(0)$ and

$$q(t, x_{01}, \tilde{\mathbf{x}}_0) = \int_0^t e^{s\mathcal{L}} \mathcal{P} \mathcal{L} e^{(t-s)\mathcal{Q}} \mathcal{L} \mathcal{Q} x_{01} ds.$$

Since $\tilde{\mathbf{x}}_0 = (x_2(0), \dots, x_N(0))$ is random, $q(t, x_{01}, \tilde{\mathbf{x}}_0)$ is a random variable. By using Jensen's inequality $[\mathbb{E}(X)]^2 \leq \mathbb{E}(X^2)$, we have the following L^∞ estimate

$$\|(\mathcal{P}q)(t, x_{01})\|_{L^\infty} \leq \|q(t, x_{01}, \cdot)\|_{L_{\rho_0}^2}. \quad (55)$$

On the other hand, we have

$$\|e^{t\mathcal{L}}\|_{L_{\rho_0}^2(V)} \leq \|e^{t\mathcal{L}}\|_{L_{\rho_0}^2} \leq e^{t\omega}, \quad \omega = -\frac{1}{2} \inf \operatorname{div}_{\rho_0}(\mathbf{A}\mathbf{x}). \quad (56)$$

For linear dynamical systems, both $\|\cdot\|_{L_{\rho_0}^2(V)}$ and $\|\cdot\|_{L_{\rho_0}^2}$ upper bounds can be used to estimate the norm of the semigroup $e^{t\mathcal{L}}$. However, for the semigroup $e^{t\mathcal{L}\mathcal{Q}}$, we can only obtain the explicit form of the $\|\cdot\|_{L_{\rho_0}^2(V)}$ bound, which is given by the following perturbation theorem [28]:

$$\|e^{t\mathcal{L}\mathcal{Q}}\|_{L_{\rho_0}^2(V)} \leq e^{t\omega_{\mathcal{Q}}}, \quad \text{where} \quad \omega_{\mathcal{Q}} = \omega + \sqrt{A_{11}^2 + \sum_{i=2}^N A_{1i}^2 \frac{\langle x_i^2(0) \rangle_{\rho_0}}{x_1^2(0)}} \geq \omega + \|\mathcal{L}\mathcal{P}\|_{L_{\rho_0}^2(V)}. \quad (57)$$

Memory growth It is straightforward at this point to compute the upper bound of the memory growth obtained in Theorem 1. Since $\|\mathcal{P}\|_{L_{\rho_0}^2} = \|\mathcal{Q}\|_{L_{\rho_0}^2} = 1$ (\mathcal{P} and \mathcal{Q} are orthogonal projections relative to ρ_0), we have the following result

$$|w_0(t)| \leq \|\mathcal{L}\mathcal{Q}\mathcal{L}x_1(0)\| \frac{e^{t\omega} - e^{t\omega_{\mathcal{Q}}}}{\omega - \omega_{\mathcal{Q}}} = \sqrt{(\mathbf{b}^T \mathbf{a})^2 x_1^2(0) + \|\mathbf{\Lambda}_{x_{i+1}(0)} \mathbf{M}_{11}^T \mathbf{a}\|_2^2} \frac{e^{t\omega} - e^{t\omega_{\mathcal{Q}}}}{\omega - \omega_{\mathcal{Q}}}, \quad (58)$$

where $\mathbf{\Lambda}_{x_{i+1}(0)}$ is a $(N-1) \times (N-1)$ diagonal matrix with $\Lambda_{ii} = \langle x_{i+1}(0) \rangle_{\rho_0}$, and $\|\cdot\|_2$ is the vector 2-norm.

Accuracy of the H -model We are interested in computing the upper bound of the approximation error generated by the H -model (see section 3.3.1 - Theorem 4). By using the matrix representation of \mathcal{L} , \mathcal{P} and \mathcal{Q} , the n -th order H -model MZ equation (51) for linear system can be explicitly written as

$$\begin{cases} \frac{d}{dt} \mathbb{E}[x_1|x_1(0)] = A_{11} \mathbb{E}[x_1|x_1(0)] + w_0^n(t) & \text{(MZ equation),} \\ \frac{dw_j^n(t)}{dt} = \mathbf{b}^T (\mathbf{M}_{11}^T)^j \mathbf{a}^T \mathbb{E}[x_1|x_1(0)] + w_{j+1}^n(t), & j = 0, 1, \dots, n-1, \\ \frac{dw_n^n(t)}{dt} = \mathbf{b}^T (\mathbf{M}_{11}^T)^n \mathbf{a}^T \mathbb{E}[x_1|x_1(0)], \end{cases} \quad (59)$$

where \mathbf{M}_{11} , \mathbf{a} and \mathbf{b} are defined as before (see equation (53)). The upper bound for the memory term approximation error is explicitly obtained as

$$\begin{aligned} |w_0(t) - w_0^n(t)| &\leq A_1 A_2 \|\mathcal{L}(\mathcal{Q}\mathcal{L})^n x_1(0)\| \frac{t^{n+1}}{(n+1)!} \\ &= A_1 A_2 \sqrt{[\mathbf{b}^T (\mathbf{M}_{11}^T)^n \mathbf{a}]^2 x_1^2(0) + \|\mathbf{\Lambda}_{x_{i+1}(0)} (\mathbf{M}_{11}^T)^{n+1} \mathbf{a}\|_2^2} \frac{t^{n+1}}{(n+1)!} \end{aligned} \quad (60)$$

where A_1, A_2 are defined in (41), while ω and $\omega_{\mathcal{Q}}$ are given in (56) and (57), respectively. Note that the error bound (60) is slightly different from the one we obtained in Theorem 4. The reason is that here we choose to bound $\|\mathcal{L}(\mathcal{Q}\mathcal{L})^n u_0\|$, instead of the quotient $\alpha_n = \|\mathcal{L}(\mathcal{Q}\mathcal{L})^{n+1} u_0\|/\|\mathcal{L}(\mathcal{Q}\mathcal{L})^n u_0\|$. For each fixed integration time T , the upper bound (60) goes to zero as we send n to infinity, i.e.,

$$\lim_{n \rightarrow +\infty} |w_0(T) - w_0^n(T)| = 0.$$

This means that the H -model converges for all linear dynamical systems with observables in the linear space (52).

3.5 Memory estimates for finite-rank projections and Hamiltonian systems

The semigroup estimates we obtained in previous sections allow us to compute explicitly an *a priori* estimate of the memory kernel in the Mori-Zwanzig equation if we employ *finite-rank* projections, e.g., Mori's projection operator (15). Hereafter we outline the procedure to obtain such estimate for Hamiltonian dynamical systems. We begin by recalling that, in general, Hamiltonian systems are necessarily divergence-free, i.e.,

$$\operatorname{div}_{\rho_{eq}}(\mathbf{F}) = 0. \quad (61)$$

Here, $\mathbf{F}(\mathbf{x})$ is the velocity field at the right hand side of (1), while $\rho_{eq} = e^{-\beta\mathcal{H}}/Z$ is the canonical Gibbs distribution. Equation (61) can be easily obtained by noticing that

$$\begin{aligned} \operatorname{div}_{\rho_{eq}}(\mathbf{F}) &= e^{\beta\mathcal{H}} \nabla \cdot \left(e^{-\beta\mathcal{H}} \mathbf{F} \right), \\ &= e^{\beta\mathcal{H}} \sum_{i=1}^N \left(\frac{\partial}{\partial q_i} \left[e^{-\beta\mathcal{H}} \frac{\partial \mathcal{H}}{\partial p_i} \right] - \frac{\partial}{\partial p_i} \left[e^{-\beta\mathcal{H}} \frac{\partial \mathcal{H}}{\partial q_i} \right] \right), \\ &= 0. \end{aligned}$$

The Koopman semigroup generated by a Hamiltonian dynamical system is always a *contraction* in the $L^2_{\rho_{eq}}$ norm, i.e.,

$$\|e^{t\mathcal{L}}\|_{L^2_{\rho_{eq}}} \leq 1. \quad (62)$$

Moreover, the MZ equation (7) with a finite-rank projection \mathcal{P} of the form (15) can be reduced to the following Volterra integro-differential equation

$$\frac{d}{dt} \mathcal{P}u_i(t) = \sum_{j=1}^M \Omega_{ij} \mathcal{P}u_j(t) - \sum_{j=1}^M \int_0^t K_{ij}(t-s) \mathcal{P}u_j(s) ds, \quad i = 1, \dots, M \quad (63)$$

where

$$G_{ij} = \langle u_i, u_j \rangle_{eq}, \quad (64a)$$

$$\Omega_{ij} = \sum_{k=1}^M (G^{-1})_{jk} \langle u_k, \mathcal{L}u_i \rangle_{eq}, \quad (64b)$$

$$K_{ij}(t-s) = - \sum_{k=1}^M (G^{-1})_{jk} \langle \mathcal{Q}\mathcal{L}u_k, e^{(t-s)\mathcal{Q}\mathcal{L}} \mathcal{Q}\mathcal{L}u_i \rangle_{eq}. \quad (64c)$$

Equation (63) is often called generalized Langevin equation (GLE) [20, 79] for the projected quantity of interest $u_i(t)$. To derive (64a)-(64c), we used the fact that \mathcal{L} is skew-adjoint and \mathcal{Q} is self-adjoint with respect to the $L^2_{\rho_{eq}}$ inner product, and that $\mathcal{Q}^2 = \mathcal{Q}$. Next, define the temporal-correlation matrix

$$C_{ij}(t) = \langle u_j(0), u_i(t) \rangle_{eq} = \langle u_j(0), \mathcal{P}u_i(t) \rangle_{eq}. \quad (65)$$

By applying $\langle u_j, (\cdot) \rangle_{eq}$ to both sides of equation (63), we obtain the following exact evolution equation for $C_{ij}(t)$

$$\frac{dC_{ij}}{dt} = \sum_{k=1}^M \Omega_{ik} C_{kj} - \sum_{k=1}^M \int_0^t K_{ik}(t-s) C_{kj}(s) ds. \quad (66)$$

Moreover, if we employ a one-dimensional Mori's basis, i.e., $M = 1$, then we obtain the simplified equation

$$\frac{dC(t)}{dt} = \Omega C(t) - \int_0^t K(t-s) C(s) ds. \quad (67)$$

where $C(t) = \langle u(0), u(t) \rangle_{eq}$. The main difficulty in solving the GLE (66) (or (67)) lies in computing the memory kernel $K_{ij}(t)$. Hereafter we prove that such memory kernels can be uniformly bounded by a computable quantity that *depends only on the initial condition of the system*. For the sake of simplicity, we will focus on the one-dimensional GLE (67).

Theorem 6. *The memory kernel $K(t)$ in the one-dimensional GLE (66) is uniformly bounded as*

$$|K(t)| \leq \frac{\|\dot{u}(0)\|_{L^2_{\rho_{eq}}}^2}{\|u(0)\|_{L^2_{\rho_{eq}}}^2} \quad \forall t \geq 0. \quad (68)$$

Proof. From the second-fluctuation dissipation theorem (64c), the memory kernel $K(t)$ satisfies

$$|K(t)| = \left| \frac{\langle e^{t\mathcal{Q}\mathcal{L}} \mathcal{Q}\mathcal{L}u(0), \mathcal{Q}\mathcal{L}u(0) \rangle_{eq}}{\langle u(0), u(0) \rangle_{eq}} \right| \leq \|e^{t\mathcal{Q}\mathcal{L}} \mathcal{Q}\|_{L^2_{\rho_{eq}}} \frac{\|\mathcal{L}u(0)\|_{L^2_{\rho_{eq}}}^2}{\|u(0)\|_{L^2_{\rho_{eq}}}^2} = \|e^{t\mathcal{Q}\mathcal{L}} \mathcal{Q}\|_{L^2_{\rho_{eq}}} \frac{\|\dot{u}(0)\|_{L^2_{\rho_{eq}}}^2}{\|u(0)\|_{L^2_{\rho_{eq}}}^2}$$

On the other hand, we know that the semigroup $e^{t\mathcal{Q}\mathcal{L}\mathcal{Q}}$ is contractive, i.e. $\|e^{t\mathcal{Q}\mathcal{L}\mathcal{Q}}\|_{L^2_{\rho_{eq}}} \leq 1$. Since \mathcal{Q} is an orthogonal projection with respect to ρ_{eq} , we have $\|e^{t\mathcal{Q}\mathcal{L}} \mathcal{Q}\|_{L^2_{\rho_{eq}}} \leq \|\mathcal{Q}\|_{L^2_{\rho_{eq}}} \|e^{t\mathcal{Q}\mathcal{L}\mathcal{Q}}\|_{L^2_{\rho_{eq}}} \leq 1$. This yields

$$|K(t)| \leq \|e^{t\mathcal{Q}\mathcal{L}} \mathcal{Q}\|_{L^2_{\rho_{eq}}} \frac{\|\dot{u}(0)\|_{L^2_{\rho_{eq}}}^2}{\|u(0)\|_{L^2_{\rho_{eq}}}^2} \leq \frac{\|\dot{u}(0)\|_{L^2_{\rho_{eq}}}^2}{\|u(0)\|_{L^2_{\rho_{eq}}}^2}.$$

□

Theorem 6 provides an *a priori* and easily computable upper bound for the memory kernel defining the dynamics of any quantity of interest u_1 that is initially in the Gibbs canonical ensemble $\rho_{eq} = e^{-\beta\mathcal{H}}/Z$. In section 5.7, we will calculate the upper bound (68) analytically and compare it with the exact memory kernel we obtain in prototype linear and nonlinear Hamiltonian systems.

Next, we provide simple numerical examples of the MZ memory approximation analysis we discussed so far. Specifically, we study Hamiltonian systems (linear and nonlinear) with finite-rank projections (Mori's projection), and non-Hamiltonian systems with infinite-rank projections (Chorin's projection). In both cases we demonstrate the accuracy of the *a priori* memory estimation method we presented in section 3.5 and section 3.4. We also compute the solution to the MZ equation for non-Hamiltonian systems with the t -model, the H -model and the H_t -model.

3.6 Hamiltonian dynamical systems with finite-rank projections

In this section we consider dimension reduction in linear and nonlinear Hamiltonian dynamical systems with finite-rank projection. In particular, we consider Mori's projection (15) and study the MZ equation for the temporal auto-correlation function of a scalar quantity of interest.

3.6.1 Harmonic chains of oscillators

Consider a one-dimensional chain of harmonic oscillators. This is a simple but illustrative example of a linear Hamiltonian dynamical system which has been widely studied in statistical mechanics, mostly in relation with the microscopic theory of Brownian motion [6, 39, 29]. The Hamiltonian of the system can be written as

$$\mathcal{H}(p, q) = \frac{1}{2m} \sum_{i=1}^N p_i^2 + \frac{k}{2} \sum_{\substack{i,j=0 \\ i < j}}^{N+1} (q_i - q_j)^2, \quad (69)$$

where q_i and p_i are, respectively, the displacement and momentum of the i -th particle, m is the mass of the particles (assumed constant throughout the network), and k is the elasticity constant that modulates the intensity of the quadratic interactions. We set fixed boundary conditions at the endpoints of the chain, i.e., $q_0(t) = q_{N+1}(t) = 0$ and $p_0(t) = p_{N+1}(t) = 0$ (particles are numbered from left to right) and $m = k = 1$. The Hamilton's equations are

$$\frac{dq_i}{dt} = \frac{\partial \mathcal{H}}{\partial p_i}, \quad \frac{dp_i}{dt} = -\frac{\partial \mathcal{H}}{\partial q_i}, \quad (70)$$

which can be written in a matrix-vector form as

$$\begin{bmatrix} \dot{p} \\ \dot{q} \end{bmatrix} = \begin{bmatrix} \mathbf{0} & kB - kD \\ \mathbf{I}/m & \mathbf{0} \end{bmatrix} \begin{bmatrix} p \\ q \end{bmatrix} \quad (71)$$

where B is the adjacency matrix of the chain and D is the degree matrix (see [8]). Note that (71) is a linear dynamical system. We are interested in the velocity auto-correlation function of a tagged oscillator, say the one at location $j = 1$. Such auto-correlation function is defined as

$$C_{p_1}(t) = \frac{\langle p_1(0)p_1(t) \rangle_{eq}}{\langle p_1(0)p_1(0) \rangle_{eq}}, \quad (72)$$

where the average is with respect to the Gibbs canonical distribution $\rho_{eq} = e^{-\beta \mathcal{H}}/Z$. It was shown in [39] that $C_{p_1}(t)$ can be obtained analytically by employing Lee's continued fraction method. The result is the well-known $J_0 - J_4$ solution

$$C_{p_1}(t) = J_0(2t) - J_4(2t), \quad (73)$$

where $J_i(t)$ is the i -th Bessel function of the first kind. On the other hand, the Mori-Zwanzig equation derived by the following Mori's projection

$$\mathcal{P}(\cdot) = \frac{\langle (\cdot), p_1(0) \rangle_{eq}}{\langle p_1(0), p_1(0) \rangle_{eq}} p_1(0) \quad (74)$$

yields the following GLE for $C_{p_1}(t)$

$$\frac{dC_{p_1}(t)}{dt} = \Omega_{p_1} C_{p_1}(t) - \int_0^t K(s) C_{p_1}(t-s) ds. \quad (75)$$

Here,

$$\Omega_{p_1} = \frac{\langle \mathcal{L}p_1(0), p_1(0) \rangle_{eq}}{\langle p_1(0), p_1(0) \rangle_{eq}} = 0$$

since $\langle p_i(0), q_j(0) \rangle_{eq} = 0$, while $K(t)$ is the MZ memory kernel. For the $J_0 - J_4$ solution, it is possible to derive the memory kernel $K(t)$ analytically. To this end, we simply insert (73) into (75) and apply the Laplace transform

$$\mathcal{L}[\cdot](s) = \int_0^\infty (\cdot) e^{-st} dt$$

to obtain

$$\hat{K}(s) = -s + \frac{1}{\hat{C}(s)}, \quad (76)$$

where $\hat{C}(s) = \mathcal{L}[C_{p_1}(t)]$ and $\hat{K}(s) = \mathcal{L}[K(t)]$. The inverse Laplace transform of (76) can be computed analytically as

$$K(t) = \frac{J_1(2t)}{t} + 1. \quad (77)$$

With $K(t)$ available, we can verify the memory estimated we derived in Theorem 6. To this end,

$$|K(t)| \leq \frac{\|\dot{p}_1(0)\|_{L^2_{\rho_{eq}}}^2}{\|p_1(0)\|_{L^2_{\rho_{eq}}}^2} = \frac{\|q_2(0) - 2q_1(0)\|_{L^2_{\rho_{eq}}}^2}{\|p_1(0)\|_{L^2_{\rho_{eq}}}^2} = 2. \quad (78)$$

Here we used the exact solution of the velocity auto-correlation function and displacement auto-correlation function of the fixed-end harmonic chain given by (see [39])

$$\langle p_i(0), p_j(0) \rangle_{eq} = \frac{k_B T}{\pi} \int_0^\pi \sin(ix) \sin(jx) dx, \quad \langle q_i(0), q_j(0) \rangle_{eq} = \frac{k_B T}{\pi} \int_0^\pi \frac{\sin(ix) \sin(jx)}{4 \sin^2(x/2)} dx.$$

In Figure 1 we plot the absolute value of the memory kernel $K(t)$ together with the theoretical bound (78). It is seen that the upper bound we obtain in this case is of the same order of magnitude as the memory kernel.

3.6.2 Chorin-Hald system

In this section, we study the Hamiltonian system studied by Chorin *et al.* in [16, 18]. The Hamiltonian function is defined as

$$\mathcal{H}(p, q) = \frac{1}{2}(q_1^2 + p_1^2 + q_2^2 + p_2^2 + q_1^2 q_2^2), \quad (79)$$

while the corresponding Hamilton's equations of motion are

$$\begin{cases} \dot{q}_1 &= p_1 \\ \dot{p}_1 &= -q_1(1 + q_2^2) \\ \dot{q}_2 &= p_2 \\ \dot{p}_2 &= -q_2(1 + q_1^2) \end{cases} \quad (80)$$

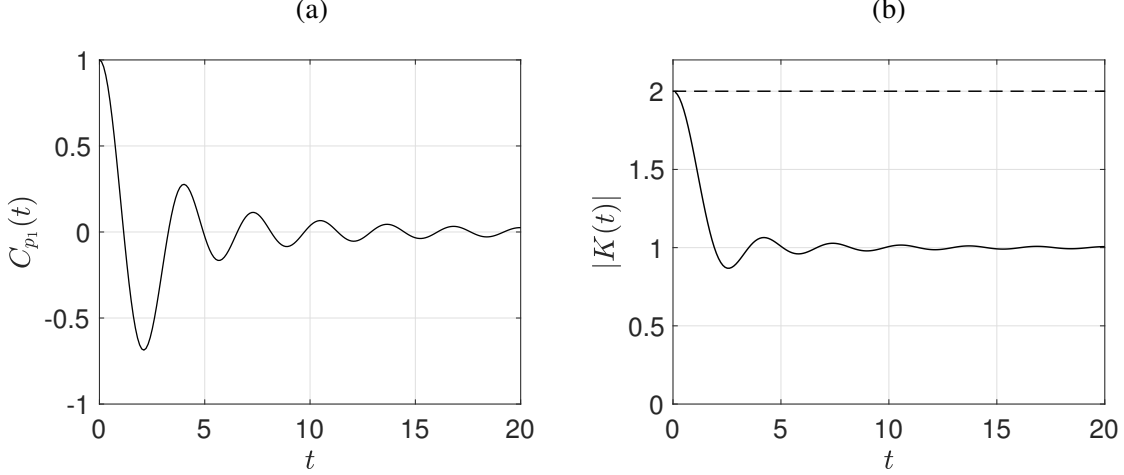


Figure 1: Harmonic chain of oscillators. (a) Velocity auto-correlation function $C_{p_1}(t)$ and (b) memory kernel $K(t)$ of the corresponding MZ equation. It is seen that our theoretical estimate (78) (dashed line) correctly bounds the MZ memory kernel. Note that the upper bound we obtain is of the same order of magnitude as the memory kernel.

We assume that the initial state is distributed according to canonical Gibbs distribution $\rho_{eq} = e^{-\mathcal{H}(p,q)}/Z$. The partition function Z is given by

$$Z = e^{1/4}(2\pi)^{3/2}K_0\left(\frac{1}{4}\right), \quad (81)$$

where $K_0(t)$ is the modified Bessel function of the second kind. We aim to study the properties of the autocorrelation function of the first component q_1 , which is defined as

$$C_{q_1}(t) = \frac{\langle q_1(0), q_1(t) \rangle_{eq}}{\langle q_1(0), q_1(0) \rangle_{eq}}.$$

Obviously, $C_{q_1}(0) = 1$. The evolution equation for $C_{q_1}(t)$ is obtained by using the MZ formulation with the Mori's projection

$$\mathcal{P}(\cdot) = \frac{\langle (\cdot), q_1(0) \rangle_{eq}}{\langle q_1(0), q_1(0) \rangle_{eq}} q_1(0). \quad (82)$$

This yields the GLE

$$\frac{dC_{q_1}(t)}{dt} = \Omega_{q_1} C_{q_1}(t) - \int_0^t K(s) C_{q_1}(t-s) ds. \quad (83)$$

The streaming term $\Omega_{q_1} C_{q_1}(t)$ is again identically zero since

$$\Omega_{q_1} = \frac{\langle \mathcal{L}q_1(0), q_1(0) \rangle_{eq}}{\langle q_1(0), q_1(0) \rangle_{eq}} = 0.$$

Theorem 6 provides the following computable upper bound for the modulus of $K(t)$

$$|K(t)| \leq \frac{\|\dot{q}_1(0)\|_{L^2_{\rho_{eq}}}^2}{\|q_1(0)\|_{L^2_{\rho_{eq}}}^2} = \frac{\|p_1(0)\|_{L^2_{\rho_{eq}}}^2}{\|q_1(0)\|_{L^2_{\rho_{eq}}}^2} = \frac{e^{1/4}K_0(1/4)}{\sqrt{\pi}U(1/2, 0, 1/2)} \approx 1.39786, \quad (84)$$

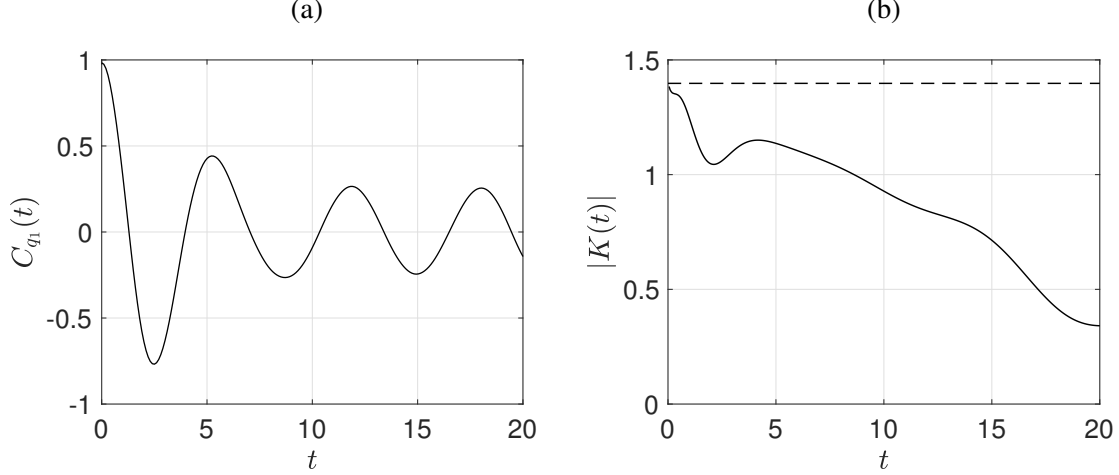


Figure 2: Hald Hamiltonian system (80). (a) Autocorrelation function of the displacement $q_1(t)$ and (b) memory kernel of the governing MZ equation. Here $C_{q_1}(t)$ is computed by Markov chain Monte-Carlo (MCMC) while $K(t)$ is determined by inverting numerically the Laplace transform in (85) with the Talbot algorithm. It is seen that the theoretical upper bound (84) (dashed line) is of the same order of magnitude as the memory kernel.

where $U(a, b, y)$ is the confluent hypergeometric function of the second kind. In Figure 2(a) we plot the correlation function $C_{q_1}(t)$ we obtained by sampling (80) and then averaging over all realizations. The samples of the initial condition are generated from the Gibbs equilibrium distribution by using Markov Chain Monte Carlo (MCMC). In Figure 2(b) we plot the memory kernel $K(t)$ we computed numerically based on $C_{q_1}(t)$. To compute such kernel, we inverted numerically the Laplace transform of (83), i.e.,

$$K(t) = \mathcal{L}^{-1} \left[-s + \frac{1}{\hat{C}(s)} \right], \quad (85)$$

where $\hat{C}(s) = \mathcal{L}[C_{q_1}(t)]$. In practice, we replaced $C_{q_1}(t)$ within the time interval $[0, 20]$ with a high-order polynomial interpolant at Gauss-Chebyshev-Lobatto nodes, computed the Laplace transform of such polynomial analytically, and then computed the inverse Laplace transform (85) numerically with the Talbot algorithm [1].

3.7 Non-Hamiltonian systems with infinite-rank projections

In this section we study the accuracy of the t -model, the H -model and the H_t model in predicting scalar quantities of interest in non-Hamiltonian systems. In particular, we consider the MZ formulation with Chorin's projection operator. For the particular case of linear dynamical systems we also compute the theoretical upper bounds we obtained in section 3.4 for the memory growth and the error in the H -model, and compare such bounds with exact results.

3.7.1 Linear Dynamical Systems

We begin by considering a low-dimensional linear dynamical system $\dot{x} = Ax$ evolving from a random initial state with density $\rho_0(x)$ to verify the MZ memory estimates we obtained in section 3.4. For simplicity,

we choose A to be negative definite

$$\mathbf{A} = e^{\mathbf{C}} \mathbf{B} e^{-\mathbf{C}}, \quad \mathbf{B} = \begin{bmatrix} -\frac{1}{8} & 0 & 0 \\ 0 & -\frac{2}{3} & 0 \\ 0 & 0 & -\frac{1}{2} \end{bmatrix}, \quad \mathbf{C} = \begin{bmatrix} 0 & 1 & 0 \\ -1 & 0 & 1 \\ 0 & -1 & 0 \end{bmatrix}. \quad (86)$$

In this case, the origin of the phase space is a stable node and it is easy to estimate $\|e^{t\mathcal{L}}\|_{\rho_0}$. We set $x_1(0) = 1$ and $x_2(0), x_3(0)$ independent standard normal random variables. In this setting, the semigroup estimates (56) and (57) are explicit

$$\|e^{t\mathcal{L}}\| \leq e^{t\omega}, \quad \omega = -\frac{1}{2}\text{trace}(\mathbf{A}) = 0.6458,$$

$$\|e^{t\mathcal{L}\mathcal{Q}}\| \leq e^{t\omega_{\mathcal{Q}}}, \quad \omega_{\mathcal{Q}} = \omega + \sqrt{A_{11}^2 + \sum_{i=2}^N \frac{A_{1i}^2}{x_1^2(0)}} = 1.1621.$$

Therefore, we obtain the following explicit upper bounds for the memory integral and the error of the H -model (see equations (58) and (60))

$$|w_0(t)| \leq 0.1964 (e^{1.1621t} - e^{0.6458t}), \quad (87)$$

$$|w_0(t) - w_0^n(t)| \leq e^{1.1624t} \sqrt{(\mathbf{b}^T (\mathbf{M}_{11}^T)^n \mathbf{a}_1)^2 x_1^2(0) + \left\| (\mathbf{M}_{11}^T)^{n+1} \mathbf{a} \right\|_2^2 \frac{t^{n+1}}{(n+1)!}}. \quad (88)$$

Next, we compare these error bounds with numerical results obtained by solving numerically the H -model (59). For example, the second-order H -model reads

$$\begin{cases} \frac{d}{dt} \mathbb{E}[x_1(t)|x_1(0)] = -0.4560 \mathbb{E}[x_1(t)|x_1(0)] + w_0^2(t), \\ \frac{dw_0^2(t)}{dt} = 0.0586 \mathbb{E}[x_1(t)|x_1(0)] + w_1^2(t), \\ \frac{dw_1^2(t)}{dt} = -0.0192 \mathbb{E}[x_1(t)|x_1(0)]. \end{cases} \quad (89)$$

In Figure 3 we demonstrate convergence of the H -model to the benchmark solution computed by Monte-Carlo simulation as we increase the H -model differentiation order. In Figure 4 we plot the bound on the memory growth (equation (87)) and the bound in the memory error (equation (88)) together with exact results.

Remark The results we just discussed can be obviously extended to higher-dimensional linear dynamical systems. In Figure 5 we plot the benchmark conditional mean path we obtained through Monte Carlo simulation together with the solution of the H -model (59) for the 100-dimensional linear dynamical system defined by the matrix ($N = 100$)

$$\mathbf{A} = \begin{bmatrix} -1 & 1 & \dots & (-1)^N \\ 1 & & & \\ \vdots & & \mathbf{B} & \\ 1 & & & \end{bmatrix}, \quad (90)$$

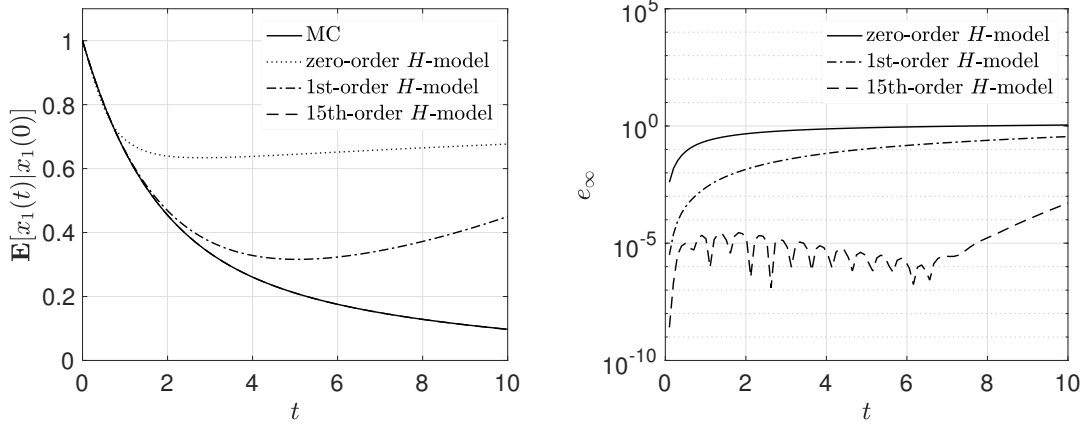


Figure 3: Convergence of the H -model for the linear dynamical system with matrix (86). The benchmark solution is computed with Monte-Carlo (MC) simulation. Also, the zero-order H -model represents the Markovian approximation to the MZ equation, i.e. the MZ equation without the memory term.

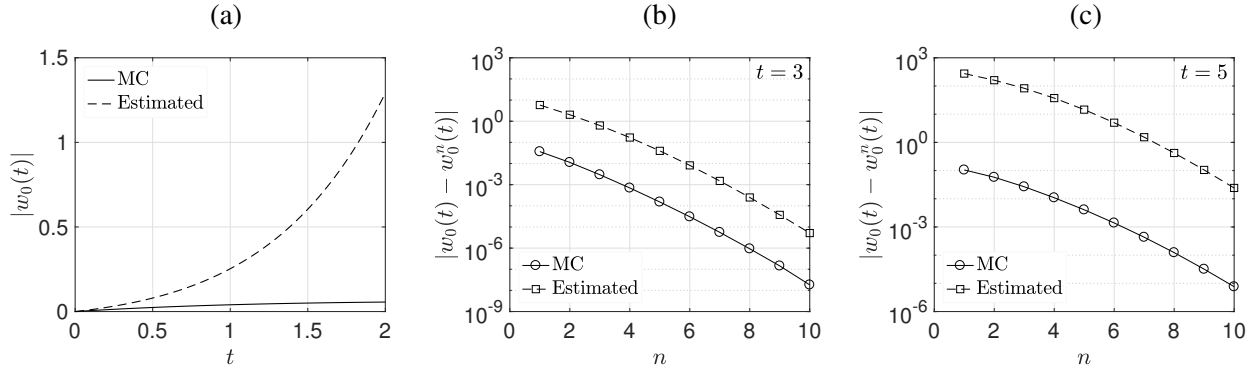


Figure 4: Linear dynamical system with matrix (86). In (a) we plot the memory term $w_0(t)$ we obtain from Monte Carlo simulation together with the estimated upper bound (87). In (b) and (c) we plot H -model approximation error $|w_0(T) - w_0^n(T)|$ together with the upper bound (88) for different differentiation orders n and at different times t .

where $B = e^C \Lambda e^{-C}$ and

$$\Lambda = \begin{bmatrix} -\frac{1}{8} & 0 & \cdots & 0 \\ 0 & -\frac{2}{9} & & \vdots \\ \vdots & & \ddots & 0 \\ 0 & \cdots & 0 & -\frac{N-1}{N+6} \end{bmatrix}, \quad C = \begin{bmatrix} 0 & 1 & & 0 \\ -1 & 0 & \ddots & \\ & \ddots & \ddots & 1 \\ 0 & & -1 & 0 \end{bmatrix}.$$

It is seen that the H -model converges as we increase the differentiation order in any finite time interval, in agreement with the theoretical prediction of section 3.4.

3.7.2 Nonlinear dynamical systems

The hierarchical memory approximation method we discussed in section 3.3 can be applied to nonlinear dynamical systems in the form (1). As we will see, if we employ the H_t -model then the nonlinearity introduces a closure problem that needs to be addressed properly.

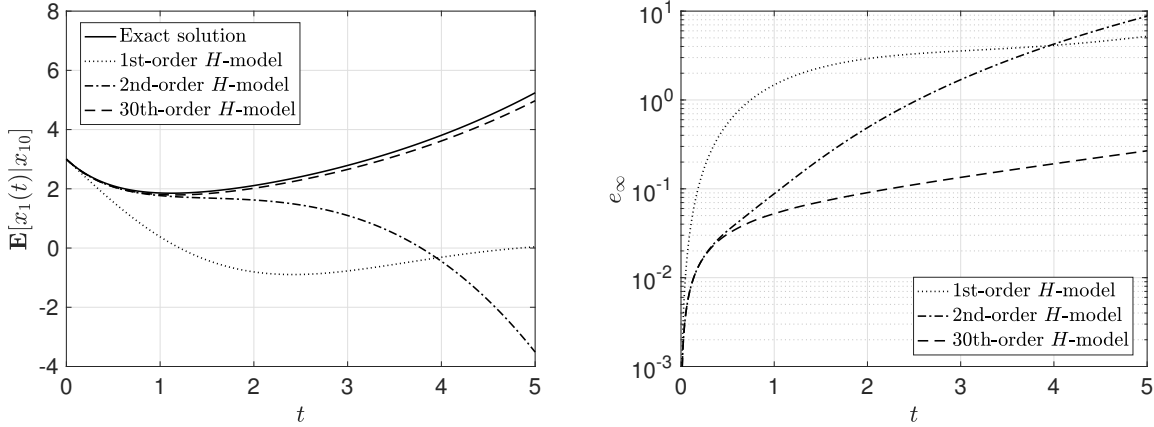


Figure 5: Linear dynamical system with matrix A (90). Convergence of the H -model to the conditional mean path solution $\mathbb{E}[x_1(t)|x_1(0)]$. The initial condition is set as $x_1(0) = 3$, while $\{x_2(0), \dots, x_{100}(0)\}$ are i.i.d. Normals.

Lorenz-63 System Consider the classical Lorenz-63 model

$$\begin{cases} \dot{x}_1 = \sigma(x_2 - x_1) \\ \dot{x}_2 = x_1(r - x_3) - x_2 \\ \dot{x}_3 = x_1x_2 - \beta x_3 \end{cases} \quad (91)$$

where $\sigma = 10$ and $\beta = 8/3$. The phase space Liouville operator for this ODE is

$$\mathcal{L} = \sigma(x_2 - x_1) \frac{\partial}{\partial x_1} + (x_1(r - x_3) - x_2) \frac{\partial}{\partial x_2} + (x_1x_2 - \beta x_3) \frac{\partial}{\partial x_3}.$$

We choose the resolved variables to be $\hat{x} = \{x_1, x_2\}$ and aim at formally integrating out $\tilde{x} = x_3$ by using the Mori-Zwanzig formalism. To this end, we set $x_3(0) \sim \mathcal{N}(0, 1)$ and consider the zeroth-order H_t -model (t -model)

$$\begin{cases} \frac{dx_{1m}}{dt} = \sigma(x_{1m} - x_{2m}), \\ \frac{dx_{2m}}{dt} = -x_{2m} + r x_{1m} - t x_{1m}^2 x_{2m}, \end{cases} \quad (92)$$

where $x_{1m}(t) = \mathbb{E}[x_1(t)|x_1(0), x_2(0)]$ and $x_{2m}(t) = \mathbb{E}[x_2(t)|x_1(0), x_2(0)]$ are *conditional mean paths*. To obtain this system we introduced the following mean field closure approximation

$$\begin{aligned} t\mathcal{P}e^{t\mathcal{L}}\mathcal{P}\mathcal{L}\mathcal{Q}\mathcal{L}x_2(0) &= -t\mathbb{E}[x_1(t)^2 x_2(t)|x_1(0), x_2(0)], \\ &\simeq -t\mathbb{E}[x_1(t)|x_1(0), x_2(0)]^2 \mathbb{E}[x_2(t)|x_1(0), x_2(0)], \\ &= -t x_{1m}^2 x_{2m}. \end{aligned} \quad (93)$$

Higher-order H_t -models can be derived based on (93). As is well known, if $r < 1$, the fixed point $(0, 0, 0)$ is a global attractor and exponentially stable. In this case, the t -model (zeroth-order H_t -model) yields accurate prediction of the conditional mean path for long time (see Figure 6). On the other hand, if we consider the chaotic regime at $r = 28$ then the t -model and its higher-order extension, i.e., the H_t -model, are accurate only for relatively short time. This is in agreement with our theoretical predictions. In fact, different from

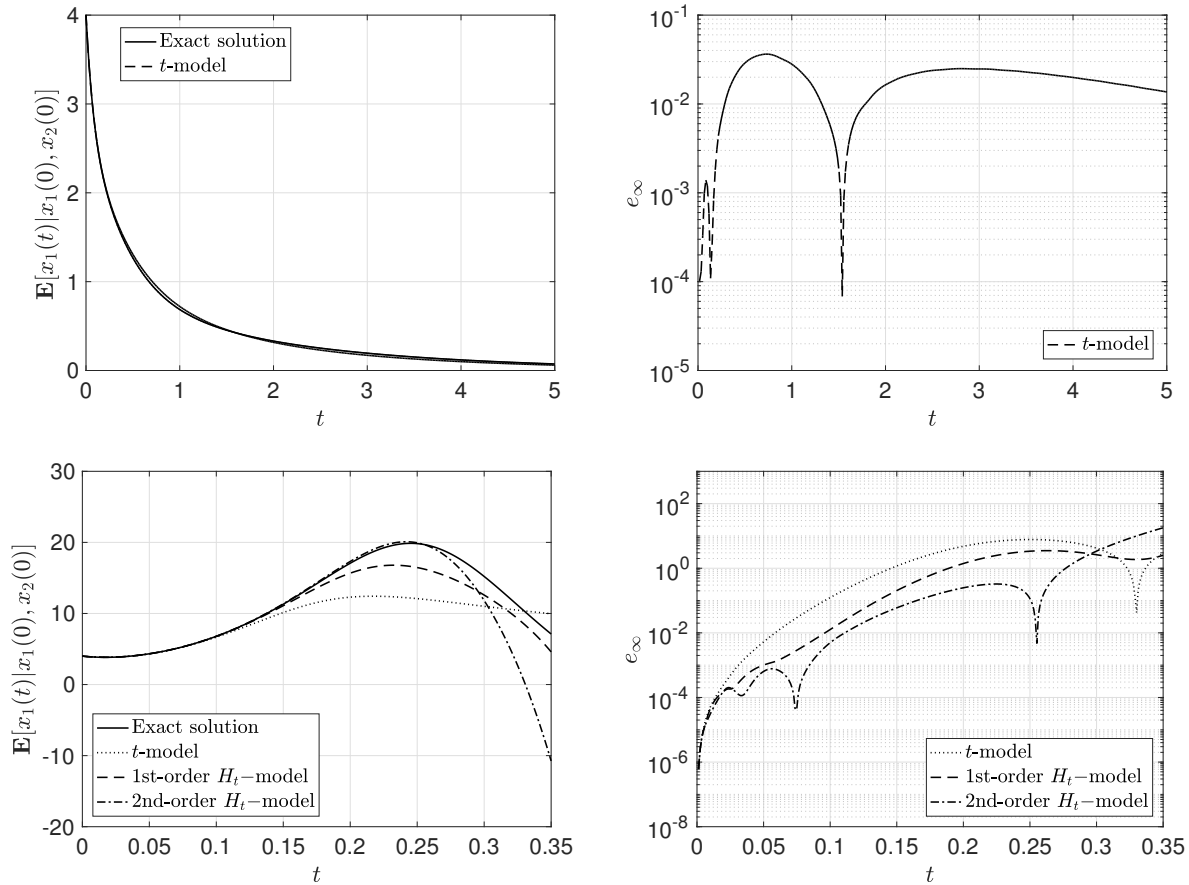


Figure 6: Accuracy of the H_t model in representing the conditional mean path in the Lorenz-63 system (91). It is seen that if $r = 0.5$ (first row), then the zeroth-order H_t -model, i.e., the t -model, is accurate for long integration times. On the other hand, if we consider the chaotic regime at $r = 28$ (second row) then we see that the t -model and its high-order extension (H_t -model) are accurate only for relatively short time.

linear systems where the hierarchical representation of the memory integral can be proven to be convergent for long time, in nonlinear systems the memory hierarchy is, in general, provably convergent only in a short time period (Theorem 5 and Corollary 4.3). This doesn't mean that the H -model or the H_t -model are not accurate for nonlinear systems. It just means that the accuracy depends on the system, the quantity of interest, and the initial condition.

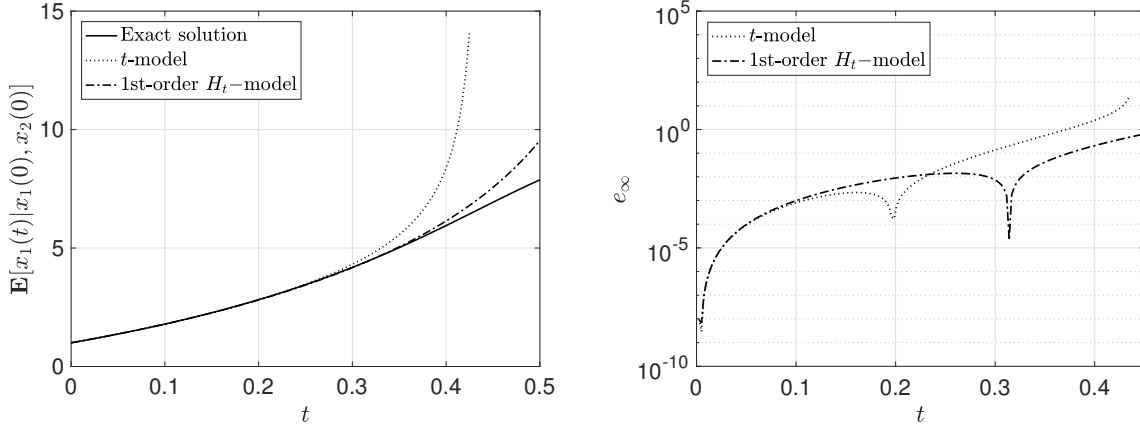


Figure 7: Accuracy of the H_t -model in representing the conditional mean path in the Lorenz-96 system (91). Here we set $F = 5$ and $N = 100$. It is seen that the H_t -model converges only for short time and provides results that are more accurate than the classical t -model.

Modified Lorenz-96 system. As an example of a high dimensional nonlinear dynamical system, we consider the following modified Lorenz-96 system [41, 57]

$$\begin{cases} \dot{x}_1 = -x_1 + x_1 x_2 + F \\ \dot{x}_2 = -x_2 + x_1 x_3 + F \\ \vdots \\ \dot{x}_i = -x_i + (x_{i+1} - x_{i-2})x_{i-1} + F \\ \vdots \\ \dot{x}_N = x_N - x_{N-2}x_{N-1} + F \end{cases} \quad (94)$$

where F is constant. As is well known, depending on the values of N and F this system can exhibit a wide range of behaviors [41]. Suppose we take the resolved variables to be $\hat{x} = \{x_1, x_2\}$. Correspondingly, the unresolved ones, i.e., those we aim at integrating through the MZ framework, are $\tilde{x} = \{x_3, \dots, x_N\}$, which we set to be independent standard normal random variables. By using the mean field approximation (93), we obtain the following zeroth-order H_t -model (t -model) of the modified Lorenz-96 system is (94)

$$\begin{cases} \dot{x}_{1m} = -x_{1m} + x_{1m}x_{2m} + F, \\ \dot{x}_{2m} = -x_{2m} + F + t(x_{1m}^2 x_{2m} - x_{1m}F). \end{cases} \quad (95)$$

In Figure 7 we study the accuracy of the H_t -model in representing the conditional mean path for with $F = 5$ and $N = 100$. It is seen that the the H_t -model converges only for short time (in agreement with the theoretical predictions) and it provides results that are more accurate than the classical t -model.

4 Mori-Zwanzig formulation for stochastic dynamical systems

In this section we develop an in-dept analysis of the Mori-Zwanzig (MZ) formulation for stochastic dynamical systems driven by multiplicative white noise. To this end, we first derive a new type of MZ equation, which we call effective Mori-Zwanzig (EMZ) equation, that governs the temporal dynamics of

noise-averaged observables. Such dynamics is generated by a Kolmogorov operator obtained by averaging Itô's representation of the stochastic Liouvillian of the system. Building upon recent work on hypoelliptic operators, we prove that the generator of the EMZ orthogonal dynamics has a spectrum that lies within cusp-shaped region of the complex plane. This allows to rigorously prove that EMZ memory kernel and fluctuation terms converge exponentially fast in time to a computable equilibrium state. We apply the new theoretical results to the Langevin dynamics of an interacting particle system widely studied in molecular dynamics simulations, and show that for smooth interaction potentials, the EMZ memory and fluctuation terms decay exponentially fast to statistical equilibrium. To illustrate the method, let us consider a d -dimensional stochastic differential equation on a smooth manifold \mathcal{M}

$$\frac{d\mathbf{x}(t)}{dt} = \mathbf{F}(\mathbf{x}(t)) + \boldsymbol{\sigma}(\mathbf{x}(t)) \underbrace{\boldsymbol{\xi}(t)}_{\text{random noise}}, \quad \mathbf{x}(0) = \mathbf{x}_0 \sim \rho_0(x) \quad (96)$$

where $\mathbf{F} : \mathcal{M} \mapsto \mathbb{R}^d$ and $\boldsymbol{\sigma} : \mathcal{M} \rightarrow \mathbb{R}^{d \times m}$ are smooth functions, $\boldsymbol{\xi}(t)$ is m -dimensional Gaussian white noise with independent components, and \mathbf{x}_0 is a random initial state characterized in terms of a probability density function $\rho_0(\mathbf{x})$ ³. The solution (96) is a d -dimensional stochastic flow on the manifold \mathcal{M} , is known as Brownian flow [50]. As is well known, if $\mathbf{F} : \mathcal{M} \mapsto \mathbb{R}^d$ and $\boldsymbol{\sigma} : \mathcal{M} \rightarrow \mathbb{R}^{d \times m}$ are of class \mathcal{C}^{k+1} ($k \geq 0$) with uniformly bounded derivatives, then the solution to (96) is global, and that the corresponding flow is a stochastic flow of diffeomorphisms [10, 96, 93] of class \mathcal{C}^k . This means that such stochastic flow is differentiable k times (with continuous derivative), with respect to the initial condition for all t . Next, consider a smooth vector-valued phase space function of the form (2). Similar to the deterministic case we discussed in section 2, it is possible to define a stochastic composition (Koopman) operator $\mathcal{E}(t, s)$ that pushes forward in time the observable $\mathbf{u}(t) = \mathbf{u}(\mathbf{x}(t))$. Specifically,

$$\mathbf{u}(\mathbf{x}(t)) = \mathcal{E}(t, s)\mathbf{u}(\mathbf{x}(s)), \quad (98)$$

The semigroup $\mathcal{E}(t, s)$ can be formally written as

$$\mathcal{E}(t, s) = \overrightarrow{\mathcal{T}} e^{\int_s^t \mathcal{L}(\tau) d\tau},$$

where $\overrightarrow{\mathcal{T}}$ is the time ordering operator placing later operators to the right, and $\mathcal{L}(\tau)$ is the (random) infinitesimal generator of the composition operator⁴. The (random) generator $\mathcal{L}(\tau)$ of the semigroup $\mathcal{E}(t, s)$ can be determined using by Dyson's series expansion [72], i.e.,

$$\mathcal{E}(t, s) = \sum_{n=1}^{\infty} \mathcal{D}_n(t, s), \quad (99)$$

where

$$\mathcal{D}_n(t, s) = \overrightarrow{\mathcal{T}} \frac{1}{n!} \int_s^t \int_s^{t_1} \cdots \int_s^{t_{n-1}} dt_1 dt_2 \cdots dt_n \mathcal{L}(t_1) \mathcal{L}(t_2) \cdots \mathcal{L}(t_n).$$

³If the system (96) evolves from a deterministic initial states then we have

$$\rho_0(x) = \prod_{i=1}^N \delta(x_i - x_i(0)). \quad (97)$$

⁴The evolution operator $\mathcal{E}(t, s)$ has a dual construction in the space of probability density functions [23].

A substitution of (99) into (98) yields

$$\mathbf{u}(\mathbf{x}(t)) = \sum_{n=1}^{\infty} \mathcal{D}_n(t, s) \mathbf{u}(\mathbf{x}(s)). \quad (100)$$

Next, we match each term of the series expansion (100) with the terms of the stochastic Taylor expansion of $\mathbf{u}(\mathbf{x}(t))$ (see [46], Chapter 5). This allows us to construct explicit expressions for the stochastic Liouvillian $\mathcal{L}(\tau)$. In particular, if we interpret the SDE (96) in the Itô sense, then we can use the classical Itô-Taylor expansion to obtain⁵

$$\mathcal{L}(t) = \sum_{k=1}^d F_k(\mathbf{x}_0) \frac{\partial}{\partial x_{0k}} + \frac{1}{2} \sum_{j=1}^m \sum_{i,k=1}^d \sigma_{ij}(\mathbf{x}_0) \sigma_{kj}(\mathbf{x}_0) \frac{\partial^2}{\partial x_{0i} \partial x_{0k}} + \sum_{j=1}^m \sum_{i=1}^d \sigma_{ij}(\mathbf{x}_0) \xi_j(t) \frac{\partial}{\partial x_{0i}}. \quad (102)$$

With the generator $\mathcal{L}(t)$ of the stochastic flow available, we can now derive the Mori-Zwanzig equation governing the evolution of the observable (98). To this end, we introduce a projection operator \mathcal{P} and the complementary projection $\mathcal{Q} = \mathcal{I} - \mathcal{P}$. By following the formal procedure outlined in [101, 23] we obtain the following evolution equation for the observable $\mathbf{u}(t) = \mathbf{u}(\mathbf{x}(t, \mathbf{x}_0))$

$$\frac{d}{dt} \mathbf{u}(t) = \mathcal{E}(t, 0) \mathcal{P} \mathcal{L}(t) \mathbf{u}(\mathbf{x}_0) + \mathcal{Y}(t, 0) \mathcal{Q} \mathcal{L}(t) \mathbf{u}(0) + \int_0^t \mathcal{E}(s, 0) \mathcal{P} \mathcal{L}(s) \mathcal{Y}(t, s) \mathcal{Q} \mathcal{L}(t) \mathbf{u}(0) ds, \quad (103)$$

where $\mathbf{u}(0) = \mathbf{u}(\mathbf{x}_0)$ and

$$\mathcal{Y}(t, s) = \overrightarrow{\mathcal{T}} e^{\int_s^t \mathcal{Q} \mathcal{L}(\tau) d\tau}. \quad (104)$$

The three terms at the right hand side of (103) are called, respectively, streaming term, fluctuation (or noise) term, and memory term. It is often more convenient (and tractable) to compute the evolution of the observable $\mathbf{u}(t)$ within a closed linear space, e.g., the image of the projection operator \mathcal{P} . To this end, we apply such projection to both sides of equation (103) to obtain⁶

$$\frac{d}{dt} \mathcal{P} \mathbf{u}(t) = \mathcal{P} \mathcal{E}(t, 0) \mathcal{P} \mathcal{L}(t) \mathbf{u}(0) + \int_0^t \mathcal{P} \mathcal{E}(s, 0) \mathcal{P} \mathcal{L}_\omega(s) \mathcal{Y}(t, s) \mathcal{Q} \mathcal{L}(t) \mathbf{u}(0) ds. \quad (105)$$

Depending on the choice of the projection operator, the MZ equation (105) can yield evolution equations for different quantities [23]. For example, if we use Chorin's projection [15, 16, 99, 88], then (105) is an evolution equation for the conditional mean of $\mathbf{u}(t)$. Similarly, if we use Mori's projection [100, 79], then (105) is an evolution equation for the temporal auto-correlation function of $\mathbf{u}(t)$.

4.1 Effective Mori-Zwanzig (EMZ) equation

The Mori-Zwanzig formulation we discussed in the previous Section provides a general framework to handle dimension reduction in stochastic dynamical systems. However, the MZ equations are not easy to use in practice because the generator $\mathcal{L}(t)$ depends on the random process $\boldsymbol{\xi}(t)$ (see Eq. (102)). To overcome this difficulty we can average the evolution (98) over $\boldsymbol{\xi}(t)$, conditional to the initial state \mathbf{x}_0 . This allows us to

⁵Similarly, by using the Stratonovich-Taylor expansion, one obtain the following infinitesimal generator

$$\mathcal{L}(t) = \sum_{k=1}^d F_k(\mathbf{x}_0) \frac{\partial}{\partial x_{0k}} + \sum_{j=1}^m \sum_{i=1}^d \sigma_{ij}(\mathbf{x}_0) \circ \xi_j(t) \frac{\partial}{\partial x_{0i}}, \quad (101)$$

where $\circ \xi_j(t)$ denotes the stochastic increment in Stratonovich's interpretation.

⁶The projected fluctuating term $\mathcal{P} \mathcal{Y}(t, 0) \mathcal{Q} \mathcal{L}(t) \mathbf{u}(\mathbf{x}_0)$ is identically zero since $\mathcal{P} \mathcal{Q} = 0$.

define an composition operator $\mathcal{M}(t, 0)$ that pushes forward in time the average of the observable $\mathbf{u}(t)$ over the noise, i.e.,

$$\mathbb{E}_{\xi(t)}[\mathbf{u}(\mathbf{x}(t))|\mathbf{x}_0] = \mathcal{M}(t, 0)\mathbf{u}(\mathbf{x}_0). \quad (106)$$

It can be shown that $\mathcal{M}(t, 0)$ is a Markovian semigroup [75]. Also, the averaging operation $\mathbb{E}_{\xi(t)}[\cdot]$ appearing in (106) is a functional integral [87] with respect to the Gaussian process $\xi(t)$. By using stochastic Taylor series, it is straightforward to show that the generator of the Markovian semigroup $\mathcal{M}(t, 0)$ is the average (over noise) of the generator \mathcal{L} defined in (102), i.e.,

$$\mathcal{K}(\mathbf{x}_0) = \sum_{k=1}^d F_k(\mathbf{x}_0) \frac{\partial}{\partial x_{0k}} + \frac{1}{2} \sum_{j=1}^m \sum_{i,k=1}^d \sigma_{ij}(\mathbf{x}_0) \sigma_{kj}(\mathbf{x}_0) \frac{\partial}{\partial x_{0i} \partial x_{0k}}, \quad (107)$$

Note that \mathcal{K} is a backward Komogorov operator [46]. The semigroup $\mathcal{M}(t, 0)$ can be now written as

$$\mathcal{M}(t, 0) = e^{t\mathcal{K}}. \quad (108)$$

This yields the following *effective Mori-Zwanzig (EMZ)* equation governing the evolution of (106)

$$\frac{\partial}{\partial t} e^{t\mathcal{K}} \mathbf{u}(0) = e^{t\mathcal{K}} \mathcal{P} \mathcal{K} \mathbf{u}(0) + e^{t\mathcal{Q}\mathcal{K}\mathcal{Q}} \mathcal{Q} \mathcal{K} \mathbf{u}(0) + \int_0^t e^{s\mathcal{K}} \mathcal{P} \mathcal{K} e^{(t-s)\mathcal{Q}\mathcal{K}\mathcal{Q}} \mathcal{Q} \mathcal{K} \mathbf{u}(0) ds. \quad (109)$$

Applying the projection operator \mathcal{P} once more yields

$$\frac{\partial}{\partial t} \mathcal{P} e^{t\mathcal{K}} \mathbf{u}(0) = \mathcal{P} e^{t\mathcal{K}} \mathcal{P} \mathcal{K} \mathbf{u}(0) + \int_0^t \mathcal{P} e^{s\mathcal{K}} \mathcal{P} \mathcal{K} e^{(t-s)\mathcal{Q}\mathcal{K}\mathcal{Q}} \mathcal{Q} \mathcal{K} \mathbf{u}(0) ds. \quad (110)$$

We notice that the projected EMZ equation for stochastic systems has the same structure as the the classical projected MZ equation for deterministic (autonomous) dynamical systems [101, 99, 100]. However, the classical Liouville operator is now replaced by a Kolmogorov operator \mathcal{K} .

By following the procedure we recently presented in [101] it possible to derive a (linear) generalized Langevin equation (GLE) for the noise-averaged observable (106) based on the EMZ equation (109) or (110). To this end, consider the weighted Hilbert space $H = L^2(\mathcal{M}, \rho)$, where ρ is a positive weight function in \mathcal{M} . For instance, ρ can be the probability density function of the random initial state \mathbf{x}_0 . Let

$$\langle h, g \rangle_\rho = \int_{\mathcal{M}} h(\mathbf{x}) g(\mathbf{x}) \rho(\mathbf{x}) d\mathbf{x} \quad h, g \in H \quad (111)$$

be the inner product in H . In H we introduce the following (Mori) projection operator

$$\mathcal{P}h = \sum_{i,j=1}^M G_{ij}^{-1} \langle u_i(0), h \rangle_\rho u_j(0), \quad h \in H. \quad (112)$$

where $G_{ij} = \langle u_i(0), u_j(0) \rangle_\rho$ and $u_i(0) = u_i(\mathbf{x}) \in V$ ($i = 1, \dots, M$) are M linearly independent functions. With \mathcal{P} defined as in (112), it is easy to show that the EMZ equation (109), and its projected version (110), take the form

$$\frac{d\mathbf{u}(t)}{dt} = \mathbf{\Omega} \mathbf{u}(t) + \int_0^t \mathbf{K}(t-s) \mathbf{u}(s) ds + \mathbf{f}(t), \quad (113)$$

$$\frac{d}{dt} \mathcal{P} \mathbf{u}(t) = \mathbf{\Omega} \mathcal{P} \mathbf{u}(t) + \int_0^t \mathbf{K}(t-s) \mathcal{P} \mathbf{u}(s) ds. \quad (114)$$

where $\mathbf{u}(t) = [u_1(t), \dots, u_M(t)]^T$ and

$$G_{ij} = \langle u_i(0), u_j(0) \rangle_\rho, \quad (115a)$$

$$\Omega_{ij} = \sum_{k=1}^M G_{jk}^{-1} \langle u_k(0), \mathcal{K}u_i(0) \rangle_\rho \quad (\text{streaming matrix}), \quad (115b)$$

$$K_{ij}(t) = \sum_{k=1}^M G_{jk}^{-1} \langle u_k(0), \mathcal{K}e^{t\mathcal{Q}\mathcal{K}\mathcal{Q}}\mathcal{K}u_i(0) \rangle_\rho \quad (\text{memory kernel}), \quad (115c)$$

$$\mathbf{f}(t) = e^{t\mathcal{Q}\mathcal{K}\mathcal{Q}}\mathcal{K}\mathbf{u}(0) \quad (\text{fluctuation term}). \quad (115d)$$

The Kolmogorov operator \mathcal{K} is not skew-adjoint relative to $\langle \cdot, \cdot \rangle_\rho$, and therefore it is not possible to represent the memory kernel as a function of the autocorrelation of \mathbf{f} using the fluctuation-dissipation theorem (see [101]).

4.1.1 An example: EMZ for the Ornstein-Uhlenbeck process

Let us consider the Ornstein-Uhlenbeck process defined by the solution to the Itô stochastic differential equation

$$\frac{d}{dt}x = \theta(\mu - x) + \sigma\xi(t), \quad (116)$$

where σ , μ , and θ are positive parameters and $\xi(t)$ is Gaussian white noise with correlation function $\langle \xi(t), \xi(s) \rangle = \delta(t - s)$. As is well-known that the Ornstein-Uhlenbeck process is ergodic and admits a stationary (equilibrium) Gaussian distribution $\rho_{eq} = \mathcal{N}(\mu, \sigma^2/2\theta)$, and we assume that $x(0) \sim \rho_{eq}$. The formal solution of Eq. (116) can be written as

$$x(t) = x(0)e^{-\theta t} + \mu(1 - e^{-\theta t}) + \sigma \int_0^t e^{-\theta(t-s)}\xi(s)ds. \quad (117)$$

Next, we consider the following quantity of interest $u(t) = x(t) - \mu$ (centered Ornstein-Uhlenbeck process). By using the formal solution (117) we obtain the following non-stationary conditional mean and conditional auto-covariance function

$$\mathbb{E}_{\xi(t)}[x(t) - \mu|x(0)] = (x(0) - \mu)e^{-\theta t}, \quad (118)$$

$$\mathbb{E}_{\xi(t)}[(x(t) - \mu)(x(s) - \mu)|x(0)] = \frac{\sigma^2}{2\theta} \left(e^{-\theta|t-s|} - e^{-\theta(t+s)} \right). \quad (119)$$

By averaging over the random initial state (distributed as ρ_{eq}) we obtain

$$\mathbb{E}_{x(0)}[\mathbb{E}_{\xi(t)}[x(t) - \mu|x(0)]] = \mathbb{E}_{x(0)}[x(0)e^{-\theta t} - \mu e^{-\theta t}] = 0, \quad (120)$$

$$\mathbb{E}_{x(0)}[\mathbb{E}_{\xi(t)}[(x(t) - \mu)(x(s) - \mu)|x(0)]] = \frac{\sigma^2}{2\theta} e^{-\theta|t-s|}. \quad (121)$$

At this point, we define the projection operator

$$\mathcal{P}h = \frac{\langle h, u(0) \rangle_{\rho_{eq}}}{\langle u(0), u(0) \rangle_{\rho_{eq}}} u(0), \quad (122)$$

The EMZ equations (113) and (114) with projection (122) can be written as

$$\frac{d}{dt}M(t) = -\theta M(t), \quad \frac{d}{dt}C(t) = -\theta C(t) \quad (123)$$

where $M(t) = \mathbb{E}_{\xi(t)}[x(t) - \mu|x(0)]$ and $C(t) = \mathbb{E}_{x(0)}[\mathbb{E}_{\xi(t)}[(x(t) - \mu)(x(0) - \mu)|x(0)]]$. Clearly, equations (123) are the exact evolution equations governing the mean and the autocovariance function of process $u(t)$ since their solution is (118) and (121), respectively.

4.2 Analysis of the EMZ equation

In this section, we develop an in-depth mathematical analysis of the effective Mori-Zwanzig equation (109) using the theory of Hörmander operators [35, 91, 68]. In particular, we build upon the analysis by Hérau and Nier [35], Eckmann and Hairer [27, 25, 26], and Helffer and Nier [34] on linear hypoelliptic operators. One of the key results of such analysis is that the spectrum of the Kolmogorov operator \mathcal{K} (see Eq. (107)) lies within a cusp-like region of the complex half-plane. This allows us to prove exponential convergence (in time) of the operator semigroup $e^{t\mathcal{K}}$ to statistical equilibrium. We will show that the same technique can be applied to the EMZ equation, in particular the orthogonal dynamics propagator $e^{t\mathcal{Q}\mathcal{K}\mathcal{Q}}$ to prove exponential relaxation to equilibrium of both the streaming term and the memory integral in (109). For consistency with the literature on hypoelliptic operators, we will use the negative of \mathcal{K} and $\mathcal{Q}\mathcal{K}\mathcal{Q}$ as semigroup generators⁷ and write the semigroups appearing in EMZ equation (109) as $e^{-t\mathcal{K}}$ and $e^{-t\mathcal{Q}\mathcal{K}\mathcal{Q}}$.

4.2.1 The Kolmogorov operator \mathcal{K}

In this section we review some of key results on the Kolmogorov operator \mathcal{K} defined in Equation (107). We begin by noticing that SDEs (96) have an associated Markovian evolution operator $\mathcal{M}(t, 0)$ (108) that is generated by a Hörmander-type operator of the form

$$\mathcal{K}(\mathbf{x}) = \sum_{i=1}^m \mathcal{X}_i^*(\mathbf{x})\mathcal{X}_i(\mathbf{x}) + \mathcal{X}_0(\mathbf{x}) + f(\mathbf{x}). \quad (124)$$

where $\mathcal{X}_i(\mathbf{x})$ ($0 \leq i \leq m$) denotes a first-order differential operator with space-dependent coefficients, \mathcal{X}_i^* is the formal adjoint of $\mathcal{X}_i(\mathbf{x})$ in $L^2(\mathbb{R}^n)$, and $f(\mathbf{x})$ is a function with at most polynomial growth. To derive useful spectral estimates for \mathcal{K} , it is convenient to first provide some background

Definition 1. Let N be a real number. Define

$$\text{Pol}_0^N = \left\{ f \in C^\infty(\mathbb{R}^n) : \sup_{\mathbf{x} \in \mathbb{R}^n} (1 + \|\mathbf{x}\|)^{-N} |\partial^\alpha f(\mathbf{x})| \leq C_\alpha \right\},$$

where α is a multi-index of arbitrary order. Note that Pol_0^N is the set of infinitely differentiable functions growing at most polynomially with \mathbf{x} .

Similarly, we define the space of k -th order differential operators with coefficients growing at most polynomially with \mathbf{x} as

$$\text{Pol}_k^N = \left\{ \mathcal{G} : C^\infty(\mathbb{R}^n) \rightarrow C^\infty(\mathbb{R}^n) : \mathcal{G}(\mathbf{x}) = G_0(\mathbf{x}) + \sum_{j=1}^n \sum_{i=1}^k G_j^i(\mathbf{x}) \partial_j^i, \quad G_j^i \in \text{Pol}_0^N \right\}$$

It is easy to verify that if $\mathcal{X} \in \text{Pol}_k^N$ and $\mathcal{Y} \in \text{Pol}_l^M$ then the operator commutator $[\mathcal{X}, \mathcal{Y}] = \mathcal{X}\mathcal{Y} - \mathcal{Y}\mathcal{X}$ is in Pol_{k+l-1}^{N+M} .

Definition 2. A family of operators

$$\mathcal{A}_i(\mathbf{x}) = \sum_{j=1}^n A_{ij}(\mathbf{x}) \partial_j \quad i = 1, \dots, m \quad (125)$$

⁷If \mathcal{K} and $\mathcal{Q}\mathcal{K}\mathcal{Q}$ are dissipative then $-\mathcal{K}$ and $-\mathcal{Q}\mathcal{K}\mathcal{Q}$ are accretive.

is called *non-degenerate* if there exist two constants N and C such that

$$\|\mathbf{y}\|^2 \leq C(1 + \|\mathbf{x}\|^2)^N \sum_{i=1}^m \langle \mathcal{A}_i(\mathbf{x}), \mathbf{y} \rangle^2 \quad \forall \mathbf{x}, \mathbf{y} \in \mathbb{R}^n$$

where $\langle \mathcal{A}_i(\mathbf{x}), \mathbf{y} \rangle = \sum_{j=1}^n A_{ij}(\mathbf{x})y_j$.

It was recently shown by Eckmann and Hairer in [26] that if the Lie algebra generated by the operators $\{\mathcal{X}_0, \dots, \mathcal{X}_m\}$ in (124) is non-degenerate then \mathcal{K} is hypoelliptic [27, 37]. The main result can be summarized as follows

Proposition 1 (Eckmann and Hairer [26]). *If $\{\mathcal{X}_0, \dots, \mathcal{X}_m\}$ and f in (124) satisfy the following conditions:*

1. $\mathcal{X}_j \in \text{Pol}_1^N$ for all $j = 0, \dots, m$, and $f \in \text{Pol}_0^N$;
2. *There exists a finite integer M such that the family of operators consisting of $\{\mathcal{X}_i\}_{i=0}^m$, $\{[\mathcal{X}_i, \mathcal{X}_j]\}_{i,j=1}^m$, $\{[\mathcal{X}_i, [\mathcal{X}_j, \mathcal{X}_k]]\}_{i,j,k=1}^m$ and so on up to the commutators of rank M is non-degenerate;*

Then the operator \mathcal{K} defined in (124) and $\partial_t + \mathcal{K}$ are both hypoelliptic.

Conditions 1 and 2 are called *poly-Hörmander conditions*. The hypoellipticity of the operator $\partial_t + \mathcal{K}$ guarantees smoothness of the transition probability density pushed forward in time by the Markovian semigroup $\mathcal{M}(t, 0)$ [25]. Let us review additional mathematical properties of the Kolmogorov operator \mathcal{K} . As a differential operator with C^∞ , tempered (i.e. with all its derivatives polynomially bounded) coefficients, \mathcal{K} and its formal adjoint \mathcal{K}^* are defined in the Schwarz space $\mathcal{S}'(\mathbb{R}^n)$, which is dense in $L^p(\mathbb{R}^n)$ ($1 \leq p < \infty$). On the other hand, \mathcal{K} and \mathcal{K}^* are both closable operators on $\mathcal{S}'(\mathbb{R}^n)$, and therefore all estimates in we obtain in this Section hold in $\mathcal{S}'(\mathbb{R}^n)$. We now introduce a family of weighted Sobolev spaces

$$\mathcal{S}^{\alpha, \beta} = \{u \in \mathcal{S}'(\mathbb{R}^n) : \Lambda^\alpha \bar{\Lambda}^\beta u \in L^2(\mathbb{R}^n), \quad \alpha, \beta \in \mathbb{R}\}, \quad (126)$$

where $\mathcal{S}'(\mathbb{R}^n)$ the space of tempered distributions in \mathbb{R}^n . The operator Λ^α is a pseudo-differential operator (see [27, 26, 35] for a rigorous definition and properties) that reduces to

$$\Lambda^2 = 1 - \Delta \quad (127)$$

for $\alpha = 2$. The weighted Sobolev space (126) is equipped with the scalar product

$$\langle h, g \rangle_{\alpha, \beta} = \langle \Lambda^\alpha \bar{\Lambda}^\beta h, \Lambda^\alpha \bar{\Lambda}^\beta g \rangle_{L^2},$$

which induces the Sobolev norm $\|\cdot\|_{\alpha, \beta}$. With the above definitions it is possible to obtain the following important estimate on spectrum of the Kolmogorov operator \mathcal{K} .

Theorem 7 (Eckmann and Hairer [26]). *Let $\mathcal{K} \in \text{Pol}_2^N$ be an operator of the form (124) satisfying conditions 1. and 2. in Proposition 1. Suppose that the closure of \mathcal{K} is a maximal-accretive operator in $L^2(\mathbb{R}^n)$ and that for every $\epsilon > 0$ there exists two constants $\delta > 0$ and $C > 0$ such that*

$$\|u\|_{\delta, \delta} \leq C(\|u\|_{0, \epsilon} + \|\mathcal{K}u\|) \quad (128)$$

for all $u \in \mathcal{S}'(\mathbb{R}^n)$. If, in addition, there exist two constants $\delta > 0$ and $C > 0$ such that

$$\|u\|_{0, \epsilon} \leq C(\|u\| + \|\mathcal{K}u\|), \quad (129)$$

then \mathcal{K} has compact resolvent when considered as an operator acting on $L^2(\mathbb{R}^n)$, whose spectrum $\sigma(\mathcal{K})$ is contained in the cusp (see Figure 8):

$$\mathcal{S}_{\mathcal{K}} = \{z \in \mathbb{C} : \text{Re } z \geq 0, \quad |\text{Im } z| < (8C_1)^{M/2}(1 + \text{Re } z)^M\} \quad (130)$$

for some positive constant C_1 and $M \in \mathbb{N}$.

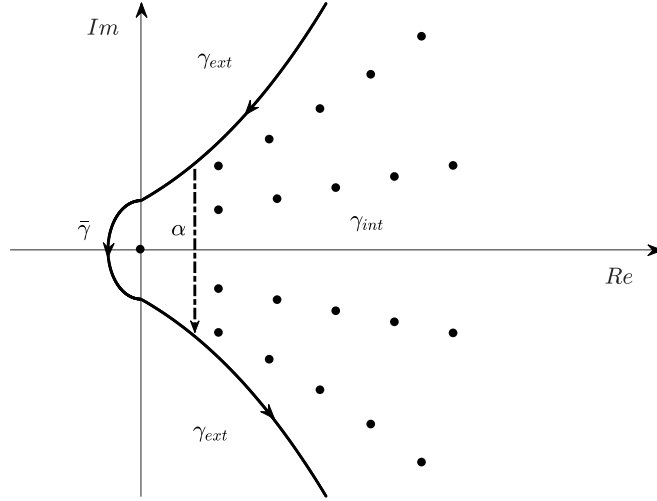


Figure 8: Sketch of the cusp-shaped region of the complex plane enclosing the spectrum of the operators \mathcal{K} and $\mathcal{Q}\mathcal{K}\mathcal{Q}$.

One of the key estimates used by Eckmann and Hairer in the proof of Theorem 7 is

$$\frac{1}{4}|z + 1|^{2/M}\|u\|^2 \leq C_1 ([1 + \operatorname{Re} z]^2\|u\|^2 + \|(\mathcal{K} - z)u\|^2), \quad \forall \operatorname{Re} z \geq 0. \quad (131)$$

In a series of papers, Hérau, Nier and Helffer [35, 34] proved that the Kolmogorov operator \mathcal{K} corresponding to classical Langevin dynamics generates a semigroup $e^{-t\mathcal{K}}$ that decays exponentially fast to an equilibrium state. Hereafter we show that similar results can be obtained for Kolmogorov operators in the general form (124). In particular, we have the following

Theorem 8. *Suppose that \mathcal{K} satisfies all conditions in Theorem 7. If the spectrum of \mathcal{K} in $L^2(\mathbb{R}^n)$ is such that*

$$\sigma(\mathcal{K}) \cap i\mathbb{R} = \{0\}, \quad (132)$$

and the eigenvalue 0 (if any) has finite algebraic multiplicity, then for any $0 < \gamma < \min(\operatorname{Re} \sigma(\mathcal{K})/\{0\})$, there exists a positive constant $C = C(\gamma)$ such that the estimate

$$\|e^{-t\mathcal{K}}u_0 - \pi_0 u_0\| \leq C e^{-\alpha t} \|u_0\| \quad (133)$$

holds for all $u_0 \in L^2(\mathbb{R}^n)$ and for all $t > 0$, where π_0 is the spectral projection onto the kernel of \mathcal{K} .

Proof. The Kolmogorov operator \mathcal{K} is closed, maximal-accretive and densely defined in $L^2(\mathbb{R}^n)$. Hence, by the Lumer-Phillips theorem, the semigroup $e^{-t\mathcal{K}}$ is a contraction in $L^2(\mathbb{R}^n)$. It was shown in [26, 35] that the core of \mathcal{K} is a Schwarz space, and that the hypoelliptic estimate (131) holds for any $u \in L^2(\mathbb{R}^n)$. According to Theorem 7, \mathcal{K} only has a discrete spectrum, i.e., $\sigma(\mathcal{K}) = \sigma_{dis}(\mathcal{K})$. Condition (132) requires that $\lambda = 0$ is the only eigenvalue on the imaginary axis $i\mathbb{R}$, and that such eigenvalue has finite algebraic multiplicity. This condition, together with Theorem 6.1 in [34], allows us to obtain a weakly convergent Dunford integral representation of the semigroup $e^{-t\mathcal{K}}$ given by

$$e^{-t\mathcal{K}}u_0 - \pi_0 u_0 = \frac{1}{2\pi i} \int_{\partial S'_\mathcal{K}} e^{-tz} (z - \mathcal{K})^{-1} u_0 dz, \quad (134)$$

where $\partial S'_K = \gamma_{int} \cup \gamma_{ext}$ is the union of the two regions shown in Figure 8, and $(z - K)^{-1}$ is the resolvent K . Equation (134) allows us to formulate the semigroup estimation problem as an estimation problem involving a complex integral. In particular, to derive the upper bound (133), we just need an upper bound for the norm of resolvent $(z - K)^{-1}$. To derive such bound, we notice that for all $z \notin S_K$ (see (130)) and $\text{Re } z \geq 0$, we have $|z + 1|^{2/M} \geq (8C_1)(1 + \text{Re } z)^2$. A substitution of this inequality into (131) yields, for all $u \in L^2(\mathbb{R}^n)$

$$\frac{1}{8}|z + 1|^{2/M}\|u\|^2 \leq C_1\|(K - z)u\|^2, \quad \forall \text{Re } z \geq 0, z \notin S_K.$$

Hence, $\|(K - z)^{-1}\| \leq \sqrt{8C_1}|z + 1|^{-1/M}$. Next, we rewrite the Dunford integral (134) as

$$\frac{1}{2\pi i} \int_{\partial S'_K} e^{-tz}(z - K)^{-1}u_0 dz = \frac{1}{2\pi i} \int_{\gamma_{int}} e^{-tz}(z - K)^{-1}u_0 dz + \frac{1}{2\pi i} \int_{\gamma_{ext}} e^{-tz}(z - K)^{-1}u_0 dz. \quad (135)$$

Since $(K - z)^{-1}$ is a compact linear operator, we have that for any $0 < \alpha < \min(\text{Re } \sigma(K)/\{0\})$ there exists a constant $C_\alpha > 0$ such that $\|(K - \alpha)u\| \geq C_\alpha\|u\|$. On the other hand, K is also a real operator, which implies that for all $z = \alpha + i\nu \notin \sigma(K)$, $\nu \in \mathbb{R}$, we have

$$\|(K - \alpha + i\nu)u\|^2 = \|(K - \alpha)u\|^2 + \nu^2\|u\|^2 \geq (C_\alpha^2 + \nu^2)\|u\|^2,$$

i.e.,

$$\|(K - \alpha + i\nu)^{-1}u\| \leq \frac{1}{\sqrt{C_\alpha^2 + \nu^2}}\|u\|. \quad (136)$$

This suggests that the resolvent $(K - z)^{-1}$ is uniformly bounded by $1/C_\alpha$ within the region γ_{int} , i.e.,

$$\left\| \frac{1}{2\pi i} \int_{\gamma_{int}} e^{-tz}(z - K)^{-1}u_0 dz \right\| \leq C e^{-\alpha t}\|u_0\|. \quad (137)$$

The region γ_{ext} is defined by all complex numbers $z = x + iy$ such that $|\text{Im } z| = (8C_1)^{M/2}(1 + \text{Re } z)^M$. Also, if $z \notin S_K$ then we have shown that the norm of the resolvent is bounded by $\|(K - z)^{-1}\| \leq \sqrt{8C_1}|z + 1|^{-1/M}$. These two inequalities allow us to write, for $M = 1$ and all $M \geq 2$,

$$\begin{aligned} \left\| \frac{1}{2\pi i} \int_{\gamma_{ext}} e^{-tz}(z - K)^{-1}u_0 dz \right\| &\leq C\|u_0\| \int_{(8C_1)^{M/2}(1+\alpha)^M}^{\infty} \exp\{-t[(8C_1)^{-\frac{1}{2}}y^{\frac{1}{M}} - 1]\}y^{-\frac{1}{M}} dy \\ &= C\|u_0\| \int_{\alpha}^{\infty} e^{-th}(h + 1)^{M-2} dh \\ &\leq C e^{-\alpha t}\|u_0\| \left[\frac{1}{t} + \frac{1}{t^2} + \dots + \frac{1}{t^M} \right], \quad t > 0. \end{aligned} \quad (138)$$

By combining (134), (135), (137) and (138) we see that there exists a constant $C = C(\alpha)$ such that

$$\|e^{-tK}u_0 - \pi_0 u_0\| \leq C e^{-\alpha t}\|u_0\|. \quad (139)$$

This completes the proof. □

Another direct consequence of the estimate (131) is the unconditional convergence of the formal power series expansion of the semigroup e^{-tK} . This is an important result that yields convergence of operator series expansions such as the MZ-Faber expansion [100] for stochastic dynamical systems.

Corollary 8.1. *Assuming that \mathcal{K} satisfies all conditions listed in Theorem 8, then for any $u_0 \in L^2(\mathbb{R}^n)$ the power series expansion*

$$e^{-(t+s)\mathcal{K}}u_0 = \lim_{m \rightarrow \infty} \sum_{n=0}^m \frac{(-s)^n}{n!} e^{-t\mathcal{K}} \mathcal{K}^n u_0 \quad (140)$$

converges in norm for any $t > 0$ and $s \geq t$.

Proof. By using the resolvent identity $(z - \mathcal{K})^{-1}\mathcal{K} = z(z - \mathcal{K})^{-1} - \mathcal{I}$, The Cauchy integral theorem, and the Dunford integral representation (134), we obtain

$$\begin{aligned} e^{-t\mathcal{K}}\mathcal{K}u_0 - \pi_0\mathcal{K}u_0 &= \frac{1}{2\pi i} \int_{\partial S'_\mathcal{K}} e^{-tz} (z - \mathcal{K})^{-1} \mathcal{K}u_0 dz \\ &= \frac{1}{2\pi i} \int_{\partial S'_\mathcal{K}} z e^{-tz} (z - \mathcal{K})^{-1} u_0 dz, \end{aligned} \quad (141)$$

which holds for any $t > 0$. As before, we split the integral in $\partial S'_\mathcal{K}$ into the sum of two integrals (see Eq. (135))

$$e^{-t\mathcal{K}}\mathcal{K}u_0 - \pi_0\mathcal{K}u_0 = \frac{1}{2\pi i} \left(\int_{\gamma_{int}} z e^{-tz} (z - \mathcal{K})^{-1} u_0 dz + \int_{\gamma_{ext}} z e^{-tz} (z - \mathcal{K})^{-1} u_0 dz \right). \quad (142)$$

If z is located within the interior of the cusp shown Figure 8, i.e., in γ_{int} we have $|z| \leq (\alpha^2 + (8C_1)^M(1 + \alpha)^{2M})^{1/2}$. This inequality, combined with the uniform boundedness of the resolvent (136), allows us to write

$$\left\| \frac{1}{2\pi i} \int_{\gamma_{int}} e^{-tz} z (z - \mathcal{K})^{-1} u_0 dz \right\| \leq C e^{-\alpha t} \|u_0\|. \quad (143)$$

If z is in γ_{ext} then $|z| = \sqrt{[(8C_1)^{-1/2}|y|^{1/M} - 1]^2 + y^2}$, where $y = \text{Im}(z)$. To derive an upper bound for the second integral in (142), we only need to consider the case where y is large enough such that $|y|^{2/M} < |y|^2$, i.e., $|z| \leq C|y|$. A substitution of this estimate into the second integral in (142) yields

$$\begin{aligned} \left\| \frac{1}{2\pi i} \int_{\gamma_{ext}} z^n e^{-tz} (z - \mathcal{K})^{-1} u_0 dz \right\| &\leq C \|u_0\| \int_{(8C_1)^{M/2(1+\alpha)} M}^{\infty} \exp\{-t[(8C_1)^{-1/2}y^{1/M} - 1]\} y^{1-1/M} dy \\ &\leq C \|u_0\| \int_{\alpha}^{\infty} e^{-th} (h+1)^{2M-2} dh \\ &\leq \underbrace{C e^{-\alpha t} \|u_0\| \left[\frac{1}{t} + \frac{1}{t^2} + \dots + \frac{1}{t^{2M-1}} \right]}_{B(t)}, \quad t > 0. \end{aligned} \quad (144)$$

Combining (143) and (144) we conclude that the Dunford integral (141) is bounded by $B(t)$. By the triangle inequality, we have for any fixed $t > 0$ and $n \in \mathbb{N}$

$$\left\| \left\| e^{-t\mathcal{K}/n} \mathcal{K}u_0 \right\| - \left\| \pi_0 \mathcal{K}u_0 \right\| \right\| \leq \left\| e^{-t\mathcal{K}/n} \mathcal{K}u_0 - \pi_0 \mathcal{K}u_0 \right\| \leq B\left(\frac{t}{n}\right).$$

Using the operator identity $e^{-t\mathcal{K}}\mathcal{K}^n = (e^{-t\mathcal{K}/n}\mathcal{K})^n$ we obtain

$$\|e^{-t\mathcal{K}}\mathcal{K}^n u_0\| \leq \left\| e^{-t\mathcal{K}/n} \mathcal{K}u_0 \right\|^n \leq \left(B\left(\frac{t}{n}\right) + \|\pi_0 \mathcal{K}u_0\| \right)^n.$$

As easily seen from the the definition of $B(t)$ given in (144), for each fixed $t > 0$ we have

$$\lim_{n \rightarrow \infty} \frac{\|e^{-t\mathcal{K}}\mathcal{K}^n u_0\|}{n!} \leq \lim_{n \rightarrow \infty} \frac{1}{n!} \left(B\left(\frac{t}{n}\right) + \|\pi_0 \mathcal{K} u_0\| \right)^n = 0. \quad (145)$$

By using the Lagrangian representation of the residual of a truncated power series [28, p. 104], we see that (145) implies that (140) converges in norm for any $t > 0$, $s \geq t$. □

4.2.2 Projected Kolmogorov operator $\mathcal{Q}\mathcal{K}\mathcal{Q}$

In this section we analyze the semigroup $e^{-t\mathcal{Q}\mathcal{K}\mathcal{Q}}$ generated by operator $\mathcal{Q}\mathcal{K}\mathcal{Q}$, where \mathcal{K} is the Kolmogorov operator and $\mathcal{Q} = \mathcal{I} - \mathcal{P}$ is the complementary projection. Such semigroup appears in the streaming term and in the memory term of the EMZ equation (113). In principle, projection operator \mathcal{P} and therefore the complementary projection \mathcal{Q} can be chosen arbitrarily [99, 16]. Here we restrict our analysis to finite-rank, self-adjoint projections in L^2 . Mori's projection (112) is one of such projections.

Theorem 9. *Let $\mathcal{P} : L^2(\mathbb{R}^n) \rightarrow L^2(\mathbb{R}^n)$ be a finite-rank self-adjoint projection operator. If \mathcal{K} satisfies all conditions listed in Theorem 7, then the operator $\mathcal{Q}\mathcal{K}\mathcal{Q}$ has a compact resolvent whose spectrum lies within the cusp*

$$\mathcal{S}_{\mathcal{Q}\mathcal{K}\mathcal{Q}} = \{z \in \mathbb{C} \mid \operatorname{Re} z \geq 0, |\operatorname{Im} z| < (8C_{\mathcal{Q}})^{M_{\mathcal{Q}}/2} (1 + \operatorname{Re} z)^{M_{\mathcal{Q}}}\} \quad (146)$$

for some the positive constants $C_{\mathcal{Q}}$ and integer $M_{\mathcal{Q}}$.

Proof. We first show that if \mathcal{K} is closely defined and maximal-accretive, so is $\mathcal{Q}\mathcal{K}\mathcal{Q}$. According to Lumer-Phillips theorem [28], the adjoint of a maximal-accretive operator is accretive, and therefore

$$\begin{aligned} \operatorname{Re}\langle \mathcal{K}f, f \rangle &\geq 0, & \forall f \in D(\mathcal{K}), \\ \operatorname{Re}\langle \mathcal{K}^*f, f \rangle &\geq 0, & \forall f \in D(\mathcal{K}^*). \end{aligned}$$

On the other hand, if \mathcal{P} is a self-adjoint operator in $L^2(\mathbb{R}^n)$ then $\mathcal{Q} = \mathcal{I} - \mathcal{P}$ is also a self-adjoint. This implies that

$$\begin{aligned} \operatorname{Re}\langle \mathcal{Q}\mathcal{K}\mathcal{Q}f, f \rangle &= \operatorname{Re}\langle \mathcal{K}\mathcal{Q}f, \mathcal{Q}f \rangle \geq 0 & \forall f \in D(\mathcal{K}) \\ \operatorname{Re}\langle (\mathcal{Q}\mathcal{K}\mathcal{Q})^*f, f \rangle &= \operatorname{Re}\langle \mathcal{K}^*\mathcal{Q}f, \mathcal{Q}f \rangle \geq 0, & \forall f \in D(\mathcal{K}^*) \end{aligned}$$

i.e., $\mathcal{Q}\mathcal{K}\mathcal{Q}$ and its adjoint $\mathcal{Q}\mathcal{K}^*\mathcal{Q}$ are both accretive. $\mathcal{Q}\mathcal{K}\mathcal{Q}$ is also a closable operator defined in $D(\mathcal{K})$. This can be seen by decomposing it as $\mathcal{Q}\mathcal{K}\mathcal{Q} = \mathcal{K} - \mathcal{K}\mathcal{P} - \mathcal{P}\mathcal{K}\mathcal{Q}$. In fact, if \mathcal{K} is a closed operator then $\mathcal{Q}\mathcal{K}\mathcal{Q}$ is also closed since $\mathcal{K}\mathcal{P}$ and $\mathcal{P}\mathcal{K}\mathcal{Q}$ are bounded [43], as we shall see hereafter. The proof is based on two steps: First, we show that the closure of $\mathcal{Q}\mathcal{K}\mathcal{Q}$ generates a contraction semigroup $e^{-t\mathcal{Q}\mathcal{K}\mathcal{Q}}$ in $L^2(\mathbb{R}^n)$. In the second step we show that if \mathcal{K} satisfies the hypoelliptic estimate $\|u\|_{\delta,\delta} \leq C(\|u\| + \|\mathcal{K}u\|)$, then so does $\mathcal{Q}\mathcal{K}\mathcal{Q}$. i.e.

$$\|u\|_{\delta,\delta} \leq C(\|u\| + \|\mathcal{Q}\mathcal{K}\mathcal{Q}u\|). \quad (147)$$

By using triangle inequality

$$\|u\|_{\delta,\delta} \leq C(\|u\| + \|\mathcal{K}u\|) \leq C(\|u\| + \|\mathcal{K}\mathcal{P}u\| + \|\mathcal{Q}\mathcal{K}\mathcal{Q}u\| + \|\mathcal{P}\mathcal{K}\mathcal{Q}u\|)$$

To prove (147), it is sufficient to show that $\mathcal{K}\mathcal{P}$ and $\mathcal{P}\mathcal{K}\mathcal{Q}$ are bounded operators in $L^2(\mathbb{R}^n)$. To this end, we recall that the set the set of finite rank operators is dense in the space of compact operators. Moreover,

compact operators between Hilbert spaces are bounded. If, in addition we assume that P is finite-rank then we have the canonical representation

$$\mathcal{P} = \sum_{i=1}^m \lambda_i \langle \cdot, \phi_i \rangle \varphi_i \quad (148)$$

, where $\{\phi_i\}_{i=1}^m$ and $\{\varphi_i\}_{i=1}^m$ are elements $L^2(\mathbb{R}^n)$. This implies that

$$\begin{aligned} \|\mathcal{K}\mathcal{P}u\| &= \left\| \sum_{i=1}^m \lambda_i \langle u, \phi_i \rangle \mathcal{K}\varphi_i \right\| \leq \sum_{i=1}^m |\lambda_i| \|\mathcal{K}\varphi_i\| \|\phi_i\| \|u\| \leq C \|u\| \\ \|\mathcal{P}\mathcal{K}\mathcal{Q}u\| &= \left\| \sum_{i=1}^m \lambda_i \langle \mathcal{K}\mathcal{Q}u, \phi_i \rangle \varphi_i \right\| = \left\| \sum_{i=1}^m \lambda_i \langle u, \mathcal{Q}\mathcal{K}^* \phi_i \rangle \varphi_i \right\| \leq \sum_{i=1}^m |\lambda_i| \|\mathcal{Q}\mathcal{K}^* \phi_i\| \|\varphi_i\| \|u\| \leq C \|u\| \end{aligned}$$

This proves that $\mathcal{K}\mathcal{P}$ and $\mathcal{P}\mathcal{K}\mathcal{Q}$ are bounded operators. At this point we notice that since $\mathcal{Q}\mathcal{K}\mathcal{Q}$ is accretive, we have that $(\mathcal{Q}\mathcal{K}\mathcal{Q} + \mathcal{I})$ invertible. Moreover,

$$\|u\|_{\delta, \delta} \leq C(\|u\| + \|\mathcal{Q}\mathcal{K}\mathcal{Q}u\|) \leq \sqrt{2}C\|(\mathcal{Q}\mathcal{K}\mathcal{Q} + \mathcal{I})u\| \Rightarrow \|(\mathcal{Q}\mathcal{K}\mathcal{Q} + \mathcal{I})^{-1}u\|_{\delta, \delta} \leq \sqrt{2}C\|u\|,$$

i.e., $(\mathcal{Q}\mathcal{K}\mathcal{Q} + \mathcal{I})^{-1}$ is bounded from L^2 to $\mathcal{S}^{\delta, \delta}$ (see (126)). Recall that $\mathcal{S}^{\delta, \delta}$ is compactly embedded into L^2 (Lemma 3.2 [26]). Hence $(\mathcal{Q}\mathcal{K}\mathcal{Q} + 1)^{-1}$ is compact from L^2 into L^2 and therefore $\mathcal{Q}\mathcal{K}\mathcal{Q}$ has compact resolvent [43]. To prove that the discrete spectrum of $\mathcal{Q}\mathcal{K}\mathcal{Q}$ lies within the cusp $\mathcal{S}_{\mathcal{Q}\mathcal{K}\mathcal{Q}}$ defined in (146), we follow the procedure outlined in [26]. To this end, let $\mathcal{K} \in \text{Pol}_2^N$. Then, for $\delta = \max\{2, N\}$ we have the bound

$$\|(\mathcal{K} + \mathcal{I})u\| \leq C\|u\|_{\delta, \delta}, \quad \forall u \in \mathcal{S}_n.$$

and

$$\|(\mathcal{Q}\mathcal{K}\mathcal{Q} + \mathcal{I})u\| \leq \|\mathcal{Q}\|(\|\mathcal{K}u\| + \|\mathcal{K}\mathcal{P}u\|) + \|u\| \leq C(\|\mathcal{K}u\| + \|u\|) \leq \sqrt{2}C\|(\mathcal{K} + \mathcal{I})u\| \leq C\|u\|_{\delta, \delta}.$$

Recall that $\mathcal{Q}\mathcal{K}\mathcal{Q} : D(\mathcal{Q}\mathcal{K}\mathcal{Q}) \rightarrow L^2(\mathbb{R}^{2d})$ is a maximal accretive operator. Therefore, by Lemma 4.5 in [26], for all $\delta > 0$ one can find an integer $M_{\mathcal{Q}} > 0$ and a constant C such that

$$\langle u, [(\mathcal{Q}\mathcal{K}\mathcal{Q} + \mathcal{I})^*(\mathcal{Q}\mathcal{K}\mathcal{Q} + \mathcal{I})]^{1/M_{\mathcal{Q}}} u \rangle \leq C\|u\|_{\delta, \delta}^2. \quad (149)$$

By using the hypoelliptic estimate (149), (147), Proposition B.1 in [34] and the triangle inequality for $z = \text{Re } z + i \text{Im } z$, we obtain

$$\begin{aligned} \frac{1}{2}|z + 1|^{2/M_{\mathcal{Q}}}\|u\|^2 &\leq C\|u\|_{\delta, \delta}^2 + \|(\mathcal{Q}\mathcal{K}\mathcal{Q} - z)\|^2 \\ &\leq C_{\mathcal{Q}}([1 + \text{Re } z]^2\|u\|^2 + \|(\mathcal{Q}\mathcal{K}\mathcal{Q} - z)u\|^2). \end{aligned}$$

This plus the compactness of the resolvent of $\mathcal{Q}\mathcal{K}\mathcal{Q}$ imply that if $z \in \sigma(\mathcal{Q}\mathcal{K}\mathcal{Q})$ (spectrum of $\mathcal{Q}\mathcal{K}\mathcal{Q}$) then

$$\frac{1}{4}|\text{Im } z|^{2/M_{\mathcal{Q}}}\|u\|^2 \leq \frac{1}{4}|z + 1|^{2/M_{\mathcal{Q}}}\|u\|^2 \leq C_{\mathcal{Q}}(1 + \text{Re } z)^2\|u\|^2.$$

Therefore the spectrum of $\mathcal{Q}\mathcal{K}\mathcal{Q}$ is contained in the cusp-shaped region $\mathcal{S}_{\mathcal{Q}\mathcal{K}\mathcal{Q}}$ defined in (146). If $z \notin \mathcal{S}_{\mathcal{Q}\mathcal{K}\mathcal{Q}}$, then we have resolvent estimate

$$\|(\mathcal{Q}\mathcal{K}\mathcal{Q} - z)^{-1}\| \leq \sqrt{8C_{\mathcal{Q}}}|z + 1|^{-1/M_{\mathcal{Q}}}. \quad (150)$$

□

Remark The main assumption at the basis of Theorem 9 is that \mathcal{P} is a finite-rank self-adjoint projection operator, e.g., Mori's projection (112). Indeed, if \mathcal{P} is of finite-rank then both $\mathcal{K}\mathcal{P}$ and $\mathcal{P}\mathcal{K}\mathcal{Q}$ are bounded operators, which yields the hypoelliptic estimate (128). On the other hand, if \mathcal{P} is an infinite-rank projection, e.g., Chorin's projection [99, 17, 18, 102], then $\mathcal{K}\mathcal{P}$ and $\mathcal{P}\mathcal{K}\mathcal{Q}$ may not be bounded. Whether Theorem 9 holds for infinite-rank projections is an open question.

With the resolvent estimate (150) available, we can now prove the analog of Theorem 8 and Corollary 8.1, where \mathcal{K} replaced by $\mathcal{Q}\mathcal{K}\mathcal{Q}$. These results establish exponential relaxation to equilibrium of $e^{-t\mathcal{Q}\mathcal{K}\mathcal{Q}}$ and convergence of its formal power series expansion.

Theorem 10. *Assume that \mathcal{K} satisfies all conditions listed in Theorem 7. Suppose that the spectrum of $\mathcal{Q}\mathcal{K}\mathcal{Q}$ as an operator from L^2 to L^2 satisfies*

$$\sigma(\mathcal{Q}\mathcal{K}\mathcal{Q}) \cap i\mathbb{R} \subset \{0\}, \quad (151)$$

where the eigenvalue 0 (if any) has finite algebraic multiplicity. Then for any $0 < \alpha_{\mathcal{Q}} < \min(\operatorname{Re} \sigma(\mathcal{Q}\mathcal{K}\mathcal{Q})/\{0\})$, there exists a positive constant $C = C(\alpha_{\mathcal{Q}})$ such that

$$\|e^{-t\mathcal{Q}\mathcal{K}\mathcal{Q}}u_0 - \pi_0^{\mathcal{Q}}u_0\| \leq Ce^{-\alpha_{\mathcal{Q}}t}\|u_0\| \quad (152)$$

holds for all $u_0 \in L^2$ and for all $t > 0$, where $\pi_0^{\mathcal{Q}}$ is the spectral projection onto the kernel of $\mathcal{Q}\mathcal{K}\mathcal{Q}$.

Proof. The proof closely follows the proof of Theorem 8. Therefore it is omitted. □

Corollary 10.1. *Suppose that \mathcal{K} satisfies all conditions listed in Theorem 8. Then for any $u_0 \in L^2(\mathbb{R}^n)$ the power series expansion*

$$e^{-(t+s)\mathcal{Q}\mathcal{K}\mathcal{Q}}u_0 = \lim_{q \rightarrow \infty} \sum_{n=0}^q \frac{(-s)^n}{n!} e^{-t\mathcal{Q}\mathcal{K}\mathcal{Q}}(\mathcal{Q}\mathcal{K}\mathcal{Q})^n u_0 \quad (153)$$

converges in norm for any $t > 0$, $s \geq t$.

Proof. The proof closely follows the proof of Corollary 8.1. Therefore it is omitted. □

Remark The convergence results in Corollary 8.1 and Corollary 10.1 hold for all $t > 0$. An immediate consequence of these results is that the operator polynomial expansion method we proposed in [100] (see also [99] and the references therein) can be proven to be convergent when applied to the EMZ equations (113)-(114) corresponding to stochastic systems of the form (96). A similar conclusion holds for the first principle MZ memory calculation method we recently developed in [101].

An important consequence of the bound (152) is that the EMZ memory kernel $K(t)$ defined in (115c) converges to an equilibrium state exponentially fast (in time). Specifically, we have the following

Corollary 10.2. *For any scalar observable $u(t) = u(x(t))$ with initial condition $u(0) = u_0$, the EMZ memory kernel (115c) converges exponentially fast to the equilibrium state $\langle \mathcal{Q}\mathcal{K}^*u_0, \pi_0^{\mathcal{Q}}\mathcal{K}u_0 \rangle$, with rate $\alpha_{\mathcal{Q}}$. In other words, there exists a positive constant C such that*

$$|K(t) - \langle \mathcal{Q}\mathcal{K}^*u_0, \pi_0^{\mathcal{Q}}\mathcal{K}u_0 \rangle| \leq Ce^{-\alpha_{\mathcal{Q}}t}. \quad (154)$$

Proof. According to the definition (115c) we have

$$\begin{aligned} |K(t) - \langle \mathcal{Q}\mathcal{K}^*u_0, \pi_0^{\mathcal{Q}}(\mathcal{K}u_0) \rangle| &= |\langle u_0, \mathcal{K}e^{t\mathcal{Q}\mathcal{K}\mathcal{Q}}\mathcal{Q}\mathcal{K}u_0 \rangle - \langle \mathcal{Q}\mathcal{K}^*u_0, \pi_0^{\mathcal{Q}}\mathcal{K}u_0 \rangle| \\ &= |\langle \mathcal{Q}\mathcal{K}^*u_0, e^{t\mathcal{Q}\mathcal{K}\mathcal{Q}}\mathcal{K}u_0 \rangle - \langle \mathcal{Q}\mathcal{K}^*u_0, \pi_0^{\mathcal{Q}}\mathcal{K}u_0 \rangle| \end{aligned} \quad (155)$$

Since $\pi_0^{\mathcal{Q}}$ is a projection, $\pi_0^{\mathcal{Q}}\mathcal{K}u_0 - \pi_0^{\mathcal{Q}}\mathcal{K}u_0 = 0$. By using the estimates (152), (155), and the Cauchy-Schwartz inequality we finally obtain

$$|K(t) - \langle \mathcal{Q}\mathcal{K}^*u_0, \pi_0^{\mathcal{Q}}\mathcal{K}u_0 \rangle| \leq C \|\mathcal{Q}\mathcal{K}^*u_0\| \|\mathcal{K}u_0 - \pi_0^{\mathcal{Q}}\mathcal{K}u_0\| e^{-\alpha_{\mathcal{Q}}t}. \quad (156)$$

□

Remark It is rather straightforward to generalize Corollary 10.2 to matrix-valued memory kernels (115c). To this end, it is sufficient to consider each entry of the memory matrix (115c) separately, and apply Corollary 10.2 to each entry. This yields,

$$\|\mathbf{K}(t) - \mathbf{G}^{-1}\mathbf{C}^{\mathcal{Q}}\|_M \leq C \|\mathbf{G}^{-1}\mathbf{D}^{\mathcal{Q}}\|_M e^{-\alpha_{\mathcal{Q}}t}, \quad (157)$$

where $\|\cdot\|_M$ denotes any matrix norm and \mathbf{G} is the Gram matrix (115a). Also, the matrix $\mathbf{C}^{\mathcal{Q}}$ has entries $C_{ij}^{\mathcal{Q}} = \langle \mathcal{Q}\mathcal{K}^*u_i(0), \pi_0^{\mathcal{Q}}\mathcal{K}u_j(0) \rangle$, while $D_{ij}^{\mathcal{Q}} = \|\mathcal{Q}\mathcal{K}u_i(0)\| \|\mathcal{K}u_j(0) - \pi_0^{\mathcal{Q}}(\mathcal{K}u_j(0))\|$. The proof of (157) follows from the following inequality

$$\begin{aligned} \langle u_i(0), \mathcal{K}e^{t\mathcal{Q}\mathcal{K}\mathcal{Q}}\mathcal{Q}\mathcal{K}u_j(0) \rangle - \langle \mathcal{Q}\mathcal{K}^*u_i(0), \pi_0^{\mathcal{Q}}(\mathcal{K}u_j(0)) \rangle &= \langle \mathcal{Q}\mathcal{K}^*u_i(0), \mathcal{K}e^{t\mathcal{Q}\mathcal{K}\mathcal{Q}}\mathcal{Q}\mathcal{K}u_j(0) - \pi_0^{\mathcal{Q}}(\mathcal{K}u_j(0)) \rangle \\ &\leq \|\mathcal{Q}\mathcal{K}u_i(0)\| \|\mathcal{K}u_j(0) - \pi_0^{\mathcal{Q}}\mathcal{K}u_j(0)\|, \end{aligned} \quad (158)$$

In fact, a substitution of (158) into (115c) yields (157).

Remark Similarly, we can prove that the fluctuation term reaches the equilibrium state exponentially fast in time. In fact, if we choose the initial condition $\mathbf{u}_0 = \mathcal{Q}\mathcal{K}\mathbf{u}_0$ then for all $j = 1, \dots, m$ we have

$$\|f_j(t) - \pi_0^{\mathcal{Q}}\mathcal{Q}\mathcal{K}u_{0j}\| = \|e^{-t\mathcal{Q}\mathcal{K}\mathcal{Q}}\mathcal{Q}\mathcal{K}u_{0j} - \pi_0^{\mathcal{Q}}\mathcal{Q}\mathcal{K}u_{0j}\| \leq C e^{-\alpha_{\mathcal{Q}}t} \|\mathcal{Q}\mathcal{K}u_{0j}\|. \quad (159)$$

Alternatively, we can introduce the norm

$$\|\mathbf{u}(t)\|_V = \|[\|u_1(t)\|, \|u_2(t)\|, \dots, \|u_m(t)\|]\|_M$$

where $\|\cdot\|$ is the standard $L^2(\mathbb{R}^n)$ norm, and $\|\cdot\|_M$ is any matrix norm. Then from (159) it follows that

$$\|\mathbf{f}(t) - \pi_0^{\mathcal{Q}}\mathcal{Q}\mathcal{K}\mathbf{u}_0\|_V \leq C e^{-\alpha_{\mathcal{Q}}t} \|\mathbf{V}\|_M,$$

where $\mathbf{V} = (\|\mathcal{Q}\mathcal{K}u_{10}\|, \dots, \|\mathcal{Q}\mathcal{K}u_{m0}\|)$.

4.3 Application to Langevin dynamics of a particle system

All results we obtained so far are based on functional analysis, and they can be applied to arbitrary stochastic dynamical systems of the form (96), provided the MZ projection operator is of finite-rank. In this section, we study in detail a specific system, namely a particle system widely used in molecular dynamics simulations and show that the EMZ memory kernel decays exponentially fast to statistical equilibrium. One of our main

focus will be on determining the projector π_0^Q appearing in Theorem 9 and Corollary 10.2. The dynamics of a system of interacting identical particles can be modeled by the following SDE [53] in $\mathbb{R}_{p,q}^{2d}$

$$\begin{cases} \frac{d\mathbf{q}}{dt} = \frac{1}{m}\mathbf{p} \\ \frac{d\mathbf{p}}{dt} = -\nabla V(\mathbf{q}) - \frac{\gamma}{m}\mathbf{p} + \sigma\xi(t) \end{cases} \quad (160)$$

where m is the mass of each particle, $V(\mathbf{q})$ is the interaction potential and $\xi(t)$ is a d -dimensional white noise process modeling Brownian motion. The parameters γ and σ represent, respectively, the magnitude of the fluctuations and the dissipation. Such parameters are linked by the fluctuation-dissipation relation $\sigma = (2\gamma/\beta)^{1/2}$, where $\beta \propto 1/T$, T being the thermodynamic temperature. The stochastic dynamical system (160) is widely used in statistical mechanics to model mesoscopic dynamics of liquids and gases. Letting the mass m in (160) go to zero, and setting $\gamma = 1$ yields the so-called overdamped Langevin dynamics, i.e., Langevin dynamics where no average acceleration takes place. The Kolmogorov operator (107) associated with the SDE (160) is given by

$$-\mathcal{K} = \frac{\mathbf{p}}{m} \cdot \nabla_{\mathbf{q}} - \nabla_{\mathbf{q}}V(\mathbf{q}) \cdot \nabla_{\mathbf{p}} + \gamma \left(-\frac{\mathbf{p}}{m} \cdot \nabla_{\mathbf{p}} + \frac{1}{\beta}\Delta_{\mathbf{p}} \right), \quad (161)$$

where “ \cdot ” denotes the dot product. If the interaction potential $V(\mathbf{q})$ is strictly positive at infinity then the Langevin equation (160) admits a unique invariant Gibbs distribution given by

$$\rho_{eq}(\mathbf{p}, \mathbf{q}) = \frac{1}{Z} e^{-\beta H(\mathbf{p}, \mathbf{q})} \quad H(\mathbf{p}, \mathbf{q}) = \frac{\|\mathbf{p}\|_2^2}{2m} + V(\mathbf{q}), \quad (162)$$

Z being is the partition function. At this point we introduce the unitary transformation $\mathcal{U} : L^2(\mathbb{R}^{2d}) \rightarrow L^2(\mathbb{R}^{2d}; \rho_{eq})$ defined by

$$(\mathcal{U}g)(\mathbf{p}, \mathbf{q}) = \sqrt{Z} e^{\beta H(\mathbf{p}, \mathbf{q})/2} g(\mathbf{p}, \mathbf{q}), \quad (163)$$

where $L^2(\mathbb{R}^{2d}; \rho_{eq})$ is a weighted Hilbert space endowed with the inner product

$$\langle h, g \rangle_{eq} = \int h(\mathbf{p}, \mathbf{q}) g(\mathbf{p}, \mathbf{q}) \rho_{eq}(\mathbf{p}, \mathbf{q}) d\mathbf{p} d\mathbf{q} \quad (164)$$

The linear transformation (163) is an isomorphism between $L^2(\mathbb{R}^{2d})$ and $L^2(\mathbb{R}^{2d}; \rho_{eq})$. In fact, for any $\tilde{u} \in L^2(\mathbb{R}^{2d})$, there exists a unique $u \in L^2(\mathbb{R}^{2d}, \rho_{eq})$ such that $\tilde{u} = (e^{-\beta H/2}/\sqrt{Z})u$ and

$$\|\tilde{u}\|_{L^2} = \|u\|_{L_{eq}^2}. \quad (165)$$

By applying (163) to (161) we construct the following Kolmogorov operator $\tilde{\mathcal{K}} = \mathcal{U}^{-1}\mathcal{K}\mathcal{U}$, i.e.,

$$\tilde{\mathcal{K}} = -\frac{\mathbf{p}}{m} \cdot \nabla_{\mathbf{q}} + \nabla V(\mathbf{q}) \cdot \nabla_{\mathbf{p}} + \frac{\gamma}{\beta} \left(-\nabla_{\mathbf{p}} + \frac{\beta}{2m}\mathbf{p} \right) \cdot \left(\nabla_{\mathbf{p}} + \frac{\beta}{2m}\mathbf{p} \right) \quad (166)$$

which can be written in the canonical form (124), i.e.,

$$\tilde{\mathcal{K}} = \sum_{i=1}^d \mathcal{X}_i^* \mathcal{X}_i - \mathcal{X}_0 \quad (167)$$

provided we set

$$\begin{cases} \mathcal{X}_0 = \frac{\mathbf{p}}{m} \cdot \nabla_{\mathbf{q}} - \nabla V(\mathbf{q}) \cdot \nabla_{\mathbf{p}} \\ \mathcal{X}_i = \sqrt{\frac{\gamma}{\beta}} \left(\partial_{p_i} + \frac{\beta}{2m} p_i \right) \\ \mathcal{X}_i^* = \sqrt{\frac{\gamma}{\beta}} \left(-\partial_{p_i} + \frac{\beta}{2m} p_i \right) \end{cases} \quad (168)$$

Note that \mathcal{X}_0 is a skew-adjoint operator in $L^2(\mathbb{R}^{2d})$. Also, \mathcal{X}_i^* and \mathcal{X}_i can be interpreted as creation and annihilation operators of a quantum harmonic oscillator. The Kolmogorov operator $\tilde{\mathcal{K}}$ and its formal adjoint $\tilde{\mathcal{K}}^*$ are both accretive, closable and with maximally accretive closure in $L^2(\mathbb{R}^{2d})$ (see [35, 34, 25]) Similarly to the Kolmogorov operator $\tilde{\mathcal{K}} = \mathcal{U}^{-1} \mathcal{K} \mathcal{U}$, we can transform the MZ projection operators \mathcal{P} and \mathcal{Q} into operators in the “flat” Hilbert space $L^2(\mathbb{R}^{2d})$ as $\tilde{\mathcal{P}} = \mathcal{U}^{-1} \mathcal{P} \mathcal{U}$ and $\tilde{\mathcal{Q}} = \mathcal{U}^{-1} \mathcal{Q} \mathcal{U}$. The relationship between $L^2(\mathbb{R}^{2d})$, $L^2(\mathbb{R}^{2d}; \rho_{eq})$ and the operators defined therein can be summarized by the following commutative diagram

$$\begin{array}{ccc} L^2(\mathbb{R}^{2d}) & \xrightarrow{\mathcal{U}} & L^2(\mathbb{R}^{2d}; \rho_{eq}) \\ \tilde{\mathcal{P}}, \tilde{\mathcal{K}}, \tilde{\mathcal{Q}} \downarrow & & \downarrow \mathcal{P}, \mathcal{K}, \mathcal{Q} \\ L^2(\mathbb{R}^{2d}) & \xleftarrow{\mathcal{U}^{-1}} & L^2(\mathbb{R}^{2d}; \rho_{eq}) \end{array}$$

The properties of all operators defined in $L^2(\mathbb{R}^{2d})$ and $L^2(\mathbb{R}^{2d}; \rho_{eq})$ are essentially the same since \mathcal{U} is an isomorphism. For instance if \mathcal{P} is compact and self-adjoint then $\tilde{\mathcal{P}}$ is also compact and self-adjoint.

Next, we apply the analytical results we obtained in Section 4.2.1 and Section 4.2.2. To this end, we just need to verify whether $\tilde{\mathcal{K}}$ is a poly-Hörmander operator, i.e., if the operators $\{\mathcal{X}_i\}_{i=0}^d$ appearing in (167)-(168) satisfy the poly-Hörmander conditions in Proposition 1 and the estimate Theorem 7 (see Section 4.2.1). This can be done by imposing additional conditions on the particle interaction potential $V(\mathbf{q})$, and then following the mathematical steps in [25, Proposition 3.7]. In particular, following Helffer and Nier [34], we assume $V(\mathbf{q})$ satisfies the following ellipticity hypothesis

Hypothesis 1. *The particle interaction potential $V(\mathbf{q})$ is of class $C^\infty(\mathbb{R}^d)$, and it satisfies*

1. $\forall \alpha \in \mathbb{N}^d, |\alpha| = 1, \forall \mathbf{q} \in \mathbb{R}^d, |\partial_{\mathbf{q}}^\alpha V(\mathbf{q})| \leq C_\alpha \sqrt{1 + \|\nabla V(\mathbf{q})\|^2}$ for some positive constant C_α ,
2. $\exists M, C \geq 1, \forall \mathbf{q} \in \mathbb{R}^d, C^{-1}(1 + \|\mathbf{q}\|^2)^{1/(2M)} \leq \sqrt{1 + \|\nabla V(\mathbf{q})\|^2} \leq C(1 + \|\mathbf{q}\|^2)^{M/2}$.

Hypothesis 1 holds for any particle interaction potential that grows at most polynomially, i.e., $V(\mathbf{q}) \simeq \|\mathbf{q}\|^M$, as $\mathbf{q} \rightarrow \infty$. With this hypothesis, it is possible to prove the following

Proposition 2 (Helffer and Nier [34]). *Consider the Langevin equation (160) with particle interaction potential $V(\mathbf{q})$ satisfying Hypothesis 1. Then the operator $\tilde{\mathcal{K}}$ defined in (166) has compact resolvent, with spectrum bounded by the cusp $\mathcal{S}_{\tilde{\mathcal{K}}}$. Moreover, there exists a positive constant C such that the estimate*

$$\|e^{-t\tilde{\mathcal{K}}} u_0 - \tilde{\pi}_0 \tilde{u}_0\| \leq C e^{-\alpha t} \|\tilde{u}_0\| \quad (169)$$

holds for all $\tilde{u}_0 \in L^2(\mathbb{R}^{2d})$ and for all $t > 0$, where $\tilde{\pi}_0$ is the orthogonal projection onto the kernel of $\tilde{\mathcal{K}}$ in $L^2(\mathbb{R}^{2d})$.

By using the isomorphism (163) we can now rewrite Proposition 2 in $L^2(\mathbb{R}^{2d}; \rho_{eq})$ as

$$\|e^{-t\mathcal{K}}u_0 - \pi_0 u_0\|_{L^2_{eq}} = \|e^{-t\tilde{\mathcal{K}}}\tilde{u}_0 - \tilde{\pi}_0 \tilde{u}_0\|_{L^2} \leq C e^{-\alpha t} \|\tilde{u}_0\|_{L^2} = C e^{-\alpha t} \|u_0\|_{L^2_{eq}}, \quad (170)$$

where $\pi_0 = \mathcal{U}\tilde{\pi}_0\mathcal{U}^{-1}$ is the orthogonal projection onto linear subspace $\mathbb{1}$ with respect to the $L^2(\mathbb{R}^{2d}; \rho_{eq})$ norm. We also notice that $\pi_0(\cdot) = \mathbb{E}[(\cdot)]$. The inequality (170) is completely equivalent to the estimate (133). It is also possible to obtain a prior estimate on the convergence rate α by building a between the Kolmogorov operator and the Witten Laplacian (see [35, 34] for further details).

Our next task is to derive an estimate for the operator $\tilde{\mathcal{Q}}\tilde{\mathcal{K}}\tilde{\mathcal{Q}}$, and for the semigroup $e^{-t\tilde{\mathcal{Q}}\tilde{\mathcal{K}}\tilde{\mathcal{Q}}}$ generated by $\tilde{\mathcal{Q}}\tilde{\mathcal{K}}\tilde{\mathcal{Q}}$. According to Theorem 9, the spectrum of $\tilde{\mathcal{Q}}\tilde{\mathcal{K}}\tilde{\mathcal{Q}}$ is bounded by the cusp $\mathcal{S}_{\tilde{\mathcal{Q}}\tilde{\mathcal{K}}\tilde{\mathcal{Q}}}$, provided \mathcal{P} is a finite-rank projection. On the other hand, Theorem 10 establishes exponential convergence of $e^{-t\tilde{\mathcal{Q}}\tilde{\mathcal{K}}\tilde{\mathcal{Q}}}$ to equilibrium if $\tilde{\mathcal{Q}}\tilde{\mathcal{K}}\tilde{\mathcal{Q}}$ satisfies condition (151). To determine the exact form of the spectral projection $\tilde{\pi}_0^{\tilde{\mathcal{Q}}}$, i.e., the projection onto the kernel of $\tilde{\mathcal{Q}}\tilde{\mathcal{K}}\tilde{\mathcal{Q}}$ (see Theorem 10) we consider a general Mori-type projection \mathcal{P} and its unitarily equivalent version $\tilde{\mathcal{P}} = \mathcal{U}^{-1}\mathcal{P}\mathcal{U}$

$$\mathcal{P}(\cdot) = \sum_{i=1}^m \langle \cdot, g_i(\mathbf{q}) \rangle_{eq} g_i(\mathbf{q}) \quad \tilde{\mathcal{P}}(\cdot) = \sum_{i=1}^m \langle \cdot, g_i(\mathbf{q}) \rangle_{eq/2} g_i(\mathbf{q}) e^{-\beta H/2}, \quad (171)$$

where $\{g_j(\mathbf{q})\}_{j=1}^m$ are zero-mean⁸ orthonormal basis functions. In (171) we used the shorthand notation

$$\langle h \rangle_{eq/2} = \frac{1}{Z} \int g(\mathbf{p}, \mathbf{q}) e^{-\beta H(\mathbf{p}, \mathbf{q})/2} d\mathbf{p} d\mathbf{q}. \quad (172)$$

Lemma 11. *Suppose that the particle interaction potential $V(\mathbf{q})$ in the SDE (161) satisfies Hypothesis 1. Then*

$$Ker(\tilde{\mathcal{Q}}\tilde{\mathcal{K}}\tilde{\mathcal{Q}}) = Ker(\tilde{\mathcal{K}}) \oplus Id(\tilde{\mathcal{P}}), \quad (173)$$

$$\sigma(\tilde{\mathcal{Q}}\tilde{\mathcal{K}}\tilde{\mathcal{Q}}) \cap i\mathbb{R} \subset \{0\}, \quad (174)$$

where $\tilde{\mathcal{K}}$ and $\tilde{\mathcal{P}}$ are defined in (166) and (171), respectively, and $Id(\tilde{\mathcal{P}}) = \{u \in L^2(\mathbb{R}^{2d}) : \tilde{\mathcal{P}}u = u\}$ is a finite-dimensional linear space.

Proof. We first prove (173). If $u \in Ker(\tilde{\mathcal{Q}}\tilde{\mathcal{K}}\tilde{\mathcal{Q}})$ then $\tilde{\mathcal{Q}}\tilde{\mathcal{K}}\tilde{\mathcal{Q}}u = 0$. Therefore we can only have one of the following three cases: i) $\tilde{\mathcal{Q}}u = 0$; ii) $\tilde{\mathcal{Q}}u \neq 0, \tilde{\mathcal{K}}\tilde{\mathcal{Q}}u = 0$; and iii) $\tilde{\mathcal{Q}}u \neq 0, \tilde{\mathcal{K}}\tilde{\mathcal{Q}}u \neq 0, \tilde{\mathcal{Q}}\tilde{\mathcal{K}}\tilde{\mathcal{Q}}u = 0$. Hereafter we discuss these cases separately.

Case 1 If $\tilde{\mathcal{Q}}u = 0$ then $\tilde{\mathcal{P}}u = u - \tilde{\mathcal{Q}}u = u$, i.e., $u \in Id(\tilde{\mathcal{P}})$.

Case 2 If $\tilde{\mathcal{Q}}u \neq 0$ and $\tilde{\mathcal{K}}\tilde{\mathcal{Q}}u = 0$, then we have that $\tilde{\mathcal{Q}}u \in Ker(\tilde{\mathcal{K}})$. We first prove that $\tilde{\mathcal{Q}}u \in Ker(\tilde{\mathcal{K}}) \Rightarrow u \in Id(\tilde{\mathcal{P}}) \oplus Ker(\tilde{\mathcal{K}})$. Since $\tilde{\mathcal{P}}$ is an orthogonal, finite-rank projection in $L^2(\mathbb{R}^n)$ (see Eq. (171)), we have that $Id(\tilde{\mathcal{P}}) = Range(\tilde{\mathcal{P}}) = \text{span}\{g_i(\mathbf{q})e^{-\beta H(\mathbf{p}, \mathbf{q})/2}\}_{i=1}^m$. At this point, we write u as

$$u = \tilde{\mathcal{P}}u + \tilde{\mathcal{Q}}u = \sum_{i=1}^m c_i g_i(\mathbf{q}) e^{-\beta H/2} + c' e^{-\beta H/2} \in Id(\tilde{\mathcal{P}}) \oplus Ker(\tilde{\mathcal{K}}), \quad c_i, c' \in \mathbb{R}$$

Let us verify that if $u \in Id(\tilde{\mathcal{P}}) \oplus Ker(\tilde{\mathcal{K}})$ then $\tilde{\mathcal{K}}\tilde{\mathcal{Q}}u = 0$, i.e. $\tilde{\mathcal{Q}}u \in Ker(\tilde{\mathcal{K}})$. To this end,

$$\tilde{\mathcal{K}}\tilde{\mathcal{Q}}u = \tilde{\mathcal{K}}(u - \tilde{\mathcal{P}}u) = \tilde{\mathcal{K}}c' e^{-\beta H/2} - c' \tilde{\mathcal{P}}\tilde{\mathcal{K}}e^{-\beta H/2} = c' e^{-\beta H/2} \in Ker(\tilde{\mathcal{K}}) \Rightarrow \tilde{\mathcal{K}}\tilde{\mathcal{Q}}u = 0.$$

⁸Zero-mean here means that $\langle g_j \rangle_{eq} = 0$.

Case 3. Let us assume that $\tilde{Q}u \neq 0$, $\tilde{K}\tilde{Q}u \neq 0$ and $\tilde{Q}\tilde{K}\tilde{Q}u = 0$. If u satisfies these three conditions, then we have

$$\langle \tilde{Q}\tilde{K}\tilde{Q}u, u \rangle = \langle \tilde{K}\tilde{Q}u, \tilde{Q}u \rangle = 0, \quad \tilde{Q}u \neq 0, \quad \tilde{K}\tilde{Q}u \neq 0. \quad (175)$$

Upon definition of $g = \tilde{Q}u$, we can write (175) as $\langle \tilde{K}g, g \rangle = 0, g \neq 0, \tilde{K}g \neq 0$. This suggests that $\text{Re}\langle \tilde{K}g, g \rangle = \sum_{i=1}^d \langle \mathcal{X}_i g, \mathcal{X}_i g \rangle = 0$, which implies that g belonging to the kernel of all annihilation operators $\mathcal{X}_i, 1 \leq i \leq d$. Therefore g must be of the form $g = \mu(\mathbf{q})e^{-\beta\|\mathbf{p}\|^2/(4m)}$. On the other hand, since $\tilde{Q}\tilde{K}\tilde{Q}u = \tilde{Q}\tilde{K}g = 0$, we have that $\tilde{P}\tilde{K}g = \tilde{K}g$. A substitution of general form of g into this expression yields

$$\tilde{K}g = \mathcal{X}_0 g = \sum_{i=1}^d p_i \left[\frac{1}{m} \partial_{q_i} \mu(\mathbf{q}) - \frac{\beta}{2m} \mu(\mathbf{q}) \partial_{q_i} V(\mathbf{q}) \right] e^{-\beta\|\mathbf{p}\|^2/(4m)} = \sum_{i=1}^d F_i(\mathbf{q}) p_i e^{-\beta\|\mathbf{p}\|^2/(4m)} \quad (176)$$

Thus,

$$\tilde{P}\tilde{K}g = \sum_{i=1}^N \langle \tilde{K}g, g_i(\mathbf{q}) \rangle_{e_{q/2} g_j(\mathbf{q})} e^{-\frac{\beta}{2}V(\mathbf{q})} e^{-\beta\|\mathbf{p}\|^2/(4m)}. \quad (177)$$

The function $\mathbf{F}(\mathbf{q})$ appearing in (176) is a d -dimensional vector field that depends on the position \mathbf{q} . It is clear that $tP\tilde{K}g = \tilde{K}g$ if and only if $\tilde{K}g$, which contradicts the assumption $\tilde{K}\tilde{Q}u \neq 0$. Hence we conclude that there is no u that simultaneously satisfies $\tilde{Q}\tilde{K}\tilde{Q}u = 0, \tilde{Q}u \neq 0$ and $\tilde{K}\tilde{Q}u \neq 0$. This means that the kernel of operator $\tilde{K}\tilde{Q}\tilde{K}$ is the finite-dimensional linear space $\text{Ker}(\tilde{K}) \oplus \text{Id}(\tilde{P})$.

Now we prove (174). Such condition states that the only eigenvalue of $\tilde{Q}\tilde{K}\tilde{Q}$ on the imaginary axis $i\mathbb{R}$ is the origin. Equivalently, this means that for all $u \in L^2(\mathbb{R}^{2d})$ such that $\tilde{Q}\tilde{K}\tilde{Q}u = i\lambda u$ ($\lambda \in \mathbb{R}$), we have that $\lambda = 0$. To see this, we choose $g = \tilde{Q}u$, $\tilde{Q}\tilde{K}\tilde{Q}u = i\lambda u$ implies $\text{Re}\langle \tilde{Q}\tilde{K}\tilde{Q}u, u \rangle = \text{Re}\langle \tilde{K}g, g \rangle = 0$, which again implies $g = \mu(\mathbf{q})e^{-\beta\|\mathbf{p}\|^2/(4m)}$. Since g is a real function and \mathcal{X}_0 a real operator, we have $\text{Im}\langle \tilde{K}g, g \rangle = \text{Im}\langle \mathcal{X}_0 g, g \rangle = 0$. Therefore, if $\tilde{Q}\tilde{K}\tilde{Q}u = i\lambda u$ and $\lambda \in \mathbb{R}$, then we must have $\lambda = 0$. \square

Lemma 11 allows us to derive the following exponential convergence result for the semigroup e^{-tQKQ} .

Proposition 3. *Suppose that the particle interaction potential $V(\mathbf{q})$ in the SDE (161) satisfies Hypothesis 1. Then there exists a positive constant C such that*

$$\|e^{-tQKQ}u_0 - \pi_0^Q u_0\|_{L_{e_q}^2} \leq C e^{-\alpha_Q t} \|u_0\|_{L_{e_q}^2} \quad (178)$$

for all $u_0 \in L^2(\mathbb{R}^{2d}, \rho_{e_q})$ and for all $t > 0$. In (178), \mathcal{P} is the finite-rank projection (171), while

$$(179)$$

$$p_i^Q(\cdot) = \pi_0(\cdot) + \mathcal{P}(\cdot) \quad (180)$$

is the orthogonal projection onto the linear space $\text{Ker}(\mathcal{K}) \oplus \text{Id}(\mathcal{P})$.

Proof. We first rewrite (178) as an $L^2(\mathbb{R}^{2d})$ estimation problem as

$$\|e^{-t\tilde{Q}\tilde{K}\tilde{Q}}\tilde{u}_0 - \tilde{\pi}_0^{\tilde{Q}}\tilde{u}_0\|_{L^2} \leq C e^{-\alpha_Q t} \|\tilde{u}_0\|_{L^2} \quad (181)$$

where $\tilde{\pi}_0^{\tilde{Q}} = \mathcal{U}^{-1}\pi_0^Q\mathcal{U}$. According to Proposition 2, The transformed Kolmogorov operator \tilde{K} is of the form (124). We know that such operator has compact resolvent and cusp-shaped spectrum. Then by Theorem 9 the operator $\tilde{Q}\tilde{K}\tilde{Q}$ has the same properties, provided \tilde{P} is a finite-rank projection. To derive the estimate (178) we can use Theorem 10. To this end, we need to make sure that the following conditions are met

1. The spectral projection appearing in Theorem 10 can be replaced by a projection operator $\tilde{\pi}_0^{\tilde{Q}}$ in $L^2(\mathbb{R}^{2d})$, which projects any $u \in L^2(\mathbb{R}^{2d})$ onto the linear subspace $Ker(\tilde{Q}\tilde{K}\tilde{Q})$, i.e., $Range(\tilde{\pi}_0^{\tilde{Q}}) = Ker(\tilde{Q}\tilde{K}\tilde{Q}) = Id(\tilde{P}) \oplus Ker(\tilde{K})$;
2. $\pi_0^{\tilde{Q}}$ is an orthogonal operator in $L^2(\mathbb{R}^{2d}; \rho_{eq})$ given by (179) (up to an isomorphism).

Proof of condition 1 The projection operator \tilde{P} is self-adjoint, and therefore $Id(\tilde{P}) = Id(\tilde{P}^*)$. In [34], Helffer and Nier proved that $Ker(\tilde{K}) = Ker(\tilde{K}^*) = \mathbb{R}e^{-\beta H}$. Hence,

$$Ker(\tilde{Q}\tilde{K}\tilde{Q}) = Ker(\tilde{Q}\tilde{K}^*\tilde{Q}) = Ker(\tilde{K}) \oplus Id(\tilde{P}) \quad (182)$$

We now consider the orthogonal decomposition of the Hilbert space $L^2(\mathbb{R}^{2d})$

$$L^2(\mathbb{R}^{2d}) = Ker(\tilde{Q}\tilde{K}\tilde{Q}) \oplus Ker(\tilde{Q}\tilde{K}\tilde{Q})^\perp,$$

If we define a projection operator $\pi_0^{\tilde{Q}}$ with range $Range(\pi_0^{\tilde{Q}}) = Ker(\tilde{Q}\tilde{K}\tilde{Q})$, then for any $u_0 \in L^2(\mathbb{R}^{2d})$, we have the orthogonal decomposition

$$\tilde{u}_0 = \pi_0^{\tilde{Q}}\tilde{u}_0 + (\tilde{u}_0 - \pi_0^{\tilde{Q}}\tilde{u}_0), \quad \text{where } \pi_0^{\tilde{Q}}\tilde{u}_0 \in Ker(\tilde{Q}\tilde{K}\tilde{Q}), \quad \tilde{u}_0 - \pi_0^{\tilde{Q}}\tilde{u}_0 \in Ker(\tilde{Q}\tilde{K}\tilde{Q})^\perp.$$

We now verify that $\tilde{Q}\tilde{K}\tilde{Q}$ maps the linear subspace $Ker(\tilde{Q}\tilde{K}\tilde{Q})^\perp$ into itself, i.e., that for any $u \in Ker(\tilde{Q}\tilde{K}\tilde{Q})^\perp$ we have that $\tilde{Q}\tilde{K}\tilde{Q}u \in Ker(\tilde{Q}\tilde{K}\tilde{Q})^\perp$. To this we first notice that if $w \in Ker(\tilde{Q}\tilde{K}\tilde{Q})$ then

$$\langle \tilde{Q}\tilde{K}\tilde{Q}u, w \rangle = \langle u, \tilde{Q}\tilde{K}^*\tilde{Q}w \rangle = 0.$$

In fact $Ker(\tilde{Q}\tilde{K}\tilde{Q}) = Ker(\tilde{Q}\tilde{K}^*\tilde{Q})$. On the other hand, if $u \in Ker(\tilde{Q}\tilde{K}\tilde{Q})^\perp$ then $\tilde{Q}\tilde{K}\tilde{Q}u \neq 0$ and therefore we must have $\tilde{Q}\tilde{K}\tilde{Q}u \in Ker(\tilde{Q}\tilde{K}\tilde{Q})^\perp$. The operator $\tilde{Q}\tilde{K}\tilde{Q}$ and its adjoint $\tilde{Q}\tilde{K}^*\tilde{Q}$ can be decomposed as

$$\tilde{Q}\tilde{K}\tilde{Q} = \tilde{Q}\tilde{K}\tilde{Q}|_{Ker(\tilde{Q}\tilde{K}\tilde{Q})} \oplus \tilde{Q}\tilde{K}\tilde{Q}|_{Ker(\tilde{Q}\tilde{K}\tilde{Q})^\perp}, \quad \tilde{Q}\tilde{K}^*\tilde{Q} = \tilde{Q}\tilde{K}^*\tilde{Q}|_{Ker(\tilde{Q}\tilde{K}\tilde{Q})} \oplus \tilde{Q}\tilde{K}^*\tilde{Q}|_{Ker(\tilde{Q}\tilde{K}\tilde{Q})^\perp}.$$

This allows us to deform the domain of the Dunford integral representing $e^{t\tilde{Q}\tilde{K}\tilde{Q}}\tilde{u}_0 - \tilde{\pi}_0^{\tilde{Q}}\tilde{u}_0$ from $[-i\infty, +i\infty]$ to the cusp $S'_{\tilde{Q}\tilde{K}\tilde{Q}}$, as we did in Theorem 8. This yields

$$e^{t\tilde{Q}\tilde{K}\tilde{Q}}\tilde{u}_0 - \tilde{\pi}_0^{\tilde{Q}}\tilde{u}_0 = e^{t\tilde{Q}\tilde{K}\tilde{Q}} \left(\tilde{u}_0 - \tilde{\pi}_0^{\tilde{Q}}\tilde{u}_0 \right) = \frac{1}{2\pi i} \int_{\partial S'_{\tilde{Q}\tilde{K}\tilde{Q}}} e^{-tz} \left(z - \tilde{Q}\tilde{K}\tilde{Q} \right)^{-1} \tilde{u}_0 dz.$$

At this point we can follow the exact same procedure in the proofs of Theorem 8 and Theorem 9, to prove the semigroup estimate (178).

Proof of condition 2 Here we show that $\tilde{\pi}_0^{\tilde{Q}}$ is an orthogonal projection in $L^2(\mathbb{R}^{2d})$ given by

$$\tilde{\pi}_0^{\tilde{Q}}(\cdot) = \tilde{\pi}_0(\cdot) + \tilde{P}(\cdot) = \langle \cdot \rangle_{eq/2} e^{-\beta H/2} + \sum_{i=1}^m \langle \cdot, g_i(\mathbf{q}) \rangle_{eq/2} g_i(\mathbf{q}) e^{-\beta H/2}, \quad (183)$$

up to an isomorphism. Since $\tilde{\pi}_0^{\tilde{Q}}$ and its adjoint are both projections, they can be used to decompose $L^2(\mathbb{R}^{2d})$ as

$$L^2(\mathbb{R}^{2d}) = Ker\left(\tilde{\pi}_0^{\tilde{Q}}\right) \oplus Range\left(\tilde{\pi}_0^{\tilde{Q}}\right), \quad L^2(\mathbb{R}^{2d}) = Ker\left(\left[\tilde{\pi}_0^{\tilde{Q}}\right]^*\right) \oplus Range\left(\left[\tilde{\pi}_0^{\tilde{Q}}\right]^*\right)$$

It follows from (182) that $\text{Range}(\tilde{\pi}_0^{\tilde{\mathcal{Q}}}) = \text{Range}([\tilde{\pi}_0^{\tilde{\mathcal{Q}}}]^*) = \text{Ker}(\tilde{\mathcal{Q}}\tilde{\mathcal{K}}\tilde{\mathcal{Q}})$. This implies $\text{Ker}(\tilde{\pi}_0^{\tilde{\mathcal{Q}}}) = \text{Ker}([\tilde{\pi}_0^{\tilde{\mathcal{Q}}}]^*)$. Since for all $u, w \in L^2(\mathbb{R}^{2d})$, $w - \tilde{\pi}_0^{\tilde{\mathcal{Q}}}w \in \text{Ker}(\tilde{\pi}_0^{\tilde{\mathcal{Q}}})$, we have that

$$\langle \tilde{p}_0^{\tilde{\mathcal{Q}}}u, w - \tilde{\pi}_0^{\tilde{\mathcal{Q}}}w \rangle = \langle u, [\tilde{\pi}_0^{\tilde{\mathcal{Q}}}]^*(w - \tilde{\pi}_0^{\tilde{\mathcal{Q}}}w) \rangle = 0.$$

Therefore $\tilde{\pi}_0^{\tilde{\mathcal{Q}}}$ is an orthogonal projection operator. On the other hand, since $\text{Id}(\tilde{\mathcal{P}}) = \text{Range}(\tilde{\mathcal{P}})$ and $\tilde{\mathcal{P}}$ itself is an orthogonal operator, the projection $\tilde{\pi}_0^{\tilde{\mathcal{Q}}}$ is therefore given by (183) (unique up to an isomorphism). \square

4.3.1 EMZ memory and fluctuation terms

Theorem 3 allows us to prove that the EMZ memory kernel (115c) and the fluctuation term (115d) converge exponentially fast to an equilibrium state. Specifically,

Corollary 11.1. *Suppose that the particle interaction potential $V(\mathbf{q})$ in the SDE (161) satisfies Hypothesis 1. Let \mathcal{P} a Mori-type projection operator associated with scalar observable $u(t) = u(x(t))$ such that $\text{Ker}(\mathcal{Q}\mathcal{K}\mathcal{Q}) = \text{Ker}(\mathcal{K}) \oplus \text{Id}(\mathcal{P})$. Then the memory kernel of (115c) converges exponentially converges to the equilibrium state $\mathbb{E}[\mathcal{K}u_0]\mathbb{E}[\mathcal{Q}\mathcal{K}^*u_0]$ with rate $\alpha_{\mathcal{Q}}$, i.e.*

$$|K(t) - \mathbb{E}[\mathcal{K}u_0]\mathbb{E}[\mathcal{Q}\mathcal{K}^*u_0]| \leq Ce^{-\alpha_{\mathcal{Q}}t}. \quad (184)$$

Proof. The Corollary follows immediately from (154), (179) and the fact that $\mathcal{P}\mathcal{Q} = 0$. \square

We emphasize that the equilibrium state $\mathbb{E}[\mathcal{K}u_0]\mathbb{E}[\mathcal{Q}\mathcal{K}^*u_0]$ the EMZ memory kernel $K(t)$ converges to can be explicitly calculated. It is straightforward to extend (184) to matrix-valued memory kernels (115c). By following the same steps that lead us to (157), we obtain

$$\|\mathbf{K}(t) - \mathbf{G}^{-1}\mathbf{C}^{\mathcal{Q}}\|_M \leq C\|\mathbf{G}^{-1}\mathbf{D}^{\mathcal{Q}}\|_M e^{-\alpha_{\mathcal{Q}}t}, \quad (185)$$

where $\|\cdot\|_M$ denotes any matrix norm, and \mathbf{G} is the Gram matrix (115a). The entries of the matrix $\mathbf{C}^{\mathcal{Q}}$ are given by $C_{ij}^{\mathcal{Q}} = \mathbb{E}[\mathcal{Q}\mathcal{K}^*u_i(0)]\mathbb{E}[\mathcal{K}u_j(0)]$, while $D_{ij}^{\mathcal{Q}} = \mathbb{E}[\mathcal{Q}\mathcal{K}u_i(0)]\mathbb{E}[\mathcal{Q}\mathcal{K}u_j(0) - \mathbb{E}[\mathcal{K}u_j(0)]]$. The components of the EMZ fluctuation term (115d) decay to an equilibrium state as well, exponentially fast in time. In fact, if we choose the initial condition as $\mathbf{u}_0 = \mathcal{Q}\mathcal{K}\mathbf{u}_0$, then (152) yields the following estimate

$$\mathbb{E}[f_i(t) - \mathbb{E}[\mathcal{Q}\mathcal{K}u_i(0)]] \leq Ce^{-\alpha_{\mathcal{Q}}t}\mathbb{E}[\mathcal{Q}\mathcal{K}u_i(0)]. \quad (186)$$

The estimate (186) can be also written in a vector form as

$$\|\mathbf{f}(t) - \mathbb{E}[\mathcal{Q}\mathcal{K}\mathbf{u}(0)]\|_V \leq Ce^{-\alpha_{\mathcal{Q}}t}\|\mathbf{V}\|_M, \quad (187)$$

where $\mathbf{V} = (\mathbb{E}[\mathcal{Q}\mathcal{K}u_1(0)], \dots, \mathbb{E}[\mathcal{Q}\mathcal{K}u_m(0)])$, $\|\cdot\|_M$ is any matrix norm and

$$\|\mathbf{h}(t)\|_V = \|\mathbb{E}[u_1(t)], \dots, \mathbb{E}[u_m(t)]\|_M. \quad (188)$$

5 Approximation methods for the MZ equation

Computing the solution to the MZ equation is a challenging task that relies on approximations and appropriate numerical schemes [84, 12, 82]. One of the main difficulties is the approximation of the memory integral (convolution term), which encodes the effects of the so-called orthogonal dynamics in the time evolution

of the quantity of interest. The orthogonal dynamics is essentially a high-dimensional flow that satisfies a complex integro-differential equation. Such flow usually has the same order of magnitude and dynamical properties as the quantity of interest, i.e., there is no scale separation between the resolved and the orthogonal dynamics [88]. In these cases, the computation of the MZ memory integral can be addressed only by problem-class-dependent approximations. The first effective technique was developed by Hazime Mori in [64]. The method relies on continued fraction expansions, and it can be conveniently formulated in terms of recurrence relations [79, 40, 52, 51, 39]. The continued fraction expansion method of Mori made it possible to compute the exact solution of important prototype problems in statistical mechanics, such as the dynamics of the auto-correlation function of a tagged oscillator in an harmonic chain [29, 44]. Other effective approaches to approximate the MZ memory integral rely on perturbation methods [94, 76, 89], mode coupling theories [2, 78, 77], or functional approximation methods [31, 33, 65]. In a parallel effort, the applied mathematics community has, in recent years, attempted to derive general easy-to-compute representations of the MZ memory integral [88, 32]. In particular, various approximations such as the t -model [15, 18, 81, 12], hierarchical perturbation methods [84, 99, 89], and data-driven methods [53, 9] were proposed to address approximation of the MZ memory integral in situations where there is no clear separation of scales between the resolved and the unresolved dynamics.

5.1 Operator series expansions

In this section, we discuss approximation methods for the MZ equation based on operator series expansions of the orthogonal dynamics propagator. Specifically, we study the Faber series, which yields asymptotically optimal approximations converging at least superlinearly with the polynomial order (for linear dynamical systems). The advantages of expanding the orthogonal dynamics propagator in terms of globally defined operator series are similar to those we obtain when we approximate a smooth function in terms of orthogonal polynomials rather than Taylor series [36]. The proposed memory approximation method can outperform in terms of accuracy the hierarchical memory approximation technique proposed by Stinis in [82] (see also [99]), which is based on Taylor series. Most of the analysis and numerical results presented in this section are for high-dimensional linear dynamical systems evolving from random initial states. The extension to nonlinear systems is straightforward, but its practical implementation is limited by the same computational bottlenecks that made it difficult to obtain high-order expansions in [15, 82, 81, 84]. To describe the method consider the Mori-Zwanzig memory integral (see Eq. (17))

$$\int_0^t \mathcal{P} e^{s\mathcal{L}} \mathcal{P} \mathcal{L} e^{(t-s)\mathcal{Q}\mathcal{L}} \mathcal{Q} \mathcal{L} \mathbf{u}_0 ds \quad (189)$$

Expand the orthogonal dynamics propagator $e^{t\mathcal{Q}\mathcal{L}}$ as

$$e^{t\mathcal{Q}\mathcal{L}} = \sum_{n=0}^{\infty} a_n(t) \Phi_n(\mathcal{Q}\mathcal{L}), \quad (190)$$

where Φ_n are polynomial basis functions, and $a_n(t)$ are temporal modes. Series expansions in the form (190) can be rigorously defined in the context of matrix theory [61, 62], i.e., for operators $\mathcal{Q}\mathcal{L}$ between finite-dimensional vector spaces. The question of whether it is possible to extend such expansions to the infinite-dimensional case, i.e., for operators acting between infinite-dimensional Hilbert or Banach spaces, is not a trivial [21]. For example, it is well-known that the classical Taylor series

$$e^{t\mathcal{L}} = \sum_{k=0}^{\infty} \frac{t^k}{k!} \mathcal{L}^k \quad (191)$$

does not hold if \mathcal{L} is an unbounded operator, e.g., the generator of the Koopman semigroup (see [43], p. 481). In the latter case, $e^{t\mathcal{L}}$ should be properly defined as

$$e^{t\mathcal{L}} = \lim_{n \rightarrow \infty} \left(1 - \frac{t\mathcal{L}}{n}\right)^{-n}. \quad (192)$$

In fact, $(1 - t\mathcal{L}/n)^{-1}$ is the resolvent of \mathcal{L} (apart from a constant factor), which can be defined for both bounded and unbounded linear operators. Despite the theoretical issues associated with the existence of convergent series expansions of semigroups generated by unbounded operators [28, 43], when it comes to computing we always need to discretize the system, most often by discretizing the generator of the semigroup. In this setting, $e^{t\mathcal{L}}$ is truly a matrix exponential, where, with some abuse of notation, we denoted by \mathcal{Q} and \mathcal{L} the finite-dimensional representation⁹ of the operators \mathcal{Q} and \mathcal{L} .

5.1.1 MZ-Dyson expansion

A substitution of the classical Taylor series expansion of the orthogonal dynamics propagator

$$e^{t\mathcal{Q}\mathcal{L}} = \sum_{n=0}^{\infty} \frac{t^n}{n!} (\mathcal{Q}\mathcal{L})^n \quad (193)$$

into the MZ equation (7) yields

$$\begin{aligned} \frac{\partial}{\partial t} \mathcal{P}e^{t\mathcal{L}}\mathbf{u}_0 &= \mathcal{P}e^{t\mathcal{L}}\mathcal{P}\mathcal{L}\mathbf{u}_0 + \int_0^t \mathcal{P}e^{s\mathcal{L}}\mathcal{P}\mathcal{L}e^{(t-s)\mathcal{Q}\mathcal{L}}\mathcal{Q}\mathcal{L}\mathbf{u}_0 ds, \\ &= \mathcal{P}e^{t\mathcal{L}}\mathcal{P}\mathcal{L}\mathbf{u}_0 + \int_0^t \sum_{n=0}^{\infty} \frac{(t-s)^n}{n!} \underbrace{\mathcal{P}e^{s\mathcal{L}}\mathcal{P}\mathcal{L}(\mathcal{Q}\mathcal{L})^n\mathcal{Q}\mathcal{L}\mathbf{u}_0}_{C_n(s)\mathbf{u}_0} ds, \\ &= \mathcal{P}e^{t\mathcal{L}}\mathcal{P}\mathcal{L}\mathbf{u}_0 + \int_0^t \underbrace{\left[\sum_{n=0}^{\infty} C_n(s) \frac{(t-s)^n}{n!} \right]}_{\mathcal{G}(t-s,s)} \mathbf{u}_0 ds, \\ &= \mathcal{P}e^{t\mathcal{L}}\mathcal{P}\mathcal{L}\mathbf{u}_0 + \int_0^t \mathcal{G}(t-s,s)\mathbf{u}_0 ds, \end{aligned} \quad (194)$$

where the *memory operator*¹⁰ $\mathcal{G}(t-s,s)$ is defined as

$$\mathcal{G}(t-s,s) = \sum_{n=0}^{\infty} \frac{(t-s)^n}{n!} C_n(s), \quad C_n(s) = \mathcal{P}e^{s\mathcal{L}}\mathcal{P}\mathcal{L}(\mathcal{Q}\mathcal{L})^n\mathcal{Q}\mathcal{L}, \quad n \geq 0. \quad (195)$$

We shall call this series expansion of the MZ equation as *MZ-Dyson expansion*. The reason for such definition is that (194) is equivalent to the hierarchical memory approximation model originally proposed by Stinis [82], which in turn is equivalent to

$$\frac{\partial}{\partial t} \mathcal{P}e^{t\mathcal{L}}\mathbf{u}_0 = \mathcal{P}e^{t\mathcal{L}}\mathcal{P}\mathcal{L}\mathbf{u}_0 + \mathbf{w}_0(t)$$

⁹The matrix representation of a linear operator \mathcal{L} , relative to the span of a finite-dimensional basis $V = \text{span}\{h_1, h_2, \dots\}$ can be easily obtained by representing each vector $\mathcal{L}h_i$ in V (provided the $\mathcal{L}V \subseteq V$). Alternatively, if \mathcal{L} operates in the Hilbert space \mathcal{H} and $\{h_1, h_2, \dots\}$ is an orthonormal basis of \mathcal{H} , then the matrix representation of \mathcal{L} has entries $\mathcal{L}_{ij} = (\mathcal{L}h_i, h_j)$, where (\cdot, \cdot) denotes the inner product in \mathcal{H} .

¹⁰Note that $\mathcal{G}(t-s,s)$ here is not a function but a linear operator.

where $w_0(t)$ is given by the Dyson series (see section 3.3.1)

$$w_0(t) = \sum_{n=1}^{\infty} \int_0^t \int_0^{\tau_{n-1}} \dots \int_0^{\tau_1} \mathcal{P}e^{s\mathcal{L}} \mathcal{P}\mathcal{L}(\mathcal{Q}\mathcal{L})^n \mathbf{u}_0 ds d\tau_1 \dots d\tau_{n-1}. \quad (196)$$

To prove such equivalence, we just need to prove that

$$\int_0^t \int_0^{\tau_{n-1}} \dots \int_0^{\tau} \mathcal{P}e^{s\mathcal{L}} \mathcal{P}\mathcal{L}(\mathcal{Q}\mathcal{L})^n ds d\tau_1 \dots d\tau_{n-1} = \int_0^t \frac{(t-s)^{n-1}}{(n-1)!} \mathcal{P}e^{s\mathcal{L}} \mathcal{P}\mathcal{L}(\mathcal{Q}\mathcal{L})^n \mathcal{Q}\mathcal{L} ds. \quad (197)$$

We proceed by induction. To this end, we first define

$$\mathcal{A}_n(t) = \int_0^t \int_0^{\tau_{n-1}} \dots \int_0^{\tau} \mathcal{P}e^{s\mathcal{L}} \mathcal{P}\mathcal{L}(\mathcal{Q}\mathcal{L})^n ds d\tau_1 \dots d\tau_{n-1}, \quad \mathcal{B}_n(t) = \int_0^t \frac{(t-s)^{n-1}}{(n-1)!} \mathcal{P}e^{s\mathcal{L}} \mathcal{P}\mathcal{L}(\mathcal{Q}\mathcal{L})^n \mathcal{Q}\mathcal{L} ds. \quad (198)$$

For $n = 1$ we have $\mathcal{A}_1 = \mathcal{B}_1$. For $n \geq 2$ we have $\mathcal{A}'_n(t) = \mathcal{A}_{n-1}(t)$, $\mathcal{B}'_n(t) = \mathcal{B}_{n-1}(t)$ and $\mathcal{A}_n(0) = \mathcal{B}_n(0)$. Hence, by induction we conclude that $\mathcal{A}_n(t) = \mathcal{B}_n(t)$, and therefore the memory integral in (194), with \mathcal{G} given in (195), is equivalent to a Dyson series.

5.2 MZ-Faber expansion

The Faber expansion of the orthogonal dynamics propagator $e^{t\mathcal{Q}\mathcal{L}}$ is an operator series of the form

$$e^{t\mathcal{Q}\mathcal{L}} = \sum_{j=0}^{\infty} a_j(t) \mathcal{F}_j(\mathcal{Q}\mathcal{L}), \quad (199)$$

where \mathcal{F}_j is the j -th order Faber polynomial, and $a_j(t)$ are suitable temporal modes defined hereafter. The series expansion (199) is *asymptotically optimal*, in the sense that its m -th order truncation uniformly approximates the best sequence of operator polynomials converging to $e^{t\mathcal{Q}\mathcal{L}}$ as $m \rightarrow \infty$ (see [66, 63]). A substitution of (199) into (189) yields the following expansion of the MZ equation (7)

$$\begin{aligned} \frac{\partial}{\partial t} \mathcal{P}e^{t\mathcal{L}} \mathbf{u}_0 &= \mathcal{P}e^{t\mathcal{L}} \mathcal{P}\mathcal{L} \mathbf{u}_0 + \int_0^t \mathcal{P}e^{s\mathcal{L}} \mathcal{P}\mathcal{L} e^{(t-s)\mathcal{Q}\mathcal{L}} \mathcal{Q}\mathcal{L} \mathbf{u}_0 ds, \\ &= \mathcal{P}e^{t\mathcal{L}} \mathcal{P}\mathcal{L} \mathbf{u}_0 + \int_0^t \sum_{j=0}^{\infty} a_j(t-s) \underbrace{\mathcal{P}e^{s\mathcal{L}} \mathcal{P}\mathcal{L} \mathcal{F}_j(\mathcal{Q}\mathcal{L}) \mathcal{Q}\mathcal{L} \mathbf{u}_0}_{\mathcal{C}_j(s)\mathbf{u}_0} ds, \\ &= \mathcal{P}e^{t\mathcal{L}} \mathcal{P}\mathcal{L} \mathbf{u}_0 + \int_0^t \mathcal{G}(t-s, s) \mathbf{u}_0 ds, \end{aligned} \quad (200)$$

where

$$\mathcal{G}(t-s, s) = \sum_{j=0}^{\infty} a_j(t-s) \mathcal{C}_j(s), \quad (201)$$

and

$$a_j(t-s) = \frac{1}{2\pi i} \int_{|w|=R} \frac{e^{(t-s)\psi(w)}}{w^{j+1}} dw, \quad \mathcal{C}_j(s) = \mathcal{P}e^{s\mathcal{L}} \mathcal{P}\mathcal{L} \mathcal{F}_j(\mathcal{Q}\mathcal{L}) \mathcal{Q}\mathcal{L}. \quad (202)$$

Here, $\psi(w)$ is the conformal map at the basis of the Faber series. The coefficients of the Laurent expansion of ψ determine the recurrence relation of the Faber polynomials. High-order Laurent series usually yield

higher convergence rates, but complicated recurrence relations. Moreover, the computation of the integrals in (202) can be quite cumbersome if high-order Laurent series are employed. To avoid such drawbacks, we choose the conformal map $\psi(w) = w + c_0 + c_1/w$. This yields the following analytical expression for the temporal modes $a_j(t - s)$

$$a_j(t - s) = \frac{e^{(t-s)c_0}}{(\sqrt{-c_1})^j} J_j(2(t - s)\sqrt{-c_1}), \quad (203)$$

where J_j denotes the j -th Bessel function of the first kind. In Section 5.6 we prove that the Faber expansion of the MZ memory integral converges for any linear dynamical system and any finite integration time with rate that is at least R -superlinear.

Remark The MZ-Dyson expansion we discussed in Section 5.1.1 is a subcase of the Faber expansion. In fact, Faber polynomials $\mathcal{F}_j(\mathcal{QL})$ corresponding to the conformal mapping $\psi(w) = w$ are simply monomials $(\mathcal{QL})^j$. Moreover, the temporal modes (203) reduce to $(t - s)^j/j!$ if we set $c_0 = 0$ and take the limit $c_1 \rightarrow 0$.

5.3 Other series expansions of the MZ-memory integral

The orthogonal dynamics propagator $e^{t\mathcal{QL}}$ can be expanded relative to basis functions other than Faber polynomials [61, 62]. This yields different approximations of the MZ memory integral and, correspondingly, different expansions of the MZ equation.

5.3.1 MZ-Lagrange expansion

The MZ-lagrange expansion is based on the following semigroup expansion

$$e^{t\mathcal{QL}} = \sum_{j=1}^n e^{\lambda_j t} \prod_{\substack{k=1 \\ k \neq j}}^n \frac{(\mathcal{QL} - \lambda_k \mathcal{I})}{(\lambda_j - \lambda_k)}, \quad (204)$$

where $\{\lambda_1, \dots, \lambda_n\} = \sigma(\mathcal{QL})$ is the spectrum of the matrix representation of the operator \mathcal{QL} (eigenvalues counted with their multiplicity). Note that (204) is in the form (190) with

$$a_j(t) = e^{\lambda_j t}, \quad \text{and} \quad \Phi_j(\mathcal{QL}) = \prod_{\substack{k=1 \\ k \neq j}}^n \frac{(\mathcal{QL} - \lambda_k \mathcal{I})}{(\lambda_j - \lambda_k)}. \quad (205)$$

A substitution of (204) into the MZ equation yields the MZ-Lagrange expansion

$$\frac{\partial}{\partial t} \mathcal{P} e^{t\mathcal{L}} \mathbf{u}_0 = \mathcal{P} e^{t\mathcal{L}} \mathcal{P} \mathcal{L} \mathbf{u}_0 + \int_0^t \mathcal{G}(t - s, s) \mathbf{u}_0 ds, \quad (206)$$

where

$$\mathcal{G}(t - s, s) = \sum_{j=1}^n e^{(t-s)\lambda_j} \mathcal{C}_j(s), \quad \text{and} \quad \mathcal{C}_j(s) = \mathcal{P} e^{s\mathcal{L}} \mathcal{P} \mathcal{L} \prod_{\substack{k=1 \\ k \neq j}}^n \frac{(\mathcal{QL} - \lambda_k \mathcal{I})}{(\lambda_j - \lambda_k)}, \quad j \geq 1. \quad (207)$$

	Type	Temporal modes	Operators $\mathcal{C}_j(s)$
Mori-Zwanzig Memory $\mathcal{G} = \sum_{j=0}^{\infty} h_j(t-s)\mathcal{C}_j(s)$	MZ-Dyson	$\frac{t^j}{j!}$	$\mathcal{P}e^{s\mathcal{L}}\mathcal{P}\mathcal{L}(\mathcal{Q}\mathcal{L})^j\mathcal{Q}\mathcal{L}$
	MZ-Faber	$e^{tc_0} \frac{J_j(2t\sqrt{-c_1})}{(\sqrt{-c_1})^j}$	$\mathcal{P}e^{s\mathcal{L}}\mathcal{P}\mathcal{L}\mathcal{F}_j(\mathcal{Q}\mathcal{L})\mathcal{Q}\mathcal{L}$
	MZ-Lagrange	$e^{t\lambda_j}$	$\mathcal{P}e^{s\mathcal{L}}\mathcal{P}\mathcal{L} \prod_{\substack{k=1 \\ k \neq j}}^n \frac{(\mathcal{Q}\mathcal{L} - \lambda_k\mathcal{I})}{(\lambda_j - \lambda_k)}$
	MZ-Newton	$f_{1,j}(t)$	$\begin{cases} \mathcal{P}e^{s\mathcal{L}}\mathcal{P}\mathcal{L} & j = 1 \\ \mathcal{P}e^{s\mathcal{L}} \prod_{k=1}^{j-1} (\mathcal{P}\mathcal{L}\mathcal{Q}\mathcal{L} - \lambda_k\mathcal{P}\mathcal{L}) & j \geq 2 \end{cases}$

Table 1: Series expansions of the Mori-Zwanzig memory operator. Here J_j is the j th Bessel function of the first kind, c_0 and c_1 are real numbers, $f_{1,j}(t)$ are defined in (209), and λ_j are the eigenvalues of any matrix representation of $\mathcal{Q}\mathcal{L}$.

5.3.2 MZ-Newton expansion

The MZ-Newton expansion is based on the following semigroup expansion

$$e^{t\mathcal{Q}\mathcal{L}} = f_{1,1}(t)\mathcal{I} + \sum_{j=2}^n f_{1,j}(t) \prod_{k=1}^{j-1} (\mathcal{Q}\mathcal{L} - \lambda_k\mathcal{I}), \quad (208)$$

where $f_{1,j}(t)$ is the divided difference defined recursively by

$$f_{1,j}(t) = \begin{cases} e^{\lambda_1 t} & j = 1, \\ \frac{e^{t\lambda_1} - e^{t\lambda_2}}{\lambda_1 - \lambda_2} & j = 2, \\ \frac{f_{1,j-1}(t) - f_{2,j}(t)}{\lambda_1 - \lambda_j} & j \geq 3. \end{cases} \quad (209)$$

A substitution of the Newton expansion (208) into the MZ equation yields the following MZ-Newton expansion

$$\frac{\partial}{\partial t} \mathcal{P}e^{t\mathcal{L}}\mathbf{u}_0 = \mathcal{P}e^{t\mathcal{L}}\mathcal{P}\mathcal{L}\mathbf{u}_0 + \int_0^t \mathcal{G}(t-s, s)\mathbf{u}_0 ds, \quad (210)$$

where

$$\mathcal{G}(t-s, s) = \mathcal{C}_1(s)e^{(t-s)\lambda_1} + \sum_{j=2}^n \mathcal{C}_j(s)f_{1,j}(t), \quad \mathcal{C}_j(s) = \begin{cases} \mathcal{P}e^{s\mathcal{L}}\mathcal{P}\mathcal{L} & j = 1 \\ \mathcal{P}e^{s\mathcal{L}} \prod_{k=1}^{j-1} (\mathcal{P}\mathcal{L}\mathcal{Q}\mathcal{L} - \lambda_k\mathcal{P}\mathcal{L}) & j \geq 2 \end{cases}. \quad (211)$$

Remark All series expansion methods we considered so far aim at representing the memory integral in the Mori-Zwanzig equation for the same phase space function. Therefore, such series should be related to each other. Indeed, as shown in Table 1, they basically represent the same memory operator $\mathcal{G}(t-s, s)$ relative to different bases. This also means that the series can have different convergence rates. For example, as we will demonstrate numerically in Section 5.7 the MZ-Faber expansion converges faster than the MZ-Dyson series.

5.4 The generalized Langevin equation (GLE)

We have seen that expanding the orthogonal dynamics propagator $e^{t\mathcal{Q}\mathcal{L}}$ in an operator series in the form (190) yields the Mori-Zwanzig equation¹¹

$$\frac{\partial}{\partial t}\mathcal{P}e^{t\mathcal{L}}\mathbf{u}_0 = \mathcal{P}e^{t\mathcal{L}}\mathcal{P}\mathcal{L}\mathbf{u}_0 + \sum_{j=0}^{\infty} \int_0^t h_j(t-s)\mathcal{C}_j(s)\mathbf{u}_0 ds, \quad (212)$$

where $h_j(t-s)$ are temporal modes, and $\mathcal{C}_j(s)$ are operators defined in Table 1. For example, if we consider the MZ-Dyson expansion, we have

$$h_j(t-s) = \frac{(t-s)^j}{j!}, \quad \mathcal{C}_j(s) = \mathcal{P}e^{s\mathcal{L}}\mathcal{P}\mathcal{L}(\mathcal{Q}\mathcal{L})^j\mathcal{Q}\mathcal{L}. \quad (213)$$

Equation (212) is the exact generalized Langevin equation (GLE) governing the projected dynamics of a quantity of interest. Such equation has different forms depending on the choice of the projection operator \mathcal{P} . In particular, if we choose Chorin's projection (8) then (212) is an equation for the conditional expectation of the quantity of interest. On the other hand, if we choose Berne's projection (24) then (212) becomes an equation for the autocorrelation function of the quantity of interest. Both these equations are, in general, *unclosed* if the dynamical system (1) is nonlinear. However, if the system is linear then, as we will see hereafter, such equations are closed.

5.4.1 Application to linear dynamical systems

Consider the linear dynamical system $\dot{\mathbf{x}} = \mathbf{A}\mathbf{x}$ and the quantity of interest $u(\mathbf{x}) = x_1$ (first component of the system). In this Section, we derive the evolution equations for the conditional mean and the autocorrelation function of $x_1(t)$ by using the MZ formulation.

5.4.2 Evolution equation for the conditional expectation

Let \mathcal{P} be Chorin's projection (8) and choose $\mathbf{u}(\mathbf{x}) = x_1$ (scalar). Then

$$\mathcal{P}e^{t\mathcal{L}}x_1(0) = \langle x_1(t) \rangle_{\rho_0} = \int x_1(t, \mathbf{x}_0)\rho_0(\mathbf{x}_0)d\mathbf{x}_0.$$

In this case, equation (212) reduces to

$$\frac{d}{dt}\langle x_1(t) \rangle_{\rho_0} = \alpha\langle x_1(t) \rangle_{\rho_0} + \beta + \int_0^t g(t-s)\langle x_1(s) \rangle_{\rho_0} ds + \int_0^t f(t-s) ds, \quad (214)$$

where the constants α, β , the *MZ memory kernel* $g(t-s)$, and the function $f(t-s)$ are defined by

$$\mathcal{P}\mathcal{L}x_1(0) = \alpha x_1(0) + \beta, \quad g(t-s) = \sum_{j=0}^{\infty} g_j h_j(t-s), \quad f(t-s) = \sum_{j=0}^{\infty} f_j h_j(t-s). \quad (215)$$

¹¹We emphasize that if we apply the semigroup expansion (199) to the unprojected Mori-Zwanzig equation (17), then we obtain a stochastic differential equation for the full dynamics. Establishing convergence of a reduced-order stochastic model derived from such stochastic equation is not easy. Moreover, for nonlinear systems, we inevitably have to introduce additional approximations to the "noise" term $e^{t\mathcal{Q}\mathcal{L}}\mathcal{Q}\mathcal{L}u_0$, to obtain a computable model. For instance, if we assume that $e^{t\mathcal{Q}\mathcal{L}}\mathcal{Q}\mathcal{L}u_0$ is random noise, then we need to introduce a suitable probability functional to characterize it [87, 47].

The coefficients g_j , f_j and the temporal bases $h_j(t-s)$ appearing in the series expansions above depend on the series expansion of the orthogonal dynamics propagator $e^{t\mathcal{QL}}$. Specifically, g_j and f_j are determined by the equation

$$\mathcal{C}_j(s)x_1(0) = g_j \langle x_1(s) \rangle_{\rho_0} + f_j, \quad (216)$$

while $h_j(t-s)$ and $\mathcal{C}_j(s)$ are defined in Table 1. To derive equation (216) we used the identity $\mathcal{P}e^{s\mathcal{L}}f_j = f_j$. In the case of MZ-Dyson and MZ-Faber expansions we explicitly obtain

$$\mathcal{PL}(\mathcal{QL})^j \mathcal{QL}x_1(0) = g_j^D x_1(0) + f_j^D, \quad \mathcal{PL}\mathcal{F}_j(\mathcal{QL}) \mathcal{QL}x_1(0) = g_j^F x_1(0) + f_j^F, \quad (217)$$

where the superscripts D and F stand for ‘‘Dyson’’ and ‘‘Faber’’, respectively.

5.4.3 Evolution equation for the autocorrelation function

If we choose the projection operator \mathcal{P} to be Berne’s projection (24), then equation (212) becomes an evolution equation for the autocorrelation function of the quantity of interest¹², i.e.,

$$\frac{dC_u(t)}{dt} = \alpha C_u(t) + \int_0^t g(t-s)C_u(s)ds, \quad (218)$$

where α and $g(t-s)$ defined by

$$\mathcal{PL}u_0 = \alpha u_0, \quad g(t-s) = \sum_{j=0}^{\infty} g_j h_j(t-s). \quad (219)$$

As before, the temporal modes h_j and the coefficients g_j in the expansion of the MZ-memory kernel $g(t-s)$ depend on the expansion of the orthogonal dynamics propagator $e^{t\mathcal{QL}}$. Specifically, in the case of MZ-Dyson and MZ-Faber expansions we obtain, respectively,

$$\mathcal{PL}(\mathcal{QL})^j \mathcal{QL}u_0 = g_j^D u_0, \quad \mathcal{PL}\mathcal{F}_j(\mathcal{QL}) \mathcal{QL}u_0 = g_j^F u_0. \quad (220)$$

It is worth noticing that Berne’s projection sends any function into the linear space spanned by the initial condition u_0 .

5.4.4 Exact solution to the MZ equation

The analytical solution to the MZ equations (214) and (218) can be computed through Laplace transforms. To this end, let us first notice that both equations are in the form of a Volterra equation

$$\frac{dy(t)}{dt} = \alpha y(t) + \beta + \int_0^t g(t-s)y(s)ds + \int_0^t f(t-s)ds. \quad (221)$$

Applying the Laplace transform

$$\mathcal{L}[\cdot](s) = \int_0^{\infty} (\cdot) e^{-st} dt \quad (222)$$

to both sides of (221) yields

$$sY(s) - y(0) = \alpha Y(s) + \frac{\beta}{s} + Y(s)G(s) + \frac{F(s)}{s}, \quad (223)$$

¹²In fact, if we apply the operator $\langle u_0, \cdot \rangle / \langle u_0, u_0 \rangle$ to both sides of equation (212) we obtain (218).

i.e.,

$$Y(s) = \frac{(F(s) + \beta)/s + y(0)}{s - G(s) - \alpha}, \quad (224)$$

where

$$Y(s) = \mathcal{L}[y(t)], \quad F(s) = \mathcal{L}[f(t)], \quad G(s) = \mathcal{L}[g(t)]. \quad (225)$$

Thus, the exact solution to the Volterra equation (221) can be written as

$$y(t) = \mathcal{L}^{-1} \left[\frac{(F(s) + \beta)/s + y(0)}{s - G(s) - \alpha} \right]. \quad (226)$$

The Laplace transform of the memory kernel $g(t)$, i.e., $G(s)$, can be computed analytically in many cases. For example, in the case of MZ-Dyson and MZ-Faber expansions we obtain, respectively

$$G(s) = \sum_{j=0}^{\infty} \frac{g_j^D}{s^{j+1}} \quad (\text{MZ-Dyson}), \quad (227)$$

$$G(s) = \sum_{j=0}^{\infty} \frac{g_j^F}{2^j (\sqrt{-c_1})^{2j}} \frac{(\sqrt{s^2 - 4c_1} - s)^j}{\sqrt{s^2 - 4c_1}} \quad (\text{MZ-Faber}). \quad (228)$$

The coefficients g_j^F and g_j^D are explicitly defined in (217), or (220), depending on whether we are interested in the mean or the correlation function of the quantity of interest.

Remark The recurrence relation at the basis of the Faber polynomials induces a recurrence relation in the Laplace transform $G(s)$ of the MZ memory kernel. Therefore, a connection between the MZ-Faber approximation method we propose here and the method of recurrence relations of Lee [64, 51] can be established.

5.5 GLEs for nonlinear systems

In the previous Sections, we employed Chorin's projection and Berne's projection to derive generalized Langevin equations for quantities of interest (phase space functions) in linear dynamical systems. Similar series expansion can be developed for nonlinear dynamical systems by following methods similar to those presented in [11, 54]. In particular, if we use Mori's projection (15), then $\mathcal{P}\mathcal{L}(\mathcal{Q}\mathcal{L})^i u_0$ is in the span of the orthogonal basis $\{A_1(u(\mathbf{x})), \dots, A_M(u(\mathbf{x}))\}$ defining the Hilbert space of observables, i.e.,

$$\mathcal{P}\mathcal{L}(\mathcal{Q}\mathcal{L})^i u_0 \in \mathcal{S} = \text{span}\{A_1, \dots, A_M\}. \quad (229)$$

As a consequence, the j -th order operator polynomial $\Phi_j(\mathcal{Q}\mathcal{L})$ and $\mathcal{P}\mathcal{L}\Phi_j(\mathcal{Q}\mathcal{L})u_0$ are both in \mathcal{S} . This means that if we choose the initial condition as $u_0 = A_k \in \mathcal{S}$, then $\mathcal{P}e^{s\mathcal{L}}\mathcal{P}\mathcal{L}\Phi_i(\mathcal{Q}\mathcal{L})A_k$ admits the matrix representation¹³

$$\mathcal{P}e^{s\mathcal{L}}\mathcal{P}\mathcal{L}\Phi_i(\mathcal{Q}\mathcal{L})A_k = \sum_{j=1}^M H_{kj}(\Phi_i)\eta_j(s), \quad (230)$$

¹³The existence of \mathbf{H} follows from (229) and simple linear algebra.

where $A_k(s) = \mathcal{P}e^{s\mathcal{L}}A_k(0)$. The $M \times M$ matrix $\mathbf{H}(\Phi_i)$ depends on the polynomial Φ_i we employ to expand the orthogonal dynamics propagator (190). Any truncation of the series (190) to n terms yields

$$\mathcal{P}e^{s\mathcal{L}}\mathcal{P}\mathcal{L}e^{(t-s)\mathcal{Q}\mathcal{L}}\mathcal{Q}\mathcal{L}A_k = \sum_{j=1}^M \sum_{i=1}^n g_i(t-s)H_{kj}(\Phi_i)A_j(s),$$

where $g_j(t-s)$ can be any of the temporal bases listed in Table 1. This yields following matrix-valued GLE

$$\frac{d}{dt}A_k(t) = \sum_{j=1}^N \Omega_{jk}A_j(t) + \sum_{j=1}^N \int_0^t K_{kj}(t-s)A_j(s)ds, \quad (231)$$

where the entries of the *streaming matrix* $\mathbf{\Omega}$ and the *memory matrix* $\mathbf{K}(t-s)$ are defined by

$$\mathcal{P}\mathcal{L}A_k = \sum_{j=1}^N \Omega_{jk}A_j \quad \text{and} \quad K_{kj}(t-s) = \sum_{i=1}^n g_i(t-s)H_{kj}(\Phi_i). \quad (232)$$

Unfortunately, for nonlinear systems it is not easy to calculate the matrix coefficients $H_{kj}(\Phi_i)$, especially for large values of i . The reason is the same that limits the practical computation of high-order expansions in [82, 81, 84]. Nevertheless, the MZ equation (231) can be used as a starting point to build approximations, e.g., based on data streams [53, 9].

5.6 Convergence analysis

In this section, we develop a thorough convergence analysis of the MZ-Faber¹⁴ equation (7). The key ideas at the basis of our analysis can be found in our recent paper [99]. Here we focus, in particular, on high-dimensional linear systems of the form

$$\dot{\mathbf{x}}(t) = \mathbf{A}\mathbf{x}(t), \quad \mathbf{x}(0) = \mathbf{x}_0(\omega), \quad (233)$$

where $\mathbf{x}_0(\omega)$ is a random initial state. Our goal is to prove that the norm of the approximation error

$$\begin{aligned} E_n(t) &= \int_0^t \mathcal{P}e^{s\mathcal{L}}\mathcal{P}\mathcal{L}e^{(t-s)\mathcal{Q}\mathcal{L}}\mathcal{Q}\mathcal{L}u_0 ds - \underbrace{\sum_{j=0}^n \int_0^t a_j(t-s)\mathcal{P}e^{s\mathcal{L}}\mathcal{P}\mathcal{L}\mathcal{F}_j(\mathcal{Q}\mathcal{L})\mathcal{Q}\mathcal{L}u_0 ds}_{\text{MZ-Faber series}} \\ &= \int_0^t \sum_{j=n+1}^{\infty} a_j(t-s)\mathcal{P}e^{s\mathcal{L}}\mathcal{P}\mathcal{L}\mathcal{F}_j(\mathcal{Q}\mathcal{L})\mathcal{Q}\mathcal{L}u_0 ds \end{aligned} \quad (234)$$

decays as we increase the polynomial order n , for any fixed integration time $t > 0$, i.e.,

$$\lim_{n \rightarrow \infty} \|E_n(t)\| = 0.$$

Throughout this Section $\|\cdot\|$ denotes either an operator norm, a norm in a function space or a standard norm in \mathbb{C}^N , depending on the context. The convergence proof of MZ-Faber series clearly depends on the choice of the projection operator, and on the phase space function $u(\mathbf{x})$ (quantity of interest). In this Section, we consider

$$u(\mathbf{x}(t)) = x_1(t), \quad (235)$$

and Chorin's projection (8). Similar results can be obtained for other projection, and vector-valued phase space functions (2). We begin with the following

¹⁴We recall that the MZ-Dyson series expansion is a subcase of the MZ-Faber expansion. Therefore convergence of MZ-Faber implies convergence of MZ-Dyson.

Lemma 12. Consider the linear dynamical system (233) and the phase space function (235). Let \mathcal{P} be Chorin's projection (8) with arbitrary initial distribution ρ_0 (not necessarily i.i.d), $\mathcal{Q} = \mathcal{I} - \mathcal{P}$, $\mathcal{L}(\mathbf{x}) = \mathbf{A}\mathbf{x} \cdot \nabla$ and p_k an arbitrary polynomial of degree k . Then we have the following operator polynomial equality

$$\mathcal{P}\mathcal{L}p_k(\mathcal{Q}\mathcal{L})\mathcal{Q}\mathcal{L}x_1(0) = [\mathbf{b} \cdot p_k(\mathbf{M}_{11}^T)\mathbf{a}] x_1(0) + [p_k(\mathbf{M}_{11}^T)\mathbf{M}_{11}^T\mathbf{a}] \cdot \langle \mathbf{x}_{-1}(0) \rangle_{\rho_0},$$

where

$$\mathbf{x}_{-1}(0) = [x_2(0), x_3(0), \dots, x_N(0)]^T, \quad \mathbf{a} = [A_{12}, \dots, A_{1N}]^T, \quad \mathbf{b} = [A_{21}, \dots, A_{N1}]^T,$$

and \mathbf{M}_{11} is the matrix obtained from \mathbf{A} by removing the first row and the first column.

Proof. By a direct calculation, it can be verified that

$$\begin{aligned} (\mathcal{Q}\mathcal{L})^n x_1(0) &= [(\mathbf{M}_{11}^T)^{n-1} \mathbf{a}] \cdot [\mathbf{x}_{-1}(0) - \langle \mathbf{x}_{-1}(0) \rangle_{\rho_0}], \\ \mathcal{L}(\mathcal{Q}\mathcal{L})^n x_1(0) &= [\mathbf{b}^T (\mathbf{M}_{11}^T)^{n-1} \mathbf{a}] x_1(0) + [(\mathbf{M}_{11}^T)^n \mathbf{a}] \cdot \mathbf{x}_{-1}(0), \\ \mathcal{P}\mathcal{L}(\mathcal{Q}\mathcal{L})^n \mathcal{Q}\mathcal{L}x_1(0) &= [\mathbf{b}^T (\mathbf{M}_{11}^T)^n \mathbf{a}] x_1(0) + [(\mathbf{M}_{11}^T)^n \mathbf{M}_{11}^T \mathbf{a}] \cdot \langle \mathbf{x}_{-1}(0) \rangle_{\rho_0}. \end{aligned} \quad (236)$$

Note that each entry of the vector $\langle \mathbf{x}_{-1}(0) \rangle_{\rho_0} = [\langle x_2(0) \rangle_{\rho_0}, \dots, \langle x_N(0) \rangle_{\rho_0}]^T$ is $\langle x_i(0) \rangle_{\rho_0} = \mathcal{P}x_i(0)$ ($i = 2, \dots, N$). Thus, for any polynomial function in the form

$$p_k(\mathcal{Q}\mathcal{L}) = \sum_{j=0}^k \beta_j (\mathcal{Q}\mathcal{L})^j, \quad (237)$$

we have

$$\begin{aligned} \mathcal{P}\mathcal{L}p_k(\mathcal{Q}\mathcal{L})\mathcal{Q}\mathcal{L}x_1(0) &= \sum_{j=0}^k \beta_j \mathcal{P}\mathcal{L}(\mathcal{Q}\mathcal{L})^j \mathcal{Q}\mathcal{L}x_1(0), \\ &= \sum_{j=0}^k \beta_j \left([\mathbf{b}^T (\mathbf{M}_{11}^T)^j \mathbf{a}] x_1(0) + [(\mathbf{M}_{11}^T)^j \mathbf{M}_{11}^T \mathbf{a}] \cdot \langle \mathbf{x}_{-1}(0) \rangle_{\rho_0} \right), \\ &= [\mathbf{b} \cdot p_k(\mathbf{M}_{11}^T)\mathbf{a}] x_1(0) + [p_k(\mathbf{M}_{11}^T)\mathbf{M}_{11}^T\mathbf{a}] \cdot \langle \mathbf{x}_{-1}(0) \rangle_{\rho_0}. \end{aligned}$$

This completes the proof of the Lemma. \square

To prove convergence of MZ-Faber series we need two more Lemmas involving Faber polynomials of a complex variable.

Lemma 13. Let γ be the capacity of $\Omega \subseteq \mathbb{C}$. If Ω is symmetric with respect to the real axis, then for any $R > \gamma$ the conformal map

$$\psi : \hat{\mathbb{C}} \setminus \{w : |w| \leq \gamma\} \rightarrow \hat{\mathbb{C}} \setminus \Omega, \quad \psi(\infty) = \infty, \quad \psi'(\infty) = 1, \quad (238)$$

where $\hat{\mathbb{C}}$ is the Riemann's sphere, satisfies

$$\psi(R) \leq \psi(\gamma) + R - \frac{\gamma^2}{R}.$$

Proof. We first notice that

$$\psi(R) = \psi(\gamma) + \int_{\gamma}^R \psi'(t) dt.$$

By using Lemma 4.2 in [66], i.e.,

$$|\psi'(t)| \leq 1 + \left(\frac{\gamma}{|t|}\right)^2, \quad |t| > \gamma$$

we have

$$\psi(R) - \psi(\gamma) \leq |\psi(R) - \psi(\gamma)| = \left| \int_{\gamma}^R \psi'(t) dt \right| \leq \int_{\gamma}^R |\psi'(t)| dt = R - \frac{\gamma^2}{R},$$

which completes the proof. □

Next, consider an arbitrary matrix \mathbf{A} and define the *field value* of \mathbf{A} as

$$FV(\mathbf{A}) = \{z^H \mathbf{A} z : z \in \mathbb{C}^N, z^H z = 1\}.$$

The field value of \mathbf{A} is a subset of the complex plane. Also, denote the truncated Faber series of the exponential matrix $e^{t\mathbf{A}}$ as

$$\mathbf{P}_m(t) = \sum_{j=0}^m a_j(t) \mathcal{F}_j(\mathbf{A}). \quad (239)$$

With this notation, we have the following

Lemma 14. *Let $\Omega \subset \mathbb{C}$ be symmetric with respect to the real axis, convex and with capacity γ . Consider an $N \times N$ matrix \mathbf{A} with spectrum $\sigma(\mathbf{A})$, and an $N \times 1$ vector \mathbf{v} . If $\sigma(\mathbf{A}) \subseteq \Omega$ and the field value $FV(\mathbf{A}) \subseteq \Omega(q)$ for some $q \geq \gamma$, then the approximation error*

$$\mathbf{e}_m(t-s)\mathbf{v} = e^{(t-s)\mathbf{A}}\mathbf{v} - \mathbf{P}_{(m-1)}(t-s)\mathbf{v} \quad t \geq s$$

satisfies

$$\|\mathbf{e}_m(t-s)\mathbf{v}\| \leq C_3 e^{(t-s)E} \left(\frac{qe^{t-s}}{m}\right)^{m-1} \quad m \geq 4q,$$

where

$$C_3 = C_3(\mathbf{v}) = 8e\|\mathbf{v}\|_q \left(1 + \frac{1}{8q}\right) \quad \text{and} \quad E = 1 + \psi(\gamma).$$

Proof. If $q \geq \gamma$ then we have, thanks to the convexity of Ω and the analyticity of the exponential function,

$$\|\mathbf{e}_m(t-s)\mathbf{v}\| \leq 8\|\mathbf{v}\| e \left(1 + \frac{1}{8q}\right) m \left(\frac{q}{m}\right)^m \max_{|z| \in \Gamma(m)} |e^{(t-s)z}| \quad m \geq 4q \quad (240)$$

(see Theorem 4.2 in [66]). On the other hand,

$$\max_{|z| \in \Gamma(m)} |e^{(t-s)z}| = e^{(t-s)\psi(m)} \quad m \geq 4q. \quad (241)$$

By using Lemma 13 we have

$$\psi(m) \leq \psi(\gamma) + m - \frac{\gamma^2}{m} \leq \psi(\gamma) + m, \quad (242)$$

and therefore

$$e^{(t-s)\psi(m)} \leq e^{(t-s)(m-1)} e^{(t-s)(1+\psi(\gamma))} \quad m \geq 4q \geq \gamma. \quad (243)$$

Combining (240) , (241) and (243), we obtain

$$\|e_m(t-s)\mathbf{v}\| \leq C_3 \exp((t-s)E) \left(\frac{qe^{t-s}}{m}\right)^{m-1}, \quad (244)$$

where

$$C_3 = 8e\|\mathbf{v}\|q \left(1 + \frac{1}{8q}\right) \quad \text{and} \quad E = 1 + \psi(\gamma).$$

□

At this point, we we have all elements to prove the following

Theorem 15. (Convergence of the MZ-Faber Expansion) *Consider the linear dynamical system (233), the phase space function (235) and the projection operator (8). The norm of the approximation error (234) satisfies¹⁵*

$$\|E_n(t)\| \leq K \left(\frac{q}{n+1}\right)^n \frac{e^{t\beta} - e^{t(E+n)}}{\beta - E - n} \quad t \geq 0, \quad n \geq 4q, \quad (245)$$

where n is the Faber polynomial order, while q , K , β and E are suitable constants defined in the proof of the theorem.

Proof. We aim at determining an upper bound for

$$\|E_n(t)\| = \left\| \int_0^t \mathcal{P}e^{s\mathcal{L}} \sum_{j=n+1}^{\infty} a_j(t-s) \mathcal{P}\mathcal{L}\mathcal{F}_j(\mathcal{Q}\mathcal{L})\mathcal{Q}\mathcal{L}x_1(0) ds \right\|. \quad (246)$$

To this end, we first notice that quantity $\mathcal{F}_j(\mathcal{Q}\mathcal{L})\mathcal{Q}\mathcal{L}$ is a $(j+1)$ -th order operator polynomial in $\mathcal{Q}\mathcal{L}$. Thus, we can apply Lemma 12 to obtain

$$\mathcal{P}\mathcal{L}\mathcal{F}_j(\mathcal{Q}\mathcal{L})\mathcal{Q}\mathcal{L}x_1(0) = [\mathbf{b} \cdot \mathcal{F}_j(\mathbf{M}_{11}^T)\mathbf{a}] x_1(0) + [\mathcal{F}_j(\mathbf{M}_{11}^T)\mathbf{M}_{11}^T\mathbf{a}] \cdot \langle \mathbf{x}_{-1}(0) \rangle_{\rho_0}. \quad (247)$$

Let us now set

$$\eta_n(t-s) = \left\| \sum_{j=n+1}^{\infty} a_j(t-s) \mathcal{P}\mathcal{L}\mathcal{F}_j(\mathcal{Q}\mathcal{L})\mathcal{Q}\mathcal{L}x_1(0) \right\|. \quad (248)$$

By using (247) and the Cauchy-Schwartz inequality we have

$$\eta_n(t-s) \leq C_4 \left\| \sum_{j=n+1}^{\infty} a_j(t-s) \mathcal{F}_j(\mathbf{M}_{11}^T)\mathbf{a} \right\| + C_5 \left\| \sum_{j=n+1}^{\infty} a_j(t-s) \mathcal{F}_j(\mathbf{M}_{11}^T)\mathbf{M}_{11}^T\mathbf{a} \right\|, \quad (249)$$

¹⁵It can be shown that the upper bound in (245) is always positive.

where $C_4 = \|\mathbf{b}^T\| |x_1(0)|$, $C_5 = \|\langle \mathbf{x}_{-1}(0) \rangle_{\rho_0}\|$. The two sums in (249) represent the error in the Faber approximation of the matrix exponential $e^{(t-s)\mathbf{M}_{11}^T}$. In fact,

$$\mathbf{e}_{(n+1)}(t-s) = e^{(t-s)\mathbf{M}_{11}^T} - \sum_{j=1}^n a_j(t-s) \mathcal{F}_j(\mathbf{M}_{11}^T) = \sum_{j=n+1}^{\infty} a_j(t-s) \mathcal{F}_j(\mathbf{M}_{11}^T). \quad (250)$$

Combining (246), (248), (249) and (244) yields

$$\begin{aligned} \|E_n(t)\| &\leq \int_0^t \eta_n(t-s) \|\mathcal{P}e^{s\mathcal{L}}\| ds, \\ &\leq \int_0^t (C_4 \|\mathbf{e}_{(n+1)}(t-s)\mathbf{a}\| + C_5 \|\mathbf{e}_{(n+1)}(t-s)\mathbf{M}_{11}^T\mathbf{a}\|) \|\mathcal{P}e^{s\mathcal{L}}\| ds, \\ &\leq \int_0^t K e^{s\beta} e^{(t-s)(E+n)} \left(\frac{q}{n+1}\right)^n ds, \\ &\leq K \left(\frac{q}{n+1}\right)^n \frac{e^{t\beta} - e^{t(E+n)}}{\beta - E - n} \quad n \geq 4q. \end{aligned} \quad (251)$$

Here we used the semigroup estimation $\|e^{s\mathcal{L}}\| \leq W e^{s\beta}$. The constants in (251) are

$$K = \|\mathcal{P}\| C_6 W, \quad C_6 = 2 \max\{C_4 C_3, C_5 C_3^*\}, \quad E = 1 + \psi(\gamma), \quad (252)$$

where

$$C_3 = 8e\|\mathbf{a}\|q \left(1 + \frac{1}{8q}\right), \quad C_3^* = 8e\|\mathbf{M}_{11}^T\mathbf{a}\|q \left(1 + \frac{1}{8q}\right). \quad (253)$$

It can be shown that the upper bound (251) is always positive, and goes to zero as we send the Faber polynomial order n to infinity. This implies that

$$\lim_{n \rightarrow \infty} \|E_n(t)\| = 0, \quad (254)$$

i.e., the MZ-Faber expansion converges for any finite time $t \geq 0$. This completes the proof. \square

Next, we estimate the convergence rate of the MZ-Faber expansion. To this end, let us define

$$R(t, n) = K \left(\frac{q}{n+1}\right)^n \frac{e^{t\beta} - e^{t(E+n)}}{\beta - E - n}, \quad n \geq 4q \quad (255)$$

to be the upper bound (251). We have the following

Corollary 15.1. (Convergence Rate of the MZ-Faber Expansion) *With the same the notation of Theorem 15, the MZ-Faber expansion converges at least superlinearly with the polynomial order, i.e.*

$$\lim_{n \rightarrow \infty} \frac{R(t, n+1)}{R(t, n)} = 0 \quad (256)$$

for any finite time $t \geq 0$.

Proof. By a direct calculation it is easy to verify that (256) holds true. In fact,

$$\frac{R(t, n+1)}{R(t, n)} = \frac{q}{n+2} \left(\frac{n+1}{n+2}\right)^n \frac{e^{t\beta} - e^{t(E+n+1)}}{e^{t\beta} - e^{t(E+n)}} \frac{\beta - E - n}{\beta - E - (n+1)}. \quad (257)$$

Therefore¹⁶,

$$\lim_{n \rightarrow +\infty} \frac{R(t, n+1)}{R(t, n)} = \lim_{n \rightarrow +\infty} \frac{qe^t}{n+2} \left(\frac{n+1}{n+2} \right)^n = 0, \quad t < \infty. \quad (259)$$

□

By using asymptotic analysis we can also show that the MZ-Dyson expansion converges superlinearly. To this end, let us define the approximation error

$$E_n(t) = \int_0^t \mathcal{P}e^{s\mathcal{L}} \mathcal{P}\mathcal{L}e^{(t-s)\mathcal{Q}\mathcal{L}} \mathcal{Q}\mathcal{L}u_0 ds - \underbrace{\sum_{j=0}^n \int_0^t a_j(t-s) \mathcal{P}e^{s\mathcal{L}} \mathcal{P}\mathcal{L}(\mathcal{Q}\mathcal{L})^j \mathcal{Q}\mathcal{L}u_0 ds}_{\text{MZ-Dyson series}}. \quad (260)$$

By following the same steps we used in the proof of Theorem 15, we can bound the norm of (260) as

$$\|E_n(t)\| \leq F(t, n). \quad (261)$$

where

$$F(t, n) = C \frac{(At)^n}{(n+1)!} \quad A, C \geq 0. \quad (262)$$

Such upper bound plays the same role as $R(t, n)$ in the MZ-Faber expansion of $E_n(t)$ (see Eqs. (251) and (255)). Taking the ratio between $F(t, n+1)$ and $F(t, n)$ we obtain

$$\lim_{n \rightarrow \infty} \frac{F(t, n+1)}{F(t, n)} = \lim_{n \rightarrow \infty} \frac{At}{n+2} = 0. \quad (263)$$

5.7 Numerical examples

In this section, we demonstrate the accuracy of the MZ-Faber expansion methods. Specifically, we study random wave propagation in an annulus with Dirichlet boundary conditions, and dynamics of harmonic chains of oscillators interacting on graphs with arbitrary topology.

5.7.1 Random wave propagation

Consider the following initial/boundary value problem for the wave equation in an annulus with radii $r_1 = 1$ and $r_2 = 11$

$$\frac{\partial^2 w}{\partial t^2} = \frac{\partial^2 w}{\partial r^2} + \frac{1}{r} \frac{\partial w}{\partial r} + \frac{1}{r^2} \frac{\partial^2 w}{\partial \theta^2}, \quad (264)$$

where

$$w(t, r_1, \theta) = 0, \quad w(t, r_2, \theta) = 0 \quad w(0, r, \theta) = w_0(r, \theta; \omega), \quad \frac{\partial w(0, r, \theta)}{\partial t} = 0. \quad (265)$$

¹⁶We recall that

$$\lim_{n \rightarrow +\infty} \left(\frac{n+1}{n+2} \right)^n = \frac{1}{e}. \quad (258)$$

The field $w(t, r, \theta)$ represents the wave amplitude at time t , while $w_0(r, \theta; \omega)$ is the wave field at initial time, which is set to be random. We seek the for an approximation of the solution $w(t, r, \theta)$ in the form

$$w_N(t, r, \theta) = \sum_{n=1}^N \widehat{w}_n(t) \psi_n(r, \theta), \quad (266)$$

where $\psi_n(r, \theta)$ is a basis constructed by taking the tensor product of polynomials (radial direction) and trigonometric functions (angular direction). The random wave field at initial time is represented as

$$w_0(r, \theta; \omega) = \sum_{n=1}^M \widehat{w}_n(0) \psi_n(r, \theta), \quad M \leq N, \quad (267)$$

where $\widehat{w}_n(0)$ are i.i.d Gaussian random variables. Substituting (266) into (264) and imposing that the residual is orthogonal to the space spanned by the basis $\{\psi_1, \dots, \psi_N\}$ (Galerkin method [42, 36]) yields the linear system

$$\frac{d^2}{dt^2} \widehat{\mathbf{w}}(t) = \mathbf{A} \widehat{\mathbf{w}}(t), \quad (268)$$

where \mathbf{A} is an $N \times N$ matrix with entries

$$A_{mn} = \frac{\int_{r_1}^{r_2} \int_0^{2\pi} \left(\frac{\partial^2 \psi_n}{\partial r^2} + \frac{1}{r} \frac{\partial \psi_n}{\partial r} + \frac{1}{r^2} \frac{\partial^2 \psi_n}{\partial \theta^2} \right) \psi_m dr d\theta}{\int_{r_1}^{r_2} \int_0^{2\pi} \psi_m^2 dr d\theta}. \quad (269)$$

We are interested in developing reduced-order model for the mean wave amplitude at a specific point within the annulus, e.g., at a location where we would like to place a sensor. To this end, we transform the system (268) from the modal space to the nodal space defined by an interpolant of at N collocation points. Such transformation can be easily defined by evaluating (266) at a set of distinct collocation nodes $\mathbf{x}_n = (r_{i(n)}, \theta_{j(n)})$ ($n = 1, \dots, N$) within the annulus. This yields

$$\mathbf{w}(t) = \Psi \widehat{\mathbf{w}}(t), \quad (270)$$

where $\mathbf{w}(t) = [w(t, \mathbf{x}_1), \dots, w(t, \mathbf{x}_N)]^T$, while Ψ is the $N \times N$ transformation matrix defined as

$$\Psi = \begin{bmatrix} \psi_1(\mathbf{x}_1) & \dots & \psi_N(\mathbf{x}_1) \\ \vdots & & \vdots \\ \psi_1(\mathbf{x}_N) & \dots & \psi_N(\mathbf{x}_N) \end{bmatrix}.$$

Differentiating (270) with respect to time yields

$$\frac{d^2}{dt^2} \mathbf{w}(t) = \Psi \mathbf{A} \Psi^{-1} \mathbf{w}(t). \quad (271)$$

This system can be conveniently transformed into a first-order system as

$$\frac{d}{dt} \begin{bmatrix} \mathbf{w} \\ \dot{\mathbf{w}} \end{bmatrix} = \mathbf{B} \begin{bmatrix} \mathbf{w} \\ \dot{\mathbf{w}} \end{bmatrix}, \quad \text{where} \quad \mathbf{B} = \begin{bmatrix} \mathbf{0} & \mathbf{I} \\ \Psi \mathbf{A} \Psi^{-1} & \mathbf{0} \end{bmatrix}. \quad (272)$$

The initial condition is set as

$$\mathbf{w}(0) = \Psi \widehat{\mathbf{w}}(0), \quad \frac{d\mathbf{w}(0)}{dt} = \mathbf{0}, \quad (273)$$

where $\widehat{\mathbf{w}}(0)$ is random. In Figure 9 we plot the mean solution of the random wave equation for initial conditions in the form (267) with different number of modes.

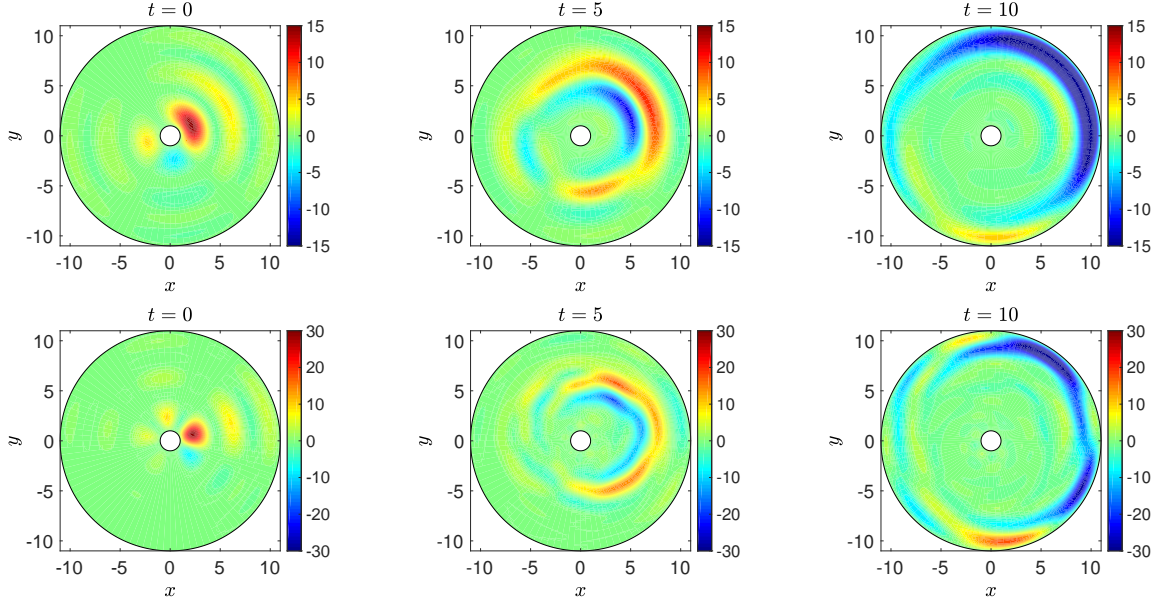


Figure 9: Mean solution of the random wave equation in the annulus. We consider two random initial conditions in the form (267), with different number of modes: $M = 25$ (first row), $M = 50$ (second row).

Generalized Langevin equation for the mean wave amplitude We are interested in developing reduced-order model for the mean wave amplitude at a specific point within the annulus, e.g., at a location where we would like to place a sensor. Such dynamical system can be constructed by using the Mori-Zwanzig formulation and Chorin's projection operator (8). To this end, let us define the quantity of interest as $u(\mathbf{w}, \dot{\mathbf{w}}) = w_1(t)$, i.e., the wave amplitude at the spatial point $(r, \theta) = (1.1, 0.1)$. The general form of the evolution equation for mean of $w_1(t)$ was derived in Section 5.4.2, and it is rewritten hereafter for convenience

$$\frac{d}{dt} \langle w_1(t) \rangle_{\rho_0} = \alpha \langle w_1(t) \rangle_{\rho_0} + \beta + \int_0^t g(t-s) \langle w_1(s) \rangle_{\rho_0} ds + \int_0^t f(t-s) ds. \quad (274)$$

The coefficients α and β are defined in terms of the matrix \mathbf{B} (Eq. (272)) and the orthogonal phase variables as¹⁷

$$\alpha = B_{11} \quad \beta = \mathbf{a} \cdot \langle \mathbf{w}_{-1}(0) \rangle_{\rho_0}, \quad (276)$$

where

$$\mathbf{w}_{-1}(0) = [w_2(0), \dots, w_N(0), \dot{w}_1(0), \dots, \dot{w}_N(0)]^T, \quad \mathbf{a} = [B_{12}, \dots, B_{1(2N)}]^T. \quad (277)$$

Note that the matrix \mathbf{B} has entries $[B_{11} \dots B_{1N}] = \mathbf{0}$, and we have $\dot{\omega}(0) = 0$ (see equation (273)). This yields, $\alpha = \beta = 0$. The memory kernel $g(t-s)$ and the function $f(t-s)$ can be expanded in terms of any

¹⁷We recall that the coefficients α and β appearing in equation (274) are computed by projecting

$$\mathcal{L}(\mathbf{w}, \dot{\mathbf{w}})w_1 = \sum_{i=1}^N \left(\dot{\omega}_i \frac{\partial}{\partial \omega_i} + [\Psi \mathbf{A} \Psi^{-1} \mathbf{w}]_i \frac{\partial}{\partial \dot{\omega}_i} \right) w_1 = \dot{\omega}_1 \quad (275)$$

i.e.,

$$\mathcal{P} \mathcal{L} w_1(0) = B_{11} w_1(0) + \mathbf{a} \cdot \langle \mathbf{w}_{-1}(0) \rangle_{\rho_0} = \alpha w_1(0) + \beta.$$

Since $\dot{\omega}_1 = 0$ (see equation (273)), in this case we obtain $\alpha = 0$ and $\beta = 0$.

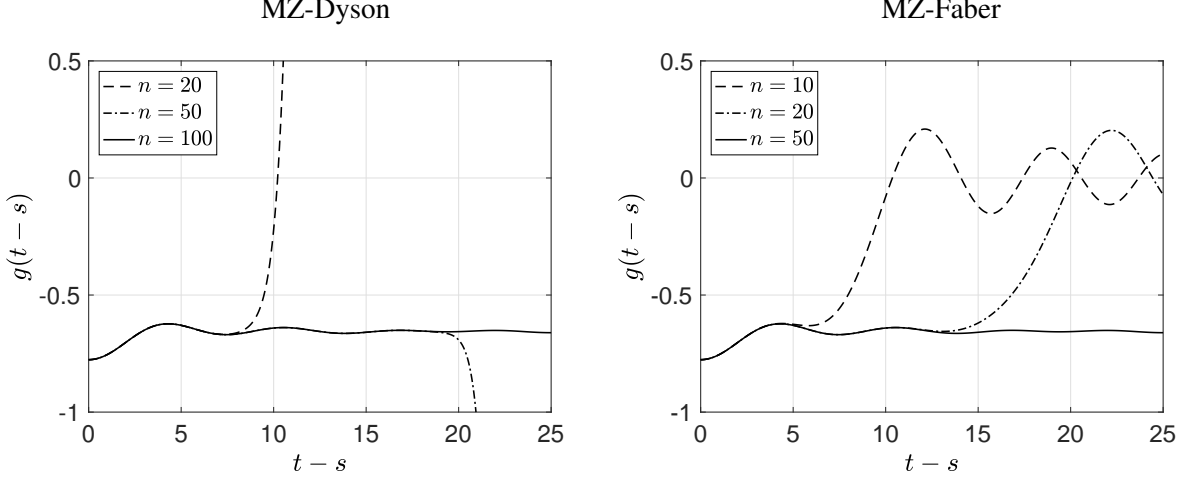


Figure 10: Dyson and Faber expansions of the Mori-Zwanzig memory kernel $g(t-s)$ in equation (278). Shown are results for different polynomial orders n . It is seen that the MZ-Faber series converges faster than the MZ-Dyson series.

of the operator series summarized in Table 1. For instance, if we employ MZ-Faber series we obtain

$$g(t-s) = \sum_{j=0}^n g_j^F e^{tc_0} \frac{J_j(2t\sqrt{-c_1})}{(\sqrt{-c_1})^j}, \quad f(t-s) = \sum_{j=0}^n f_j^F e^{tc_0} \frac{J_j(2t\sqrt{-c_1})}{(\sqrt{-c_1})^j}. \quad (278)$$

The coefficients g_j^F and f_j^F are explicitly obtained as

$$g_j^F = \mathbf{b}^T \mathcal{F}_j (\mathbf{M}_{11}^T) \mathbf{a}, \quad f_j^F = [\mathcal{F}_j (\mathbf{M}_{11}^T) \mathbf{M}_{11}^T \mathbf{a}] \cdot \langle \boldsymbol{\omega}_{-1}(0) \rangle_{\rho_0}, \quad (279)$$

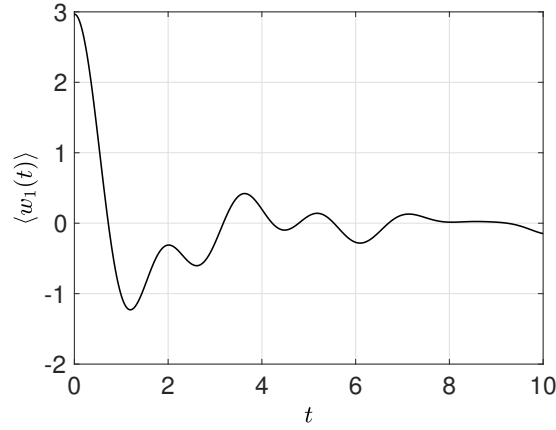
where $\boldsymbol{\omega}_{-1}$ and \mathbf{a} are defined in (277), while $\mathbf{b} = [B_{21}, \dots, B_{(2N)1}]^T$. Also, \mathbf{M}_{11} is the matrix obtained from \mathbf{B} by removing the first row and the first column. In Figure 10 we study convergence of MZ-Dyson and MZ-Faber series expansions of the memory kernel. In Figure 11 we study the accuracy of the MZ-Dyson and the MZ-Faber expansions in representing the mean wave solution as a function of the polynomial order n . To this end, we solve (274) numerically with a linear multi-step (explicit) time integration scheme (3rd-order Adams-Bashforth) combined with a trapezoidal rule to discretize the memory integral. It clearly appears that the MZ-Faber expansion converges faster than the MZ-Dyson expansion.

5.7.2 Harmonic oscillator chains on the Bethe lattice

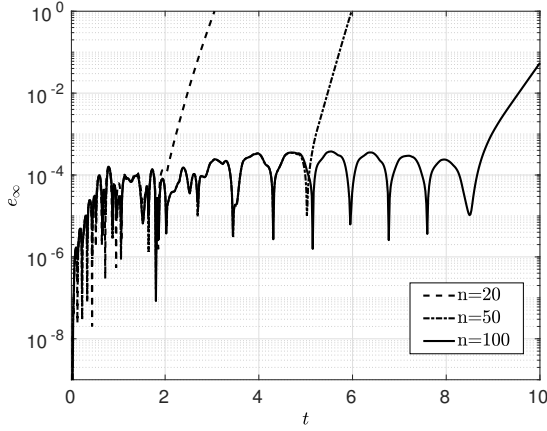
Dynamics of harmonic chains on Bethe lattices is a simple but illustrative Hamiltonian dynamical system that has been widely studied in statistical mechanics, mostly in relation to Brownian motion [6, 39, 29, 30, 44]. A Bethe lattice is a connected cycle-free graph in which each node interacts only with its neighbors. The number of such neighbors, is a constant of the graph called *coordination number*. This means that each node in the graph (with the exception of the leaf nodes) has the same number of edges connecting it to its neighbors. In Figure 12 we show two Bethe lattices with coordination numbers $l = 2$ and $l = 3$, respectively. The Bethe graph is hierarchical and therefore it can be organized into shells, emanating from an arbitrary node. The number of nodes in the k -th shell is given by $N_k = l(l-1)^{k-1}$, while the total number of nodes within S shells is

$$N = 1 + \sum_{k=1}^S N_k. \quad (280)$$

Mean Wave Amplitude at $(r, \theta) = (1.1, 0.1)$



MZ-Dyson Error



MZ-Faber Error

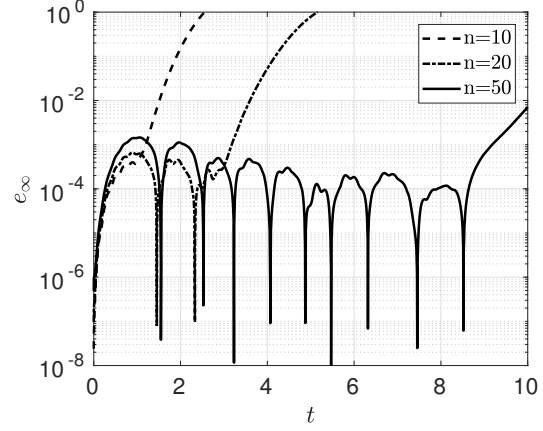


Figure 11: MZ-Dyson and MZ-Faber approximation errors of the mean wave amplitude at $(r, \theta) = (1.1, 0.1)$ as a function of the polynomial order n . It is seen that the MZ-Faber expansion converges faster than the MZ-Dyson series.

Next, we consider a coupled system of N harmonic oscillators¹⁸ whose mutual interactions are defined by the adjacency matrix $\mathbf{B}^{(l)}$ of a Bethe graph with coordination number l [8]. The Hamiltonian of such system can be written as

$$H(\mathbf{p}, \mathbf{q}) = \frac{1}{2m} \sum_{i=1}^N p_i^2 + \frac{k}{2l} \sum_{i,j=1}^N B_{ij}^{(l)} (q_i - q_j)^2, \quad (281)$$

where q_i and p_i are, respectively, the displacement and momentum of the i -th particle, m is the mass of the particles (assumed constant throughout the network), and k is the elasticity constant that modulates the intensity of the quadratic interactions. We emphasize that the harmonic chain we consider here is one-dimensional. The Bethe graph basically just sets the interaction among the different oscillators. The dynamics of the harmonic chain on the Bethe lattice is governed by the Hamilton's equations

$$\frac{dq_i}{dt} = \frac{\partial H}{\partial p_i}, \quad \frac{dp_i}{dt} = -\frac{\partial H}{\partial q_i}. \quad (282)$$

¹⁸The number of oscillators cannot be set arbitrarily as it must satisfy the topological graph constraints prescribed by (280).

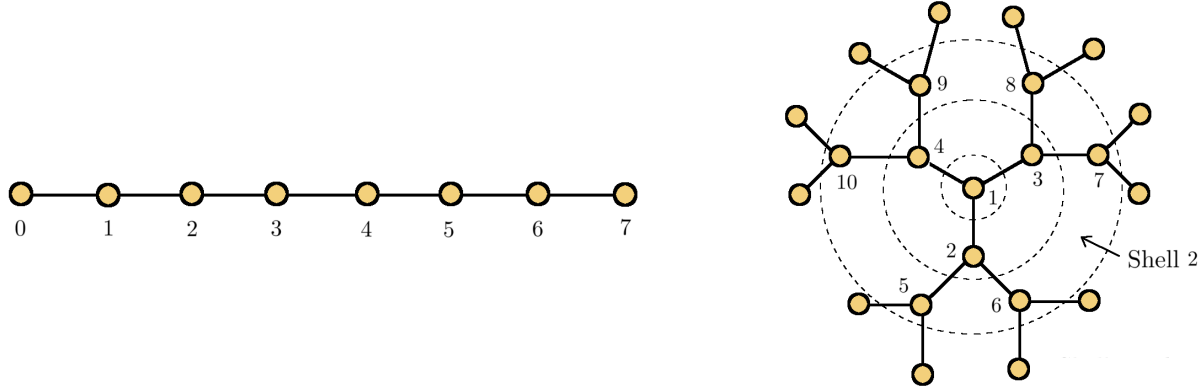


Figure 12: Bethe lattices with coordination numbers 2 (left), and 3 (right).

These equations can be written in a matrix-vector form as

$$\begin{bmatrix} \dot{\mathbf{p}} \\ \dot{\mathbf{q}} \end{bmatrix} = \begin{bmatrix} \mathbf{0} & k\mathbf{B}^{(l)} - k\mathbf{D}^{(l)} \\ \mathbf{I}/m & \mathbf{0} \end{bmatrix} \begin{bmatrix} \mathbf{p} \\ \mathbf{q} \end{bmatrix} = \mathbf{C} \begin{bmatrix} \mathbf{p} \\ \mathbf{q} \end{bmatrix}, \quad (283)$$

where $\mathbf{B}^{(l)}$ is the adjacency matrix of the graph and $\mathbf{D}^{(l)}$ is the degree matrix. Note that (283) is a linear dynamical system. The time evolution of any phase space function $u(\mathbf{q}, \mathbf{p})$ (quantity of interest) satisfies

$$\frac{du}{dt} = \{u, H\},$$

where

$$\{u, H\} = \sum_{i=1}^N \left(\frac{\partial u}{\partial q_i} \frac{\partial H}{\partial p_i} - \frac{\partial H}{\partial q_i} \frac{\partial u}{\partial p_i} \right) \quad (284)$$

denotes the Poisson Bracket. A particular phase space function we consider hereafter is the velocity autocorrelation function of a tagged oscillator, say the one at location $j = 1$ (see Figure 12). Such correlation function is defined as

$$C_{p_1}(t) = \frac{\langle p_1(t)p_1(0) \rangle_{eq}}{\langle p_1(0)p_1(0) \rangle_{eq}}, \quad (285)$$

where the average is an integral over the Gibbs canonical distribution.

Analytical expressions for the velocity autocorrelation function The simple structure of harmonic chains on the Bethe lattice allows us to determine analytical expressions for the velocity autocorrelation function (285), e.g., [6, 44, 39].

Bethe lattice with coordination number 2: Let us set $l = 2$. In this case, the Bethe lattice is a path graph, i.e., a one-dimensional chain of harmonic oscillators where each oscillator interacts only with the one at the left and at the right. We set fixed boundary conditions at the endpoint of the chain, i.e., $q_0(t) = q_{N+1}(t) = 0$ and $p_0(t) = p_{N+1}(t) = 0$ (particles are numbered from left to right). In this setting, the velocity autocorrelation function of the particle labeled with $j = 1$ can be obtained analytically by employing Lee's continued fraction method [39]. This yields the well-known $J_0 - J_4$ solution

$$C_{p_1}(t) = J_0(2\omega t) - J_4(2\omega t), \quad (286)$$

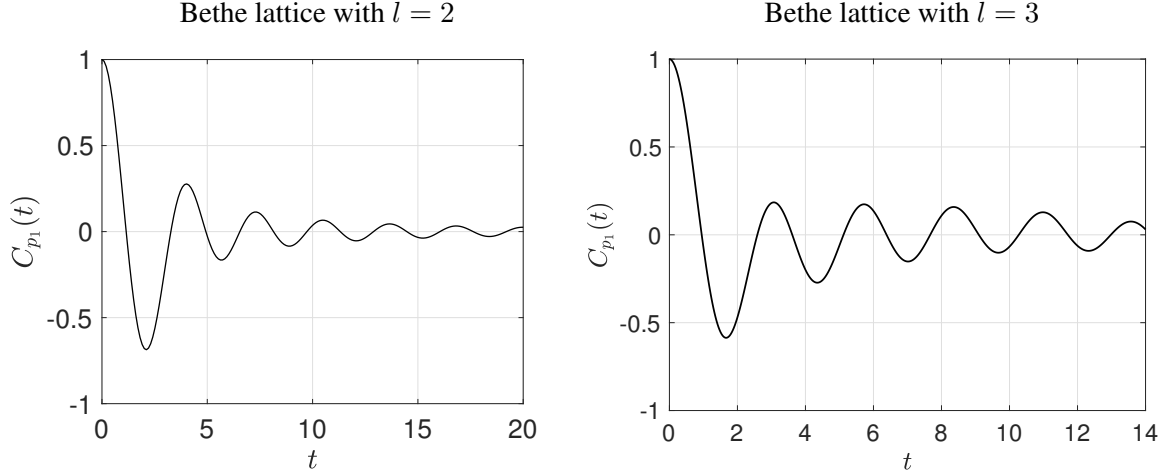


Figure 13: Velocity auto-correlation functions (286) (left) and (289) (right) of a tagged oscillator in a harmonic chain interacting on a Bethe lattice with coordination number $l = 2$ and $l = 3$, respectively.

where $J_i(t)$ is the i -th Bessel function of the first kind, and $\omega = k/m$. Here we choose $k = m = 1$. The Hamilton's equations (283) for the inner oscillators¹⁹ take the form

$$\begin{bmatrix} \dot{\mathbf{p}} \\ \dot{\mathbf{q}} \end{bmatrix} = \begin{bmatrix} \mathbf{0} & \mathbf{B}^{(2)} - \mathbf{D}^{(2)} \\ \mathbf{I} & \mathbf{0} \end{bmatrix} \begin{bmatrix} \mathbf{p} \\ \mathbf{q} \end{bmatrix}, \quad (287)$$

where $\mathbf{B}^{(2)}$ and $\mathbf{D}^{(2)}$ are the adjacency matrix and the degree matrix of the Bethe lattice with $l = 2$ (see Figure 12). As an example, if we consider $N = 5$ oscillators then $\mathbf{B}^{(2)}$ and $\mathbf{D}^{(2)}$ are given by

$$\mathbf{B}^{(2)} = \begin{bmatrix} 0 & 1 & 0 \\ 1 & 0 & 1 \\ 0 & 1 & 0 \end{bmatrix}, \quad \mathbf{D}^{(2)} = \begin{bmatrix} 2 & 0 & 0 \\ 0 & 2 & 0 \\ 0 & 0 & 2 \end{bmatrix}. \quad (288)$$

Bethe lattice with coordination number 3: Bethe graphs with $l = 3$ can be represented as planar graphs (see Figure 12). The velocity auto-correlation function at the center node can be expressed analytically [44], in the limit of an infinite number of oscillators ($N \rightarrow \infty$)²⁰, as

$$C_{p_1}(t) = \sum_{n=-\infty}^{+\infty} [G_n(t) + H_n(t)] J_{2n}(bt) \quad (289)$$

where

$$G_n(l) = \sum_{k=0}^{\infty} \frac{g_k(l)}{b^{2k-2}} \frac{1}{2\pi} \int_a^{\pi/2} d\theta \frac{\cos^2(\theta)}{\sin^{2k}(\theta)} \cos(2n\theta), \quad g_k(l) = - \sum_{j=k}^{\infty} \frac{(2j-1)!!}{[2^j(2j-1)j!]} a^{2j} c^{2(k-j)},$$

$$H_n(l) = \sum_{k=0}^{\infty} \frac{h_k(l)}{b^{-2k-2}} \frac{1}{2\pi} \int_a^{\pi/2} d\theta \frac{\cos^2(\theta)}{\sin^{-2k}(\theta)} \cos(2n\theta), \quad h_k(l) = - \sum_{j=k}^{\infty} \frac{(2j-1)!!}{[2^j(2j-1)j!]} a^{2(j-k)} c^{-2j}$$

¹⁹We exclude the two oscillators at the endpoints of the harmonic chain, since their dynamics is trivial.

²⁰Thanks to the symmetry of the Bethe lattice, in the limit $n \rightarrow \infty$ the velocity auto-correlation function is the same at each node.

and $a = \sqrt{2} - 1$, $b = \sqrt{2} + 1$ and $c = \sqrt{6}$. The Hamilton's equations of motion in this case are²¹ ($k = m = 1$)

$$\begin{bmatrix} \dot{\mathbf{p}} \\ \dot{\mathbf{q}} \end{bmatrix} = \begin{bmatrix} \mathbf{0} & \mathbf{B}^{(3)} - \mathbf{D}^{(3)} \\ \mathbf{I} & \mathbf{0} \end{bmatrix} \begin{bmatrix} \mathbf{p} \\ \mathbf{q} \end{bmatrix}. \quad (290)$$

where $\mathbf{B}^{(3)}$, $\mathbf{D}^{(3)}$ are the adjacency matrix and the degree matrix of the Bethe lattice with $l = 3$ (see Figure 12). For example, if we label the oscillators as in Figure 12, and assume that the Bethe lattice has only three shells, i.e., 10 oscillators (4 inner nodes, and 6 leaf nodes) then the adjacency matrix and the degree matrix are

$$\mathbf{B}^{(3)} = \begin{bmatrix} 0 & 1 & 1 & 1 & 0 & 0 & 0 & 0 & 0 & 0 \\ 1 & 0 & 0 & 0 & 1 & 1 & 0 & 0 & 0 & 0 \\ 1 & 0 & 0 & 0 & 0 & 0 & 1 & 1 & 0 & 0 \\ 1 & 0 & 0 & 0 & 0 & 0 & 0 & 0 & 1 & 1 \\ 0 & 1 & 0 & 0 & 0 & 0 & 0 & 0 & 0 & 0 \\ 0 & 1 & 0 & 0 & 0 & 0 & 0 & 0 & 0 & 0 \\ 0 & 0 & 1 & 0 & 0 & 0 & 0 & 0 & 0 & 0 \\ 0 & 0 & 1 & 0 & 0 & 0 & 0 & 0 & 0 & 0 \\ 0 & 0 & 0 & 1 & 0 & 0 & 0 & 0 & 0 & 0 \\ 0 & 0 & 0 & 1 & 0 & 0 & 0 & 0 & 0 & 0 \end{bmatrix}, \quad \mathbf{D}^{(3)} = \begin{bmatrix} 3 & 0 & 0 & 0 & 0 & 0 & 0 & 0 & 0 & 0 \\ 0 & 3 & 0 & 0 & 0 & 0 & 0 & 0 & 0 & 0 \\ 0 & 0 & 3 & 0 & 0 & 0 & 0 & 0 & 0 & 0 \\ 0 & 0 & 0 & 3 & 0 & 0 & 0 & 0 & 0 & 0 \\ 0 & 0 & 0 & 0 & 1 & 0 & 0 & 0 & 0 & 0 \\ 0 & 0 & 0 & 0 & 0 & 1 & 0 & 0 & 0 & 0 \\ 0 & 0 & 0 & 0 & 0 & 0 & 1 & 0 & 0 & 0 \\ 0 & 0 & 0 & 0 & 0 & 0 & 0 & 1 & 0 & 0 \\ 0 & 0 & 0 & 0 & 0 & 0 & 0 & 0 & 1 & 0 \\ 0 & 0 & 0 & 0 & 0 & 0 & 0 & 0 & 0 & 1 \end{bmatrix}. \quad (291)$$

Generalized Langevin Equation for the Velocity Autocorrelation Function The evolution equation for the velocity autocorrelation function (285) was obtained in Section 5.4.3 and it is hereafter rewritten for convenience

$$\frac{dC_{p_1}(t)}{dt} = \alpha C_{p_1}(t) + \int_0^t g(t-s)C_{p_1}(s)ds. \quad (292)$$

The initial condition is set as $C_{p_i}(0) = 1$. As before, it can be shown that the coefficient α in (292) is identically zero. This implies that the dynamics of the velocity autocorrelation function is entirely determined by the MZ memory term. The MZ-Dyson and MZ-Faber series expansions of the the memory kernel $g(t-s)$ are given by

$$g(t-s) = \sum_{j=0}^n \frac{g_j^D}{j!} (t-s)^j, \quad g(t-s) = \sum_{j=0}^n g_j^F e^{tc_0} \frac{J_j(2t\sqrt{-c_1})}{(\sqrt{-c_1})^j}$$

where

$$g_j^D = \mathbf{b}^T (\mathbf{M}_{11}^T)^j \mathbf{a}, \quad g_j^F = \mathbf{b}^T \mathcal{F}_j (\mathbf{M}_{11}^T) \mathbf{a}.$$

The definition of the matrix \mathbf{M}_{11}^T and the vectors \mathbf{a} , \mathbf{b} is the same as before. Here we used the fact that for any quadratic Hamiltonian we have $\langle p_i(0), q_i(0) \rangle_{eq} = 0$ and $\langle p_i(0), p_j(0) \rangle_{eq} = 0$.

In Figure 14 we study convergence of the MZ-Dyson and the MZ-Faber series expansion of the memory kernel in equation (218). As before, the MZ-Faber series converges faster than the MZ-Dyson series. In Figure 15 and Figure 16, we study the accuracy of the MZ-Dyson and the MZ-Faber expansions in representing the velocity auto-correlation functions (286) and (289) (see Figure 13). Specifically, in these simulations we considered a chain of $N = 100$ oscillators for the case $l = 2$, and 8 shells of oscillators for the case $l = 3$, i.e., a total number of $N = 766$ oscillators. The results in Figure 15 and Figure 16 show that both the

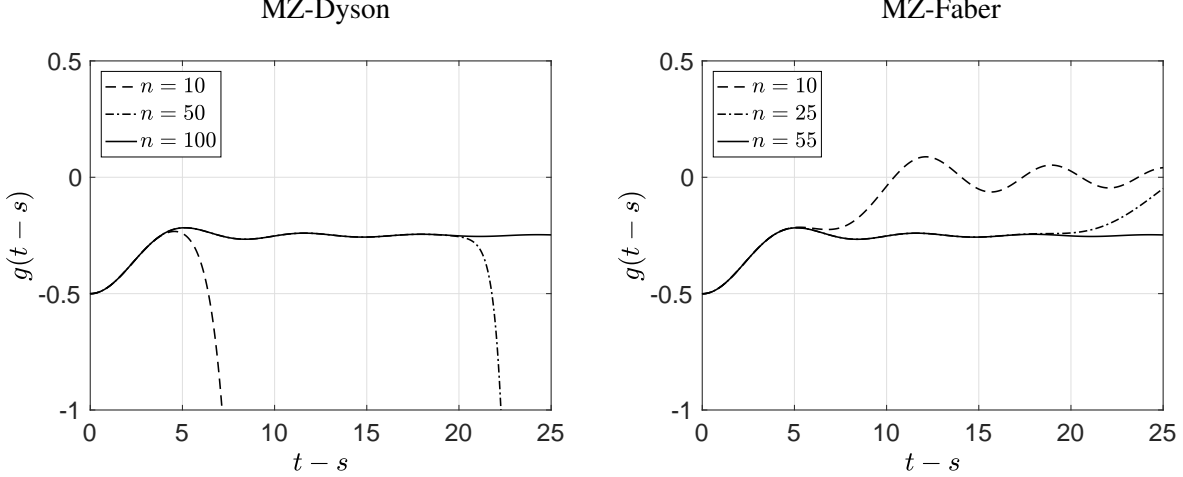


Figure 14: Harmonic chains of oscillators. Dyson and Faber expansions of the Mori-Zwanzig memory kernel $g(t - s)$. Shown are results for different polynomial orders n . It is seen that the MZ-Faber series converges faster than the MZ-Dyson series.

MZ-Dyson and the MZ-Faber expansions of the memory integral yield accurate approximations of the velocity autocorrelation function, and that convergence is uniform with the polynomial order. The expansion of the MZ memory integral we developed can be employed to calculate phase space functions of harmonic oscillators on graphs with arbitrary topological structure. The following example shows the effectiveness of the proposed technique in calculating the velocity auto-correlation function of a tagged oscillator in a network sampled from the Erdős–Rényi random graph.

6 Systems with local polynomial interactions

Building upon the Faber operator series expansion we discussed in section 5.1, in this section we show that it is possible to develop a formally exact algorithm to calculate the MZ memory kernel (64c). Such algorithm is based on a combinatorial approach originally proposed by Amati, Meyer and Schilling in [3].

6.1 Calculation of the MZ memory kernel from first principles

Let us consider the dynamical system (1) and a one-dimensional (scalar) phase space function of the form (2), i.e., $u(t) = u(\mathbf{x}(t, \mathbf{x}_0))$. A substitution of (190) into (64c) allows us to write the MZ memory kernel as

$$K(t) \simeq \sum_{q=0}^n g_q(t) M_q, \quad \text{where} \quad M_q = \frac{\langle u(0), \mathcal{L} \Phi_q(\mathcal{Q} \mathcal{L}) \mathcal{Q} \mathcal{L} u(0) \rangle_\rho}{\langle u(0), u(0) \rangle_\rho}. \quad (293)$$

Note that $K(t)$ depends only on the set of parameters $\{M_0, \dots, M_n\}$, since the temporal modes $g_q(t)$ are explicitly available given the polynomial set $\{\Phi_0, \dots, \Phi_n\}$ (see Table 1). We aim at determining $\{M_0, \dots, M_n\}$ from first principles. For one-dimensional phase space functions, Mori's projection (15) reduces to

$$\mathcal{P}f = \frac{\langle f, u(0) \rangle_\rho}{\langle u(0), u(0) \rangle_\rho} u(0). \quad (294)$$

²¹Here we implemented a free boundary condition at the outer shell of the chain.

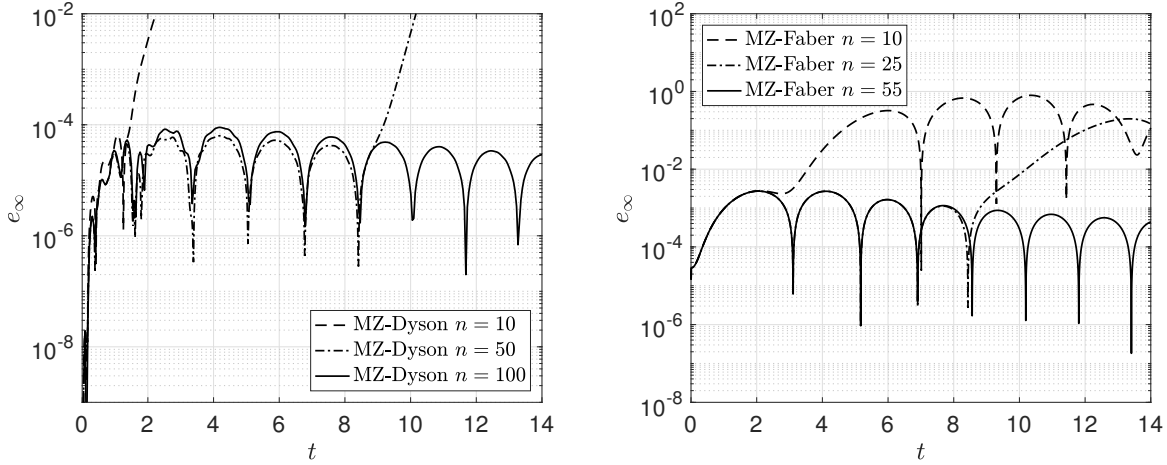


Figure 15: Accuracy of the MZ-Dyson and MZ-Faber expansions in representing the velocity auto-correlation function of the tagged oscillator $j = 2$ in an harmonic chain interacting on the Bethe lattice with coordination number 2. It is seen that the MZ-Dyson and the MZ-Faber expansions yield accurate predictions as we increase the polynomial order n . Moreover, the MZ-Faber expansion converges faster than the MZ-Dyson expansion.

At this point, it is convenient to introduce the following notation

$$\mu_i = \frac{\langle \mathcal{L}(\mathcal{QL})^{i-1} u(0), u(0) \rangle_\rho}{\langle u(0), u(0) \rangle_\rho}, \quad \gamma_i = \frac{\langle \mathcal{L}^i u(0), u(0) \rangle_\rho}{\langle u(0), u(0) \rangle_\rho}. \quad (295)$$

Each coefficient μ_i represents the rescaling of $u(0)$ under the action of the operator $\mathcal{PL}(\mathcal{QL})^{i-1}$, i.e. we have

$$\mu_i u(0) = \mathcal{PL}(\mathcal{QL})^{i-1} u(0). \quad (296)$$

Clearly, if we are given $\{\mu_1, \dots, \mu_{n+2}\}$ then we can easily compute M_q in (293), and therefore the memory kernel $K(t)$ for any given polynomial function Φ_q . For example, if $\Phi_q(\mathcal{QL}) = (\mathcal{QL})^q$ then $M_q = \mu_{q+2}$ ($q = 0, \dots, n$). On the other hand, if $\{\Phi_0, \dots, \Phi_n\}$ are Faber polynomials [100], then we can write each Φ_q as a linear combination of monomials $(\mathcal{QL})^j$ ($j = 0, \dots, q$) and therefore represent M_q as a linear combination of $\{\mu_1, \dots, \mu_{q+2}\}$. Computing μ_i using the definition (295) involves taking operator powers and averaging, which may be computationally expensive. An alternative effective algorithm relies on the following recursive formula [19, 79, 7]

$$\mu_1 = \gamma_1, \quad \mu_2 = \gamma_2 - \mu_1 \gamma_1, \quad \dots, \quad \mu_n = \gamma_n - \sum_{j=1}^{n-1} \mu_{n-j} \gamma_j. \quad (297)$$

In practice, (297) shifts the problem of computing $\{\mu_1, \dots, \mu_n\}$ to the problem of evaluating the coefficients $\{\gamma_1, \dots, \gamma_n\}$ defined in (295). This will be discussed extensively in the subsequent Section 6.2. If the Liouville operator \mathcal{L} is skew-adjoint relative to the inner product (111), then all μ_j and γ_j corresponding to odd indices are identically zero. This allows us to simplify the recursion (297) as

$$\mu_{2j} = \gamma_{2j} - \sum_{k=1}^{j-1} \mu_{2j-2k} \gamma_{2k} \quad j = 1, 2, \dots \quad (298)$$

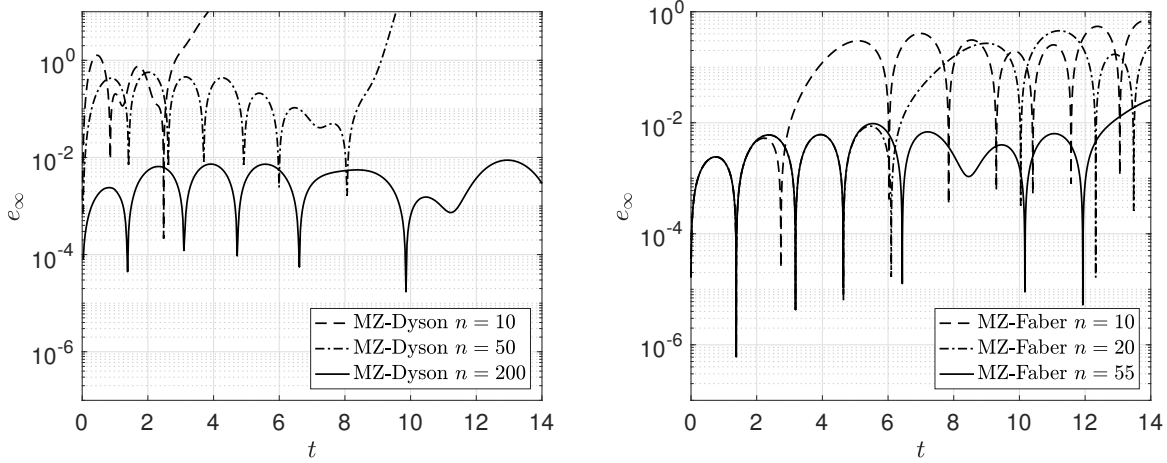


Figure 16: Accuracy of the MZ-Dyson and MZ-Faber expansions in representing the velocity auto-correlation function of the oscillator at the center of a Bethe lattice with coordination number 3, 8 shells and $N = 766$ oscillators. It is seen that the MZ-Dyson and the MZ-Faber expansion yield accurate predictions as we increase the polynomial order n . Moreover, the MZ-Faber expansion converges faster than the MZ-Dyson series.

As a consequence, the streaming term (115b) in the MZ equation vanishes identically since $\Omega = \mu_1 = \gamma_1 = 0$. We recall that skew-adjoint Liouville operators arise naturally, e.g., in Hamiltonian dynamical systems at statistical equilibrium.

6.2 Systems with polynomial nonlinearities

In this Section, we address the problem of calculating the coefficients $\{\gamma_1, \dots, \gamma_n\}$ defined in (295) and appearing in the recursion relation (297). With such coefficients available, we can compute $\{\mu_1, \dots, \mu_n\}$ and therefore the MZ memory kernel (293). The calculation we propose is based on first principles, meaning that we do not rely on any assumption or model to evaluate the averages $\gamma_i = \langle \mathcal{L}^i u(0), u(0) \rangle_\rho / \langle u(0), u(0) \rangle_\rho$. Instead, we develop a combinatorial algorithm that allows us to track all terms in $\mathcal{L}^i u(0)$, hence representing γ_i exactly as a superimposition of a finite, although possibly large, number of terms. The algorithm we develop is built upon the combinatorial algorithm recently proposed by Amati, Meyer and Schiling in [3]. To describe the algorithm, consider the nonlinear dynamical system (1) and assume that $\mathbf{F}(\mathbf{x})$ is a multivariate polynomial in the phase variables \mathbf{x} . A simple example of such system is the Kraichnan-Orszag three-mode problem [67, 92, 9]

$$\dot{x}_1 = x_1 x_3, \quad \dot{x}_2 = -x_2 x_3, \quad \dot{x}_3 = x_2^2 - x_1^2. \quad (299)$$

Other examples are the semi-discrete form of the Navier-Stokes equations, or the semi-discrete form of the nonlinear wave equation discussed in Section 6.6. The key observation to compute γ_j for systems with polynomial nonlinearities is that the action of the operator power \mathcal{L}^i on a polynomial observable $u(\mathbf{x})$ yields a polynomial function. For instance, consider $u(\mathbf{x}) = x_1^3$, and the Liouville operator associated with the system (299)

$$\mathcal{L} = x_1 x_3 \frac{\partial}{\partial x_1} - x_2 x_3 \frac{\partial}{\partial x_2} + (x_2^2 - x_1^2) \frac{\partial}{\partial x_3}. \quad (300)$$

We have

$$\mathcal{L}x_1^3 = 3x_1^3x_3, \quad (301)$$

$$\mathcal{L}^2x_1^3 = 9x_1^3x_3^2 + 3x_1^3x_2^2 - 3x_1^5, \quad (302)$$

$$\mathcal{L}^3x_1^3 = 27x_1^3x_3^3 + 18x_1^3x_2^2x_3 - 18x_1^5x_3 + 27x_1^3x_2^2x_3 - 6x_1^3x_2^2x_3 - 15x_1^5x_3. \quad (303)$$

Clearly, the number of terms in $\mathcal{L}^i x_1^3$ can rapidly increase, if high-order powers of \mathcal{L} are considered. For higher-dimensional systems with non-local interactions, i.e., for systems where each $F_i(\mathbf{x})$ ($i = 1, \dots, N$) depends on all components of \mathbf{x} , this problem is serious, and requires multi-core computer-based combinatorics to systematically track all terms in the expansion of $\mathcal{L}^i x_j^q$. Let us introduce the following notation

$$\mathcal{L}^n x_j^q = \sum_{\mathbf{b}_i \in B^{(n)}} a_{\mathbf{b}_i}^{(n)} x_{k_1}^{m_{k_1}^{(i)}} \cdots x_{k_r}^{m_{k_r}^{(i)}}, \quad (304)$$

where $\{a_{\mathbf{b}_i}^{(n)}\}$ are polynomial coefficients, and $\{m_{k_j}^{(i)}\}$ are polynomial exponents. The set of indexes representing the relevant phase variables appearing in $\mathcal{L}^n x_j^q$, i.e., $\{k_1, \dots, k_r\}$, is collected in the index set $K(n, j) = \{k_1, \dots, k_r\}$, which depends on n and j . For example, in (301)-(303) we have

$$K(1, 1) = \{1, 3\}, \quad K(2, 1) = \{1, 2, 3\}, \quad K(3, 1) = \{1, 2, 3\}. \quad (305)$$

Of course, for low-dimensional dynamical systems, the simplest choice for the relevant variables would be the complete set of variables $\{x_1, \dots, x_N\}$. However, for high-dimensional systems with local interactions this choice could lead to unnecessary computations. In fact, it can be shown that the variables appearing in the polynomial $\mathcal{L}^n x_j^q$ are usually a (possibly small) subset of the phase variables if the system has local interactions. The vector $\mathbf{b}_i = [m_{k_1}^{(i)}, \dots, m_{k_r}^{(i)}]$, collects the exponents of the i -th monomial appearing in the expansion (304). Similarly, $a_{\mathbf{b}_i}^{(n)}$ is the coefficient multiplying i -th monomial in (304). For example, in (301) and (302) we have, respectively,

$$\mathbf{b}_1 = [3, 1], \quad a_{\mathbf{b}_1}^{(1)} = 3,$$

$$\mathbf{b}_1 = [3, 0, 2], \quad \mathbf{b}_2 = [3, 2, 0], \quad \mathbf{b}_3 = [5, 0, 0], \quad a_{\mathbf{b}_1}^{(2)} = 9, \quad a_{\mathbf{b}_2}^{(2)} = 3, \quad a_{\mathbf{b}_3}^{(2)} = -3.$$

At this point, it is convenient to define the set of polynomial exponents $B^{(n)} = \{\mathbf{b}_1, \mathbf{b}_2, \dots\}$, the set of polynomial coefficients $A^{(n)} = \{a_{\mathbf{b}_1}^{(n)}, a_{\mathbf{b}_2}^{(n)}, \dots\}$, and the combined index set

$$\mathcal{I}^{(n)} = \{A^{(n)}, B^{(n)}\}. \quad (306)$$

Clearly, $\mathcal{I}^{(n)}$ identifies uniquely the polynomial (304), i.e., there is a one-to-one correspondence between $\mathcal{I}^{(n)}$ and $\mathcal{L}^n x_j^q$. For example, in the case of (301)-(303) we have

$$\mathcal{I}^{(1)} = \underbrace{\{\{3\}\}}_{A^{(1)}} \cup \underbrace{\{\{3, 0, 1\}\}}_{B^{(1)}}, \quad (307)$$

$$\mathcal{I}^{(2)} = \underbrace{\{\{9, 3, -3\}\}}_{A^{(2)}} \cup \underbrace{\{\{3, 0, 2\}, [3, 2, 1], [5, 0, 0]\}}_{B^{(2)}}, \quad (308)$$

$$\mathcal{I}^{(3)} = \underbrace{\{\{27, 18, -18, 27, -6, -15\}\}}_{A^{(3)}} \cup \underbrace{\{\{3, 0, 3\}, [3, 2, 1], [5, 0, 1], [3, 2, 1], [3, 2, 1], [5, 0, 1]\}}_{B^{(3)}}. \quad (309)$$

If we apply \mathcal{L} to (304) we obtain

$$\begin{aligned}
\mathcal{L}^{n+1}x_j^q &= \mathcal{L}\mathcal{L}^n x_j^q, \\
&= \mathcal{L} \sum_{\mathbf{b}_i \in B^{(n)}} a_{\mathbf{b}_i}^{(n)} x_{k_1}^{m_{k_1}^{(i)}} \cdots x_{k_r}^{m_{k_r}^{(i)}}, \\
&= \sum_{\mathbf{b}_i \in B^{(n+1)}} a_{\mathbf{b}_i}^{(n+1)} x_{k_1}^{m_{k_1}^{(i)}} \cdots x_{k_r}^{m_{k_r}^{(i)}}.
\end{aligned} \tag{310}$$

Clearly, if we can compute the mapping $\mathcal{I}^{(n)} \xrightarrow{\mathcal{L}} \mathcal{I}^{(n+1)}$, induced by the action of the Liouville operator \mathcal{L} to the polynomial (304) (represented by $\mathcal{I}^{(n)}$), then we can compute the *exact* series expansion of $\mathcal{L}^n x_j^q$ for arbitrary n . With such expansion available, we can immediately determine the coefficients γ_j in (295) by averaging over the probability density ρ as

$$\gamma_n = \frac{\langle \mathcal{L}^n x_j^q, x_j^q \rangle_\rho}{\langle x_j^q, x_j^q \rangle_\rho} = \sum_{\mathbf{b}_i \in B^{(n)}} a_{\mathbf{b}_i}^{(n)} \frac{\langle x_{k_1}^{m_{k_1}^{(i)}} \cdots x_{k_r}^{m_{k_r}^{(i)}} x_j^q \rangle_\rho}{\langle x_j^q, x_j^q \rangle_\rho}. \tag{311}$$

If the operator \mathcal{L} is skew-adjoint in $L^2(\mathcal{M}, \rho)$, i.e., if $\langle \mathcal{L}f, g \rangle_\rho = -\langle f, \mathcal{L}g \rangle_\rho$, then we have

$$\gamma_{2n} = \frac{\langle \mathcal{L}^{2n} x_j^q, x_j^q \rangle_\rho}{\langle x_j^q, x_j^q \rangle_\rho} = (-1)^n \sum_{\mathbf{b}_i, \mathbf{b}_j \in B^{(n)}} a_{\mathbf{b}_j}^{(n)} a_{\mathbf{b}_i}^{(n)} \frac{\langle x_{k_1}^{m_{k_1}^{(i)}+m_{k_1}^{(j)}} \cdots x_{k_r}^{m_{k_r}^{(i)}+m_{k_r}^{(j)}} \rangle_\rho}{\langle x_j^q, x_j^q \rangle_\rho}. \tag{312}$$

As pointed out by Maiocchi *et al.* in [58], the value of the first few coefficients $\{\gamma_n\}$ in (311) or (312) can be used to identify non-exponential relaxation patterns to equilibrium.

Remark To enhance numerical stability when computing the Faber expansion of the MZ memory kernel we scale the Liouville operator \mathcal{L} by a parameter $\delta < 1$ (see [100, 38]), i.e., we compute the Faber operator polynomial series relative to $\delta\mathcal{L}$. Correspondingly, the generalized Langevin equation (63) is solved on a time scale t/δ . In this setting, the coefficients (311) are also calculated relative to the rescaled Liouville operator $\delta\mathcal{L}$.

Remark Computing γ_j for linear systems reduces to a classical numerical linear algebra problem, i.e., computing the Rayleigh quotient of a matrix power. To show this, consider the N -dimensional linear system $\dot{\mathbf{x}} = \mathbf{A}\mathbf{x}$, evolving from the random initial state $\mathbf{x}_0 \sim \rho_0$ (\mathbf{x}_0 column vector). Suppose we are interested in the first component of the system, i.e., set the observable as $u(t) = x_1(t, \mathbf{x}_0)$. Define the linear subspace $V = \text{span}\{x_{01}, x_{02}, \dots, x_{0N}\} \subset L^2(\mathcal{M}, \rho_0)$. Clearly $u(t) \in V$ for all $t \geq 0$ [99, 100]. This allows us to calculate γ_j as

$$\gamma_j = \langle [\mathbf{A}^T]^j \mathbf{x}_0 \cdot \mathbf{e}_1 \rangle_{\rho_0}, \quad j = 1, \dots, n \tag{313}$$

where $\mathbf{e}_1 = [1, 0, \dots, 0]^T$.

6.3 Mapping the index set $\mathcal{I}^{(n)}$

Here we describe the algorithm that allows us to compute the polynomial $\mathcal{L}^{n+1}x_k^q$ given the polynomial $\mathcal{L}^n x_k^q$ and the Liouville operator \mathcal{L} , i.e., the mapping defined by equation (310). This is equivalent to develop a set of algebraic rules to transform the combined index set $\mathcal{I}^{(n)}$ defined in (306) into $\mathcal{I}^{(n+1)}$, for arbitrary n . Once such rules are known, we can apply them recursively to compute the polynomial sequence

$$x_j^q \rightarrow \mathcal{L}x_j^q \rightarrow \mathcal{L}^2x_j^q \rightarrow \mathcal{L}^3x_j^q \rightarrow \cdots \rightarrow \mathcal{L}^n x_j^q$$

to any desired order. In this way, we can determine γ_n through (311) (or (312)), μ_n through (297) (or (298)), and therefore the MZ memory kernel (293). Before formulating the algorithm in full generality, it is useful to examine how it operates in a concrete example. To this end, consider again the Kraichnan-Orszag system (299), and the transformation between the polynomials (302) and (303) defined by the action of the Liouville operator (300). We are interested in formulating such transformation in terms of a set of algebraic operations mapping the index set $\mathcal{I}^{(2)}$ into $\mathcal{I}^{(3)}$ (Eqs. (308)-(309)). We begin by decomposing the three-dimensional Liouville operator (300) as

$$\mathcal{L} = \mathcal{L}_1 + \mathcal{L}_2 + \mathcal{L}_3, \quad \text{where} \quad \mathcal{L}_1 = x_1 x_3 \frac{\partial}{\partial x_1}, \quad \mathcal{L}_2 = -x_2 x_3 \frac{\partial}{\partial x_2}, \quad \mathcal{L}_3 = (x_2^2 - x_1^2) \frac{\partial}{\partial x_3}. \quad (314)$$

The action of \mathcal{L}_i on any monomial generates a polynomial with S_i terms. In the present example, we have $S_1 = S_2 = 1$ and $S_3 = 2$. Let us now consider the first monomial in (302), i.e., $9x_1^3 x_2^2$. Such monomial is represented by the first element of $A^{(2)}$ and $B^{(2)}$ in (309). The corresponding combined set is $\{9, [3, 0, 2]\}$. At this point, we apply the operators \mathcal{L}_1 , \mathcal{L}_2 and \mathcal{L}_3 to the polynomial $\{9, [3, 0, 2]\}$. This yields

$$\underbrace{\{9, [3, 0, 2]\}}_{9x_1^3 x_2^2} \xrightarrow{\mathcal{L}_1} \underbrace{\{27, [3, 0, 3]\}}_{27x_1^3 x_3^3}, \quad (315)$$

$$\underbrace{\{9, [3, 0, 2]\}}_{9x_1^3 x_2^2} \xrightarrow{\mathcal{L}_2} \underbrace{\{0, [3, -1, 2]\}}_0, \quad (316)$$

$$\underbrace{\{9, [3, 0, 2]\}}_{9x_1^3 x_2^2} \xrightarrow{\mathcal{L}_3} \underbrace{\{18, [3, 2, 1]\} \uplus \{-18, [5, 0, 1]\}}_{18x_1^3 x_2^2 x_3 - 18x_1^5 x_3} = \{\{18, -18\}, \{[3, 2, 1], [5, 0, 1]\}\}. \quad (317)$$

The transformation associated with \mathcal{L}_3 generates the sum of two monomials, namely $18x_1^3 x_2^2 x_3 - 18x_1^5 x_3$, which we represent as a union between two index sets. Such union, here denoted as \uplus , is an ordered union that pushes to the left polynomial coefficients and to the right polynomial exponents. Proceeding in a similar manner for all other monomials in (302) and taking ordered unions of all sets, yields the desired mapping $\mathcal{I}^{(2)} \rightarrow \mathcal{I}^{(3)}$. Let us now examine the action of a more general Liouville operator

$$\mathcal{L}_j = z x_1^{c_1} \cdots x_N^{c_N} \frac{\partial}{\partial x_j} \quad (318)$$

on the monomial $ax_1^{m_1} \cdots x_N^{m_N}$ represented by the index set $\{a, [m_1, \dots, m_N]\}$. We have

$$\{a, [m_1, \dots, m_N]\} \xrightarrow{\mathcal{L}_j} \{z m_j a, [m_1 + c_1, \dots, m_j + c_j - 1, \dots, m_N + c_N]\}. \quad (319)$$

This defines two linear transformations: a scaling transformation in the space of coefficients, and an addition in the space of exponents

$$a \rightarrow (z m_1) a, \quad [m_1, \dots, m_N] \rightarrow [m_1, \dots, m_N] + [c_1, \dots, c_j - 1, \dots, c_N]. \quad (320)$$

In a vector notation, upon definition of $\mathbf{b} = [m_1, \dots, m_N]$, $\boldsymbol{\theta}_j = [c_1, \dots, c_j - 1, \dots, c_N]$ and $\alpha_j = zm_j$, we can write (320) in compact form as

$$a \rightarrow \alpha_j a, \quad \mathbf{b} \rightarrow \mathbf{b} + \boldsymbol{\theta}_j. \quad (321)$$

Let us now consider the general case where the Liouville operator is defined as

$$\mathcal{L}(\mathbf{x}) = \sum_{k=1}^N \mathcal{L}_k(\mathbf{x}) \quad \mathcal{L}_k(\mathbf{x}) = F_k(\mathbf{x}) \frac{\partial}{\partial x_k} \quad (322)$$

and $F_k(\mathbf{x})$ is a polynomial involving S_k monomials in either all variables $\{x_1, \dots, x_N\}$ or a subset of them. The action of \mathcal{L} on each monomial in (310) can be written as

$$\mathcal{L} x_{k_1}^{m_{k_1}^{(i)}} \dots x_{k_r}^{m_{k_r}^{(i)}} = \sum_{q \in K(n, j)} \mathcal{L}_q x_{k_1}^{m_{k_1}^{(i)}} \dots x_{k_r}^{m_{k_r}^{(i)}}, \quad (323)$$

where $K(n, j) = \{k_1, \dots, k_r\}$ is the set of relevant variables at iteration n . The polynomial (323) involves $S_{k_1} + \dots + S_{k_r}$ terms, each one of which can be explicitly constructed by applying the linear transformation rules (321). In summary, we have

$$\mathcal{I}^{(n+1)} = \biguplus_{q \in K(n, j)} \biguplus_{i=1}^{\#B^{(n)}} \biguplus_{s=1}^{S_q} \{\alpha_s^q a_{\mathbf{b}_i}^{(n)}, \mathbf{b}_i + \boldsymbol{\theta}_s^q\}, \quad (324)$$

where $\#B^{(n)}$ denotes the number of elements in $B^{(n)}$. Note that both α_s^q and $\boldsymbol{\theta}_s^q$ depend on $q \in K(n, j)$ (index set of relevant variables).

Remark The recursive algorithm summarized by formula (324) is a modified version of the algorithm originally proposed by Amati, Meyer and Schiling in [3]. The key idea is the same, i.e., to compute the expansion coefficients γ_n in (311) using polynomial differentiation. However, there are a few differences between our algorithm and the algorithm proposed in [3] which we emphasize hereafter. In [3], the index set $B^{(n)}$ is pre-computed using the so-called spreading operators. Essentially, for each n , the iterative scheme generates a new set of polynomial coefficients $A^{(n)}$, which is subsequently matched with the corresponding indexes in $B^{(n)}$. In our algorithm, the sets $B^{(n)}$ and $A^{(n)}$ are computed on-the-fly at each step of the recursion. By doing so, we avoid calculating the spreading operators. This, in turn, allows us to avoid using numerical tensors to store index sets, since in our formulation there is no matching procedure between the polynomial exponents and the polynomial coefficients. Another difference between the two algorithms is that we utilized a rescaled Liouville operator $\delta \mathcal{L}$ ($\delta \in \mathbb{R}$) to enhance numerical stability when computing the operator polynomials $\Phi_q(\mathcal{Q}\mathcal{L})$ in (190). The algorithm in [3], on the other hand, is based on a Taylor series expansion of the operator exponential $e^{t\mathcal{L}}$, with unscaled Liouville operator²².

6.4 An example: the Fermi-Pasta-Ulam (FPU) model

Consider a one-dimensional chain of N anharmonic oscillators with Hamiltonian

$$\mathcal{H}(\mathbf{p}, \mathbf{q}) = \sum_{j=0}^{N-1} \frac{p_j^2}{2m} + \sum_{j=1}^{N-1} V(q_j - q_{j-1}). \quad (325)$$

²²In our recent work [100] (section 3.1) we proved that a Taylor series of the orthogonal dynamical propagation $e^{t\mathcal{Q}\mathcal{L}}$ yields an expansion of the MZ memory integral that resembles the classical Dyson series in scattering theory.

In (325) $\{q_j, p_j\}$ are, respectively, the generalized coordinate and momentum of the j -th oscillator, while $V(q_i - q_{i-1})$ is the potential energy between two adjacent oscillators. Suppose that the oscillator chain is closed (periodic), i.e., that $q_0 = q_N$ and $p_0 = p_N$. Define the distance between two oscillators as $r_j = q_j - q_{j-1}$. This allows us to write the Hamilton's equations of motion as

$$\begin{cases} \frac{dr_j}{dt} = \frac{1}{m}(p_i - p_{i-1}), \\ \frac{dp_j}{dt} = \frac{\partial V(r_{j+1})}{\partial r_{j+1}} - \frac{\partial V(r_j)}{\partial r_j}. \end{cases}$$

The Liouville operator corresponding to this system is

$$\mathcal{L}(\mathbf{p}, \mathbf{r}) = \sum_{i=1}^{N-1} \left[\left(\frac{\partial V(r_{i+1})}{\partial r_{i+1}} - \frac{\partial V(r_i)}{\partial r_i} \right) \frac{\partial}{\partial p_i} + \frac{1}{m}(p_i - p_{i-1}) \frac{\partial}{\partial r_i} \right].$$

Setting $V(x) = \alpha x^2/2 + \beta x^4/4$ yields the well-known Fermi-Pasta-Ulam β -model [60], which we study hereafter. To this end, suppose we are interested in the distance between the oscillators j and $j - 1$, i.e., in the polynomial observable $u(\mathbf{p}, \mathbf{r}) = r_j$. The action of \mathcal{L}^n on r_j can be explicitly written as

$$\mathcal{L}^n r_j = \sum_{\mathbf{b}_i \in B^{(n)}} a_{\mathbf{b}_i}^{(n)} r_{k_1}^{m_{k_1}^{(i)}} \cdots r_{k_u}^{m_{k_u}^{(i)}} p_{l_1}^{s_{l_1}^{(i)}} \cdots p_{l_v}^{s_{l_v}^{(i)}}, \quad (326)$$

where $\{k_1, \dots, k_u\}$ and $\{l_1, \dots, l_v\}$ are the relevant degrees of freedom for the polynomials of \mathbf{r} and \mathbf{p} , respectively, at iteration n . We can explicitly compute the sets of such relevant degrees of freedom as

$$K_r(n, j) = \left\{ j - \left\lfloor \frac{n}{2} \right\rfloor, \dots, j + \left\lfloor \frac{n}{2} \right\rfloor \right\} \quad L_p(n, j) = \left\{ j - \left\lfloor \frac{n+1}{2} \right\rfloor, \dots, j + \left\lfloor \frac{n-1}{2} \right\rfloor \right\}, \quad (327)$$

The action of the Liouville operator on each monomial appearing in (326) can be written as

$$\mathcal{L} r_{k_1}^{m_{k_1}^{(i)}} r_{k_u}^{m_{k_u}^{(i)}} p_{l_1}^{s_{l_1}^{(i)}} \cdots p_{l_v}^{s_{l_v}^{(i)}} = \sum_{v \in K_r(n, j)} \sum_{h \in L_p(n, j)} (\mathcal{L}_{r_v} + \mathcal{L}_{p_h}) r_{k_1}^{m_{k_1}^{(i)}} \cdots r_{k_u}^{m_{k_u}^{(i)}} p_{l_1}^{s_{l_1}^{(i)}} \cdots p_{l_v}^{s_{l_v}^{(i)}}, \quad (328)$$

where

$$\mathcal{L}_{r_v} = \frac{1}{m}(p_v - p_{v-1}) \frac{\partial}{\partial r_v}, \quad \text{and} \quad \mathcal{L}_{p_h} = [\alpha(r_{h+1} - r_h) + \beta(r_{h+1}^3 - r_h^3)] \frac{\partial}{\partial p_h}. \quad (329)$$

By computing the action of \mathcal{L}_{r_v} and \mathcal{L}_{p_h} on the monomial $r_{k_1}^{m_{k_1}^{(i)}} \cdots r_{k_u}^{m_{k_u}^{(i)}} p_{l_1}^{s_{l_1}^{(i)}} \cdots p_{l_v}^{s_{l_v}^{(i)}}$ we obtain explicit linear maps of the form (321), involving the polynomial exponents

$$\mathbf{b}_i = [\mathbf{m}^{(i)}, \mathbf{s}^{(i)}], \quad \mathbf{m}^{(i)} = [m_{k_1}^{(i)}, \dots, m_{k_u}^{(i)}], \quad \mathbf{s}^{(i)} = [s_{l_1}^{(i)}, \dots, s_{l_v}^{(i)}], \quad (330)$$

and the polynomial coefficients $a_{\mathbf{b}_i}^{(n)}$. With such maps available, we can transform the combined index set $\mathcal{I}^{(n)}$ (representing $\mathcal{L}^n r_j$) to $\mathcal{I}^{(n+1)}$ (representing $\mathcal{L}^{n+1} r_j$) using (324). Specifically, we obtain

$$\mathcal{I}^{(n+1)} = \mathcal{I}_r^{(n+1)} \uplus \mathcal{I}_p^{(n+1)},$$

where

$$\begin{aligned}\mathcal{I}_r^{(n+1)} &= \bigoplus_{v \in K_r(n,j)} \bigoplus_{i=1}^{\#B^{(n)}} \bigoplus_{k=0}^1 \left\{ m_v^{(i)} (-1)^k a_{\mathbf{b}_i}^{(n)}, [\mathbf{m}^{(i)} - \mathbf{e}_v, \mathbf{s}^{(i)} + \mathbf{e}_{v-k}] \right\}, \\ \mathcal{I}_p^{(n+1)} &= \bigoplus_{h \in L_p(n,j)} \bigoplus_{i=1}^{\#B^{(n)}} \bigoplus_{k=0}^1 \left\{ \{s_h^{(i)} (-1)^{k+1} \alpha a_{\mathbf{b}_i}^{(n)}, s_h^{(i)} (-1)^{k+1} \beta a_{\mathbf{b}_i}^{(n)}\}, \right. \\ &\quad \left. \{[\mathbf{m}^{(i)} + \mathbf{e}_{h+k}, \mathbf{s}^{(i)} - \mathbf{e}_h], [\mathbf{m}^{(i)} + 3\mathbf{e}_{h+k}, \mathbf{s}^{(i)} - \mathbf{e}_h]\} \right\}.\end{aligned}$$

6.5 Modeling the MZ fluctuation term

In previous section we discussed an algorithm to approximate the memory kernel in the MZ equation (113) or (20) based on the microscopic equations of motion (first-principle calculation). In this Section we construct a statistical model for the fluctuation term $\mathbf{f}(t)$ appearing in (113). A possible way to build such model is to expand (19d) in a finite-dimensional series²³ (see Eq. (190)) as

$$\mathbf{f}(t) \simeq \sum_{q=0}^n g_q(t) \Phi_q(\mathcal{QL}) \mathcal{QL} \mathbf{u}(0), \quad (331)$$

and evaluate the coefficients $\Phi_q(\mathcal{QL}) \mathcal{QL} \mathbf{u}(0)$ using the combinatorial approach discussed in Section 6.2. However, this may not be straightforward since $\Phi_q(\mathcal{QL}) \mathcal{QL} \mathbf{u}(0)$ is a high-dimensional random field. An alternative approach is to ignore the mathematical structure of $\mathbf{f}(t)$, i.e., equation (19d) or the series expansions (331), and simply model $\mathbf{f}(t)$ as a stochastic process. In doing so, we need to make sure that the statistical properties of the reduced-order model, e.g., the equilibrium distribution, are consistent with the full model. Such consistency conditions carry over a certain number of constraints on $\mathbf{f}(t)$, which allow for its *partial* identification. As an example, consider the following MZ model recently proposed by Lei *et al.* in [53] to study the dynamics of a tagged particle in a large particle system

$$\begin{cases} \dot{\mathbf{q}} &= \frac{\mathbf{p}}{m} \\ \dot{\mathbf{p}} &= \mathbf{F}(\mathbf{q}) + \mathbf{d} \\ \dot{\mathbf{d}} &= \mathbf{B}_0 \mathbf{d} - \mathbf{A}_0 \frac{\mathbf{p}}{m} + \mathbf{f}(t) \end{cases} \quad (332)$$

It was shown in [53] that if $\mathbf{f}(t)$ is Gaussian white noise (in time) with auto-correlation function

$$\langle \mathbf{f}(t) \mathbf{f}(t') \rangle = -\beta (\mathbf{B}_0 \mathbf{A}_0 + \mathbf{A}_0 \mathbf{B}_0^T) \delta(t - t'), \quad (333)$$

then the equilibrium distribution of the particle system has the Boltzmann-Gibbs form

$$\rho(\mathbf{p}, \mathbf{q}, \mathbf{d}) \propto \exp \left\{ -\beta \left(\frac{1}{2m} |\mathbf{p}|^2 + \frac{1}{2} \mathbf{d}^T \mathbf{A}_0^{-1} \mathbf{d} + V(\mathbf{q}) \right) \right\}, \quad (334)$$

$V(\mathbf{q})$ being the inter-particle potential. However, modeling $\mathbf{f}(t)$ as a Gaussian process does not provide satisfactory statistics in MZ equations if we use Mori's projection. In fact, equation (113) is linear and therefore the equilibrium distribution of $\mathbf{u}(t)$ (assuming it exists) under Gaussian noise $\mathbf{f}(t)$ will be necessarily Gaussian. In most applications, however, the equilibrium distribution of $\mathbf{u}(t)$ is strongly non-Gaussian.

²³Note that $\mathbf{f}(t)$ is a random process obtained by mapping the random initial state $\mathbf{u}(0) = \mathbf{u}(\mathbf{x}_0)$ forward in time using the orthogonal dynamics propagator $e^{t\mathcal{QL}(\mathbf{x}_0)}$.

To overcome this difficulty Chu and Li [19] recently developed a multiplicative Gaussian noise model that generalizes (113) in the sense that it is not based on additive noise, and it allows for non-Gaussian responses.

In this Section we propose a different stochastic modeling approach for $f(t)$ based on bi-orthogonal representations random processes [86, 90, 85, 5, 4]. To describe the method, we study the case where the observable $u(t)$ is real valued (one-dimensional) and square integrable. This allows us to develop the theory in a clear and concise way. We also assume that the system is in statistical equilibrium, i.e., that there exists an equilibrium distribution $\rho_{eq}(\mathbf{x})$ (or more generally an invariant measure) for the phase variables $\mathbf{x}(t, \mathbf{x}_0)$, and that \mathbf{x}_0 is sampled from such distribution. The MZ equation (113) for one-dimensional phase space functions $u(t) = u(\mathbf{x}(t, \mathbf{x}_0))$ reduces to

$$\frac{du(t)}{dt} = \Omega u(t) + \int_0^t K(t-s)u(s)ds + f(t), \quad (335)$$

where

$$\Omega = \frac{\langle u(0), \mathcal{L}u(0) \rangle_{eq}}{\langle u(0), u(0) \rangle_{eq}}, \quad K(t) = \frac{\langle u(0), \mathcal{L}f(t) \rangle_{eq}}{\langle u(0), u(0) \rangle_{eq}}, \quad f(t) = e^{t\mathcal{Q}\mathcal{L}}\mathcal{Q}\mathcal{L}u(0). \quad (336)$$

Since $u(t)$ is assumed to be a second-order random process in the time interval $[0, T]$, we can expand it in a truncated Karhunen-Loéve series

$$u(t) \simeq \bar{u} + \sum_{k=1}^K \sqrt{\lambda_k} \xi_k e_k(t), \quad t \in [0, T] \quad (337)$$

where \bar{u} denotes the mean of $u(t)$ relative to the equilibrium distribution²⁴, $\{\xi_1, \dots, \xi_K\}$ are uncorrelated random variables ($\langle \xi_i \xi_j \rangle_{eq} = \delta_{ij}$), and $\{\lambda_k, e_k(t)\}$ ($k = 1, \dots, K$) are, respectively, eigenvalues and eigenfunctions of the homogeneous Fredholm integral equation of the second kind

$$\int_0^T \langle u(t)u(s) \rangle_{eq} e_k(s)ds = \lambda_k e_k(t), \quad t \in [0, T]. \quad (338)$$

We recall that for ergodic systems in statistical equilibrium the auto-correlation function $\langle u(t)u(s) \rangle_{eq}$ decays to zero as $|t-s| \rightarrow \infty$. Also, the integral operator at the left hand side of (338) is positive-definite and compact [4]. The orthogonal random variables ξ_k and the temporal modes $e_k(t)$ are related to each other by the following dispersion relations [5, 86]

$$\xi_k = \frac{1}{\sqrt{\lambda_k}} \int_0^T u(t)e_k(t)dt, \quad e_k(t) = \frac{\langle u(t)\xi_k \rangle_{eq}}{\sqrt{\lambda_k}} \quad k = 1, 2, \dots \quad (339)$$

Equation (339) suggests that if $u(t)$ is a Gaussian random process (e.g., a Wiener process) then $\{\xi_1, \dots, \xi_K\}$ are necessarily independent Gaussian random variables. On the other hand, if $u(t)$ is non-Gaussian then the joint distribution of $\{\xi_1, \dots, \xi_K\}$ is unknown, although it can be in principle computed by using the transformation $u(t) \rightarrow \xi_k$ ($k = 1, \dots, K$) defined in (339), given λ_k and $e_k(t)$.

An alternative approach to identify the PDF of $\{\xi_1, \dots, \xi_K\}$ relies on sampling. In particular, as recently shown by Phoon *et al.* [74, 73], it is possible to develop effective sampling algorithms for the KL expansion (337). Such algorithms allow to sample the uncorrelated variables $\{\xi_1, \dots, \xi_K\}$ in a way that makes the PDF of $u(t)$ consistent with the equilibrium distribution, which can be calculated by mapping $\mathbf{x}_0 \sim \rho_{eq}(\mathbf{x}_0)$ to $u(\mathbf{x}_0)$. At this point, we have available a consistent bi-orthogonal representation of the random process $u(t)$ defined by the series expansion (337). It is straightforward to see that such representation yields a corresponding series expansion of the fluctuation term $f(t)$ in (335). In fact we have the following

²⁴The mean of $u(t) = u(\mathbf{x}(t, \mathbf{x}_0))$ is necessarily time-independent at statistical equilibrium. In fact, at equilibrium we have that $\mathbf{x}_0 \sim \rho_{eq}$ implies that $\mathbf{x}(t) \sim \rho_{eq}$ for all $t \geq 0$. A statistically stationary process however, may not be stationary in phase space. Indeed, $\mathbf{x}(t)$ evolves in time, eventually in a chaotic way as it happens for systems with strange attractors and invariant measures.

Proposition 4. For any bi-orthogonal series expansion (337) of the solution to the MZ-equation (335), there exists a unique series expansion of the fluctuation term $f(t)$ of the form

$$f(t) = \bar{f} + \sum_{k=1}^K \sqrt{\lambda_k} \xi_k h_k(t). \quad (340)$$

Proof. It is sufficient to prove the theorem for zero-mean processes. To this end, we set $\bar{u} = 0$ and $\bar{f} = 0$ in (337) and (340). A substitution of (337) into (335) yields, for all $t \in [0, T]$

$$f(t) = \sum_{k=1}^K \sqrt{\lambda_k} \xi_k \left(\frac{de_k(t)}{dt} - \Omega e_k(t) - \int_0^t K(t-s) e_k(s) ds \right). \quad (341)$$

Define,

$$h_k(t) = \frac{de_k(t)}{dt} - \Omega e_k(t) - \int_0^t K(t-s) e_k(s) ds. \quad (342)$$

This equation does not allow us to compute h_k explicitly quite yet. In fact, the MZ memory kernel $K(t-s)$ depends on $f(t)$ (see Eq. (336)). However, a substitution of (340) (with $\bar{f} = 0$) into the analytical expression of $K(t)$ yields

$$K(t) = \sum_{i,j=1}^K \sqrt{\lambda_i \lambda_j} v_{ij} e_i(0) h_j(t), \quad \text{where} \quad v_{ij} = \frac{\langle \xi_i, \mathcal{L} \xi_j \rangle_{eq}}{\langle u(0), u(0) \rangle_{eq}}. \quad (343)$$

To evaluate $\langle \xi_i, \mathcal{L} \xi_j \rangle_{eq}$ we need to express $\{\xi_1, \dots, \xi_K\}$ as a function of \mathbf{x}_0 (recall that \mathcal{L} operates on functions of \mathbf{x}_0 , see Eq. (3)), and then integrate over $\rho_{eq}(\mathbf{x}_0)$. This is easily achieved by using the dispersion relation (339). Specifically, we have

$$\xi_k(\mathbf{x}_0) = \frac{1}{\sqrt{\lambda_k}} \int_0^T u(\mathbf{x}(t, \mathbf{x}_0)) e_k(t) dt. \quad (344)$$

At this point, we substitute (343) into (342) to obtain

$$h_k(t) = \frac{de_k(t)}{dt} - \Omega e_k(t) - \sum_{i,j=1}^K \sqrt{\lambda_i \lambda_j} v_{ij} e_i(0) \int_0^t h_j(t-s) e_k(s) ds. \quad (345)$$

Given $\{e_1(t), \dots, e_K(t)\}$, Ω and v_{ij} , this equation can be solved uniquely for $\{h_1(t), \dots, h_K(t)\}$ by using Laplace transforms. Note that $\{h_1(t), \dots, h_K(t)\}$ are not necessarily orthogonal in $L^2([0, T])$. \square

Remark If the dynamical system (1) is Hamiltonian then the MZ steaming term vanishes, and the MZ memory kernel can be written in terms the fluctuation term as (see Eq. (23))

$$K(t) = \frac{\langle f(0), f(t) \rangle_{eq}}{\langle u(0), u(0) \rangle_{eq}}. \quad (346)$$

A substitution of this expression into (335) yields, after projection onto ξ_k

$$\frac{de_k(t)}{dt} = \int_0^t \sum_{j=1}^K \lambda_j [h_j(0) h_{k'}(t-s)] e_k(s) ds + h_k(t). \quad (347)$$

This equation establishes a one-to-one correspondence between the temporal modes of the KL expansion (337) and the temporal modes of the fluctuation term (341). In particular, given $\{e_1(t), \dots, e_K(t)\}$, we can determine $\{h_1(t), \dots, h_K(t)\}$ directly by using Laplace transforms, without building the MZ memory kernel (343).

6.5.1 Building MZ-KL stochastic models from first principles

Proposition 4 establishes a one-to-one correspondence between the noise process in the MZ equation (335) and the biorthogonal series expansion of the solution. This new paradigm allows us to build stochastic models for the observable $u(t)$ at statistical equilibrium from first principles. To this end,

1. Compute the solution to the MZ equation for the temporal correlation function of $u(t)$ (see Eq. (66))

$$\frac{dC(t)}{dt} = \Omega C(t) + \int_0^t K(t-s)C(s)ds. \quad (348)$$

The memory kernel $K(t-s)$ can be expanded as in (293), and computed from first-principles using the combinatorial approach we discussed in Section 6.2.

2. Build the Karhunen-Loève expansion (337) by spectrally decomposing the correlation function $C(t) = \langle u(0)u(t) \rangle_{eq}$ obtained at point 1. Recall that at statistical equilibrium we have $C(t-s) = \langle u(0)u(t-s) \rangle_{eq} = \langle u(s)u(t) \rangle_{eq}$. This yields eigenvalues $\{\lambda_j\}$ and the eigenfunctions $e_j(t)$. The uncorrelated random variables ξ_k appearing in (337) can be sampled consistently with the equilibrium distribution ρ_{eq} by using, e.g., the iterative algorithm recently proposed by Phoon *et al.* [73, 74].
3. With $\{\xi_1, \dots, \xi_K\}$, $\{e_1(t), \dots, e_K(t)\}$ and $\{\lambda_1, \dots, \lambda_K\}$ available, we can uniquely identify the noise process $f(t)$ in the MZ equation (335). To this end, we simply use Proposition 4, with the temporal modes $h_k(t)$ obtained by solving equation (345) or (347) with the Laplace transform.
4. With $K(t)$ computed from first principles, and $f(t)$ modeled based on the auto-correlation function $C(t)$, we can generate samples of the observable $u(t)$ by solving equation (335).

Remark We emphasize that the correlation function $C(t)$ can be also computed directly from data, e.g., by using a Monte-Carlo or a quasi Monte Carlo method [22]. With $C(t)$ available it is possible to determine the fluctuation term $f(t)$ with equation (340) and the MZ memory kernel $K(t)$ using equation (343).

The results of this Section can be generalized to vector-valued phase space functions $\mathbf{u}(t)$ at statistical equilibrium. The starting point is the KL expansion for multi-correlated stochastic processes we recently proposed in [13]. Such expansion is constructed based on cross-correlation information²⁵, and can be made consistent with the equilibrium distribution of $\mathbf{u}(t)$, e.g., by using the sampling strategy proposed in [73, 74]. The correspondence between the KL expansions of $\mathbf{u}(t)$ and the vector-valued fluctuation term $\mathbf{f}(t)$ can be established by following the same arguments we used in the proof of Proposition 4.

6.6 Application to random wave propagation

In this Section, we demonstrate the accuracy of the MZ memory calculation method and the reduced-order stochastic modeling technique we discussed in Section 6.1 and Section 6.5, respectively. To this end, we study nonlinear random wave propagation described by Hamiltonian partial differential equations (PDEs). To derive such PDEs consider the nonlinear functional

$$\mathcal{H}([p], [u]) = \int_0^{2\pi} \left[\frac{p^2}{2} + \frac{\alpha}{2} u_x^2 + G(p, u_x, u) \right] dx, \quad (349)$$

²⁵At statistical equilibrium the cross correlation functions are invariant under temporal shifts. This means that $\langle u_i(s), u_j(t) \rangle_{eq} = \langle u_i(0), u_j(t-s) \rangle_{eq}$ for all $t \geq s$. Hence, the solution to the projected MZ equation (66) is sufficient to compute the KL expansion of the multi-correlated process $\mathbf{u}(t)$, e.g., using the series expansion method proposed in [13].

where $u = u(x, t)$ represents the wave displacement, $p = p(x, t)$ is the canonical momentum (field variable conjugate to $u(x, t)$), $u_x = \partial u / \partial x$, and $G(p, u_x, u)$ is the nonlinear interaction term. By taking functional derivatives of (349) with respect to p and u (see, e.g., [87]) we obtain the Hamilton's equations of motion

$$\begin{cases} \partial_t u &= \frac{\delta \mathcal{H}(p, u)}{\delta p(x, t)} = p + \partial_p G(p, u_x, u), \\ \partial_t p &= -\frac{\delta \mathcal{H}(p, u)}{\delta u(x, t)} = \alpha u_{xx} + \partial_x \partial_{u_x} G(p, u_x, u) - \partial_u G(p, u_x, u). \end{cases} \quad (350)$$

The corresponding nonlinear wave equation is

$$u_{tt} = \alpha u_{xx} + \partial_t \partial_p G(p, u_x, u) + \partial_x \partial_{u_x} G(p, u_x, u) - \partial_u G(p, u_x, u). \quad (351)$$

This equation has been studied extensively in mathematical physics [45, 24, 59, 71], in particular in general relativity, statistical mechanics, and in the theory of viscoelastic fluids. In Figure 17 and Figure 18, we plot a few sample numerical solutions to (351) corresponding to different initial conditions and different nonlinear interaction term $G(p, u_x, u)$. These solutions are computed by an accurate Fourier spectral method with $N = 512$ modes (periodic boundary conditions in $x \in [0, 2\pi]$). Throughout this Section, we assume that the initial state $\{u(x, 0), p(x, 0)\}$ is random and distributed according to the functional Boltzmann-Gibbs equilibrium distribution²⁶

$$\rho_{eq}([p], [u]) = \frac{1}{Z(\alpha, \gamma)} e^{-\gamma \mathcal{H}([p], [u])}, \quad \text{where} \quad Z(\alpha, \gamma) = \int e^{-\gamma \mathcal{H}(p, u)} \mathcal{D}[p(x)] \mathcal{D}[u(x)]. \quad (352)$$

We emphasize that $\rho_{eq}([p], [u])$ is invariant under the infinite-dimensional flow generated by (351) with periodic boundary conditions, since the Hamiltonian (349) is a constant of motion (conserved quantity) in this case.

6.6.1 Linear waves

Setting the interaction term $G(p, u_x, u)$ in (349) and (351) equal to zero yields the well-known linear wave equation

$$u_{tt} = \alpha u_{xx}. \quad (353)$$

We discretize (353) in space using second-order finite differences on the (periodic) grid $x_j = 2\pi j/N$ ($j = 0, \dots, N$). This yields the following linear dynamical system

$$\frac{du_j}{dt} = p_j, \quad \frac{dp_j}{dt} = \frac{\alpha}{h^2} (u_{j+1} - 2u_j + u_{j-1}), \quad (354)$$

where $u_j(t) = u(x_j, t)$, $p_j(t) = p(x_j, t)$, and $h = 2\pi/N$ is the mesh size. The Hamilton's function corresponding to the finite-difference scheme (354) is obtained by discretizing the integral (349), e.g., with the rectangle rule. This yields

$$\mathcal{H}_1(\mathbf{p}, \mathbf{u}) = \sum_{j=0}^{N-1} \frac{h}{2} p_j^2 + \frac{\alpha_1 h}{2} \sum_{j=0}^{N-1} (u_{j+1} - u_j)^2, \quad (355)$$

²⁶The partition function $Z(\alpha, \gamma)$ is defined as a functional integral over $u(x)$ and $p(x)$ (see, e.g., [87]).

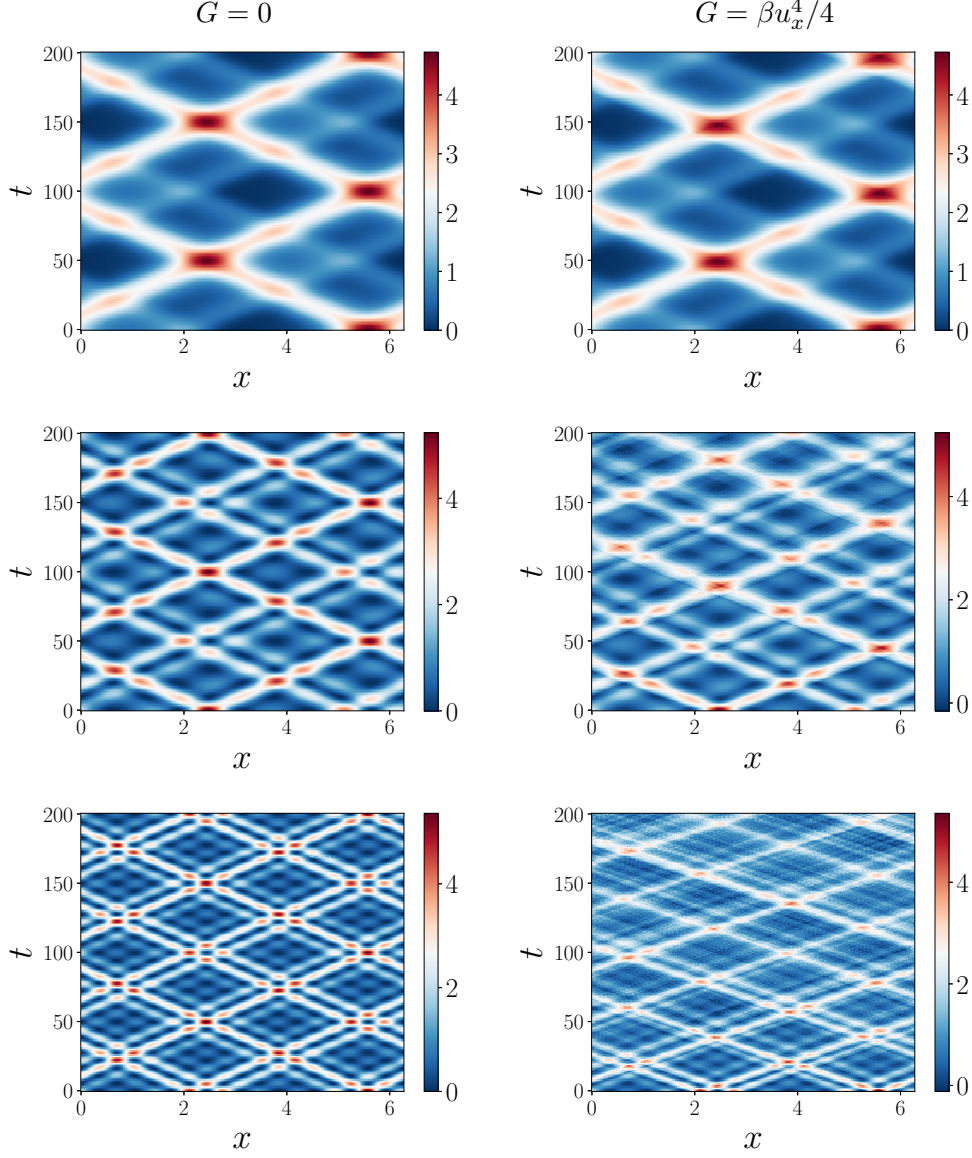


Figure 17: Sample solutions of the nonlinear wave equation (351) with initial conditions $u(x, 0) = e^{-\sin(2x)}(1 + \cos(x))$ (first row), $u(x, 0) = e^{-\sin(2x)}(1 + \cos(5x))$ (second row), and $u(x, 0) = e^{-\sin(2x)}(1 + \cos(9x))$ (third row). We set the group velocity α to $(2\pi/100)^2$ and consider different nonlinear interaction terms: $G = 0$ (first column – linear waves), $G = \beta u_x^4/4$ with $\beta = (2\pi/100)^4$ (second column – nonlinear waves). It is seen that as the initial condition becomes rougher, the nonlinear effects become more important.

where we defined $\alpha_1 = \alpha/h^2$. The corresponding finite-dimensional Gibbs distribution can be written as

$$\rho_{eq}(\mathbf{p}, \mathbf{u}) = \frac{1}{Z_1(\alpha_1, \gamma)} \exp \left\{ -\gamma \left(\sum_{j=0}^{N-1} \frac{1}{2} p_j^2 + \frac{\alpha_1}{2} \sum_{j=0}^{N-1} (u_{j+1} - u_j)^2 \right) \right\}, \quad (356)$$

$Z_1(\alpha_1, \gamma)$ being the partition function (normalization constant). Note that we absorbed the scaling factor h in the parameter $\gamma > 0$. It is straightforward to verify that the lattice Hamiltonian (355) is preserved if $u_0 = u_N$ and $p_0 = p_N$ (periodic boundary conditions). This implies that the PDF (356) is invariant

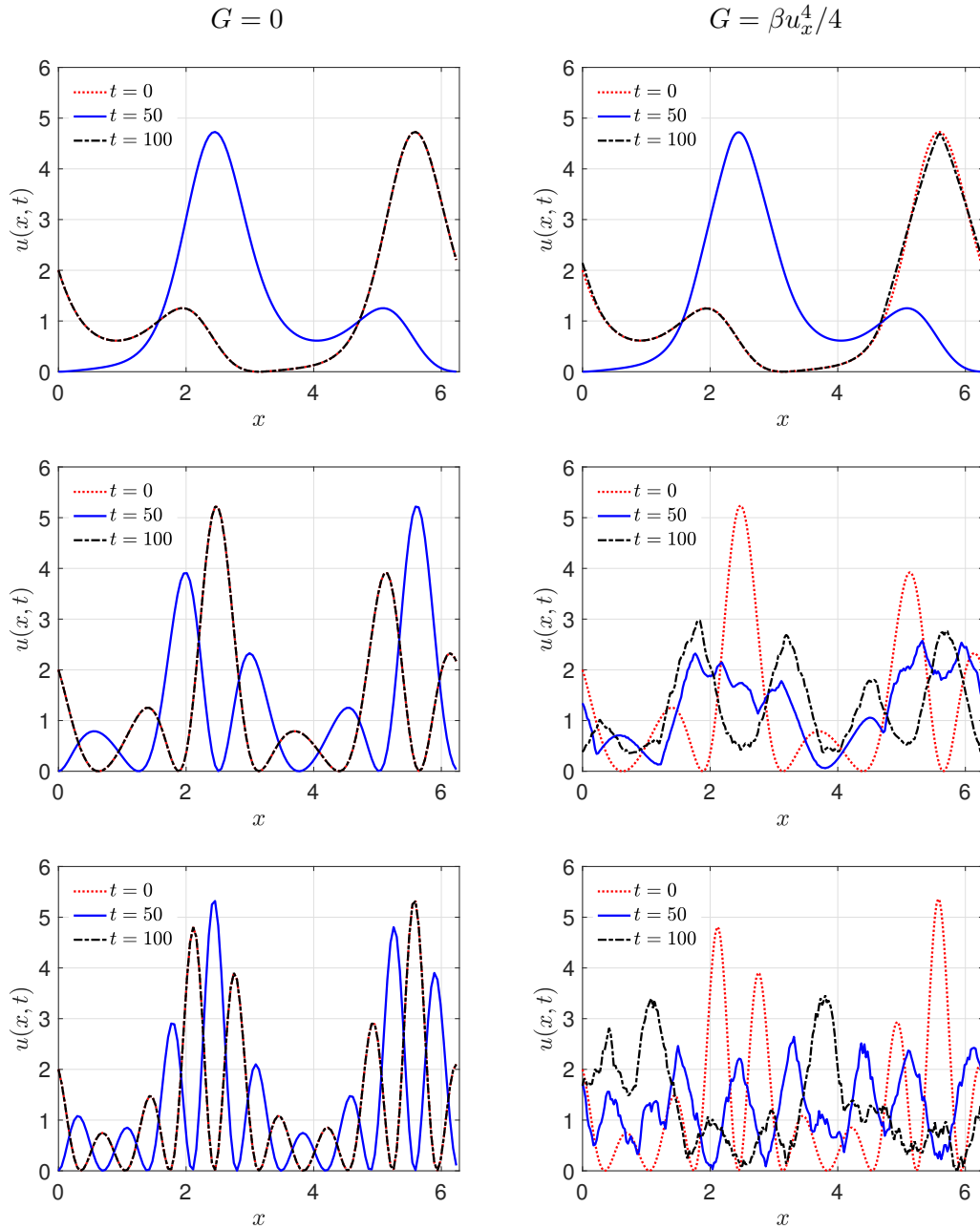


Figure 18: Snapshots of the solution shown in Figure 17.

under the flow generated by the linear ODE (354). Note that the lattice Hamiltonian (355) coincides with the Hamiltonian of a one-dimensional chain of harmonic oscillators with uniform mass $m = 1$ and spring constants $k = \alpha_1$. We set $N = 100$ and $\alpha = (2\pi/100)^2$ in equation (354). In this way, the system (354) is 200-dimensional and the modeling parameter α_1 in (355)-(356) is equal to 1.

MZ memory kernel and auto-correlation functions The Hamiltonian system (354) with periodic boundary conditions has many symmetries. In particular, the statistical properties of wave displacement $u(x, t)$ at any point x_j are the same, if the initial state is distributed according to (356). In addition, the PDF of the

wave momentum²⁷ $p(x_j, t)$ and the wave displacement $r(x_j, t) = u(x_{j+1}, t) - u(x_j, t)$ are both Gaussian (see Eq. (356)). Suppose we are interested in the temporal auto-correlation function of the wave momentum $p(x_j, t) = p_j$, at an arbitrary location x_j , i.e.,

$$C_{p_j}(t) = \langle p_j(t), p_j(0) \rangle_{eq}, \quad (357)$$

where $\langle \cdot, \cdot \rangle_{eq}$ is an integral over the equilibrium distribution (356). Such correlation function admits the analytical expression (see [39])

$$C_{p_j}(t) = J_0(2t), \quad \forall \gamma > 0, \quad (358)$$

where J_0 is the zero-order Bessel function of the first kind. With $C_{p_j}(t)$ available, we can solve the MZ equation

$$\frac{d}{dt} C_{p_j}(t) = \int_0^t K(t-s) C_{p_j}(s) ds \quad (359)$$

for the memory kernel $K(t)$ by using Laplace transforms. This yields the exact MZ kernel

$$K(t) = \frac{J_1(2t)}{t}, \quad \forall \gamma > 0, \quad (360)$$

where J_1 is the first-order Bessel function of the first kind. In Figure 19, we compare the exact memory kernel (360) and the correlation function (359) with the results we obtained using the iterative algorithm discussed in Section 6.3. Note that the system (354) is linear. Therefore, we can use the formula (313) to compute the coefficients $\{\gamma_1, \dots, \gamma_{n+2}\}$. With such coefficients available, we then compute $\{\mu_1, \dots, \mu_{n+2}\}$ using the recurrence relation (298), and the MZ memory kernel (293). In Figure (19) we demonstrate that the MZ-Faber expansion rapidly converges to the exact auto-correlation function (357) of the wave momentum as we increase the Faber expansion order n . This is not surprising since the linear wave equation is a well-known integrable system for which convergence of the MZ-Faber series can be rigorously established (section 5 in [100]).

Reduced-order stochastic modeling Suppose we are interested in building a consistent reduced-order stochastic model for the wave momentum $p(x_j, t) = \partial u(x_j, t) / \partial t$ at statistical equilibrium. To this end, we employ the spectral expansion technique we discussed in Section 6.5. The auto-correlation function of the process $p(t) = p(x_j, t)$ (at any location x_j), i.e., (357), is obtained by solving the MZ equation (359) with the kernel computed using the combinatorial algorithm described in Section 6.3. Following the stochastic modeling paradigm we developed in Section 6.5, we expand $p(t)$ as

$$p(t) \simeq \sum_{k=1}^K \sqrt{\lambda_k} \xi_k(\omega) e_k(t), \quad (361)$$

where $(\lambda_k, e_k(t))$ are eigenvalues and eigenfunctions of (357). By enforcing consistency of (361) with the equilibrium distribution (356) at each fixed time we obtain that the random variables $p(t_j)$ are normally distributed with zero mean and variance $1/\gamma$, for all $t_j \in [0, 10]$. In other words $p(t)$ is a centered, stationary Gaussian random process with correlation function (357). In Figure 20, we plot the auto-correlation functions

$$C_p(t) = \langle p_j(t), p_j(0) \rangle_{eq}, \quad C_p^2(t) = \langle p_j^2(t), p_j^2(0) \rangle_{eq}, \quad C_p^4(t) = \langle p_j^4(t), p_j^4(0) \rangle_{eq}, \quad (362)$$

we obtained with an MZ-Faber expansion of degree $n = 6$.

²⁷Note that for linear waves the wave momentum $p(x, t)$ is equal to $\partial u(x, t) / \partial t$ (see Eq. (350)).

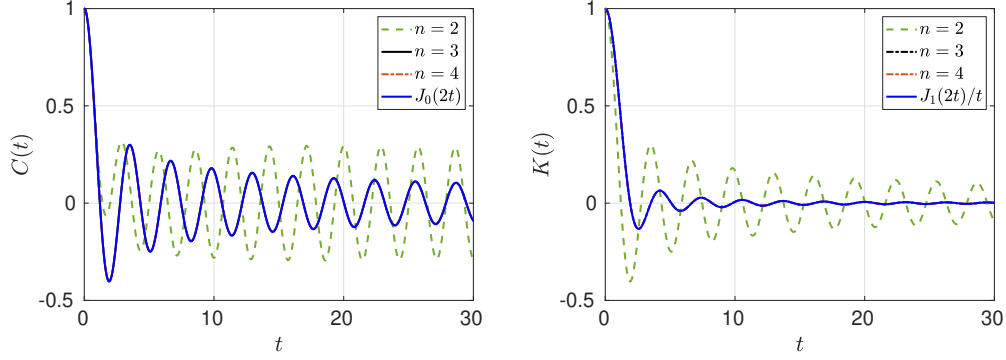


Figure 19: Linear wave equation (353). Temporal auto-correlation function of the wave momentum $p(x_j, t) = \partial u(x_j, t)/\partial t$ (Eq. (357), any location x_j) and MZ memory kernel $K(t)$. We compare the analytical results (358) and (360), with results we obtained by using the recursive algorithm we presented in Section 6.1 for different Faber polynomial orders n . It is seen that the MZ-Faber expansion rapidly converges to the exact MZ-kernel and auto-correlation function we increase the polynomial order.

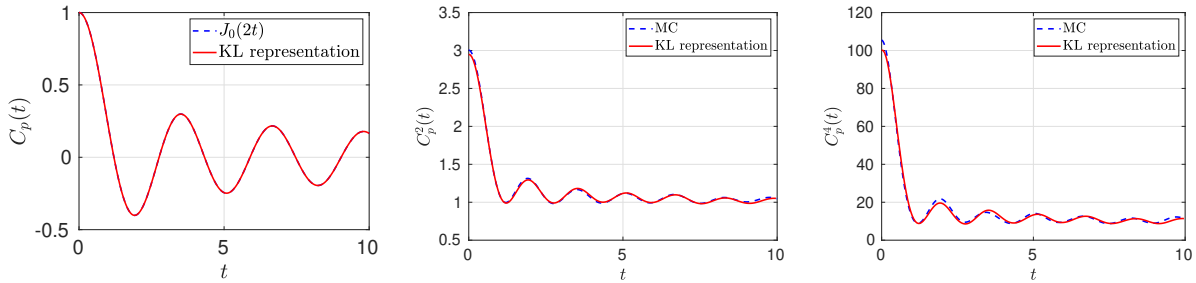


Figure 20: Linear wave equation (353). Temporal auto-correlation functions (362) of the wave momentum. The MZ kernel here is approximated with a Faber polynomial series of degree $n = 10$.

6.6.2 Nonlinear waves

Here we study the nonlinear wave equation (351) with interaction term $G(p, u_x, u) = \beta u_x^4/4$, i.e.,

$$u_{tt} = \alpha u_{xx} + 3\beta u_x^2 u_{xx}, \quad \alpha, \beta > 0. \quad (363)$$

In Figure 17 and Figure 18 we plot sample solutions of (363) corresponding to different initial conditions. It is clearly seen that the nonlinearity $u_x^2 u_{xx}$ breaks the periodicity of traveling wave. This effect is more pronounced if the initial condition is rougher in x , as u_x^2 and u_{xx} are larger in this case, thereby increasing magnitude of the nonlinear term in (363). As before, we discretize (363) and the Hamiltonian (349) with finite differences on a periodic spatial grid (N points in $[0, 2\pi]$). This yields

$$\mathcal{H}_2(\mathbf{p}, \mathbf{u}) = \sum_{j=0}^{N-1} \frac{h p_j^2}{2} + \sum_{j=0}^{N-1} \frac{h \alpha_1}{2} (u_{j+1} - u_j)^2 + \sum_{j=0}^{N-1} \frac{h \beta_1}{4} (u_{j+1} - u_j)^4, \quad (364)$$

where $u_j(t) = u(x_j, t)$ and $p_j(t) = \partial u(x_j, t)/\partial t$ represent the wave amplitude and momentum at location $x_j = hj$ ($j = 0, \dots, N, h = 2\pi/N$), $\alpha_1 = \alpha/h^2$ and $\beta_1 = \beta/h^4$. The discretized equilibrium distribution

(352) then becomes

$$\rho_{eq}(\mathbf{p}, \mathbf{u}) = \frac{1}{Z_2(\alpha_1, \beta_1, \gamma)} \exp \left\{ -\gamma \left(\sum_{j=0}^{N-1} \frac{p_j^2}{2} + \sum_{j=0}^{N-1} \frac{\alpha_1}{2} (u_{j+1} - u_j)^2 + \sum_{j=0}^{N-1} \frac{\beta_1}{4} (u_{j+1} - u_j)^4 \right) \right\}. \quad (365)$$

As before, we absorbed the factor h into the parameter γ . Note that the lattice Hamiltonian (364) coincides with the Hamiltonian of the Fermi-Pasta-Ulam β -model (325), with $m_j = 1$. We emphasize that if a different scheme is used to discretize the wave equation (363), then the lattice Hamiltonian (364) may not be a conserved quantity.

MZ memory term and auto-correlation functions We choose the wave momentum $p_j(t)$ and the wave displacement $r_j(t) = u_{j+1}(t) - u_j(t)$ as quantities of interest. Moreover, we set $N = 100$ and $\alpha = (2\pi/100)^2$. To study the effects of the nonlinear interaction term, we consider different values of $\beta = \beta_1 \alpha^2$, with β_1 ranging from 0.01 to 1. This corresponds to the FPU models with mild and strong nonlinearities, respectively. Based on the structure of the Hamiltonian (364) and the equilibrium distribution (365), we expect that the dynamics of $p_j(t)$ and $r_j(t)$ will be different for different parameters β . To calculate the temporal auto-correlation function of $p_j(t)$ and $r_j(t)$ at an arbitrary spatial point x_j , we solve the corresponding MZ equations. Such equations are of the form (359), where the memory kernel $K(t - s)$ is computed from first-principles (i.e., from the microscopic equations of motion) using the algorithm we presented in Section 6.3. In Figure 21, we compare the temporal auto-correlation function we obtained for the wave displacement $r_j(t)$ with results of Markov-Chain-Monte-Carlo (MCMC) (10^6 sample paths) for FPU systems with mild nonlinearities ($\beta_1 = 0.01$ and $\beta_1 = 0.1$) at different temperatures ($\gamma = 1$ and $\gamma = 40$). It is seen that the Faber approximation of the MZ memory kernel yields relatively accurate results for FPU systems with mild nonlinearities at both low ($\gamma = 40$) and high temperature ($\gamma = 1$) as we increase the polynomial order n .

Reduced-order stochastic modeling We employ the spectral approach of Section 6.5 to build stochastic low-dimensional models of the wave momentum $p_j(t)$ and wave displacement $r_j(t) = u_{j+1}(t) - u_j(t)$ at statistical equilibrium. Since we assumed that we are at statistical equilibrium, the statistical properties of the random processes representing $p_j(t)$ and $r_j(t)$ are time-independent. For instance, by integrating (365) we obtain the following expression for the one-time PDF of $r_j(t)$

$$r_j(t) \sim e^{-\gamma(\frac{1}{2}\alpha_1 r^2 + \frac{1}{4}\beta_1 r^4)} \quad \forall t \in [0, T], \quad \forall j = 0, \dots, N-1. \quad (366)$$

Clearly, $r_j(t)$ is a stationary non-Gaussian process. To sample the KL expansion of $r_j(t)$ in a way that is consistent with the PDF (366) we used the algorithm discussed in [74, 73]. For the FPU system with $\alpha_1 = \beta_1 = 1$, it is straightforward to show that for all $m \in \mathbb{N}$

$$\mathbb{E}\{r_j^{2m}(t)\} = \frac{\int_{-\infty}^{+\infty} r^{2m} e^{-\gamma(\frac{1}{2}r^2 - \frac{1}{4}r^4)} dr}{\int_{-\infty}^{+\infty} e^{-\gamma(\frac{1}{2}r^2 - \frac{1}{4}r^4)} dr} = \frac{\sqrt{2}\gamma^{-\frac{1}{4} - \frac{m}{2}} \Gamma(\frac{1}{2} + m) U(\frac{1}{4} + \frac{m}{2}, \frac{1}{2}, \frac{\gamma}{4})}{e^{\gamma/8} K_{1/4}(\frac{\gamma}{8})},$$

where $\Gamma(x)$ is the Gamma function, $K_n(z)$ is the modified Bessel function of the second kind and $U(x, y, z)$ is Tricomi's confluent hypergeometric function. Therefore, for all positive γ and finite m we have that $\mathbb{E}\{r_j^{2m}(t)\} < \infty$, i.e., $r_j(t)$ is L^{2m} process. This condition guarantees convergence of the KL expansion to temporal correlation functions of order greater than two. In Figure 22 we plot the temporal auto-correlation

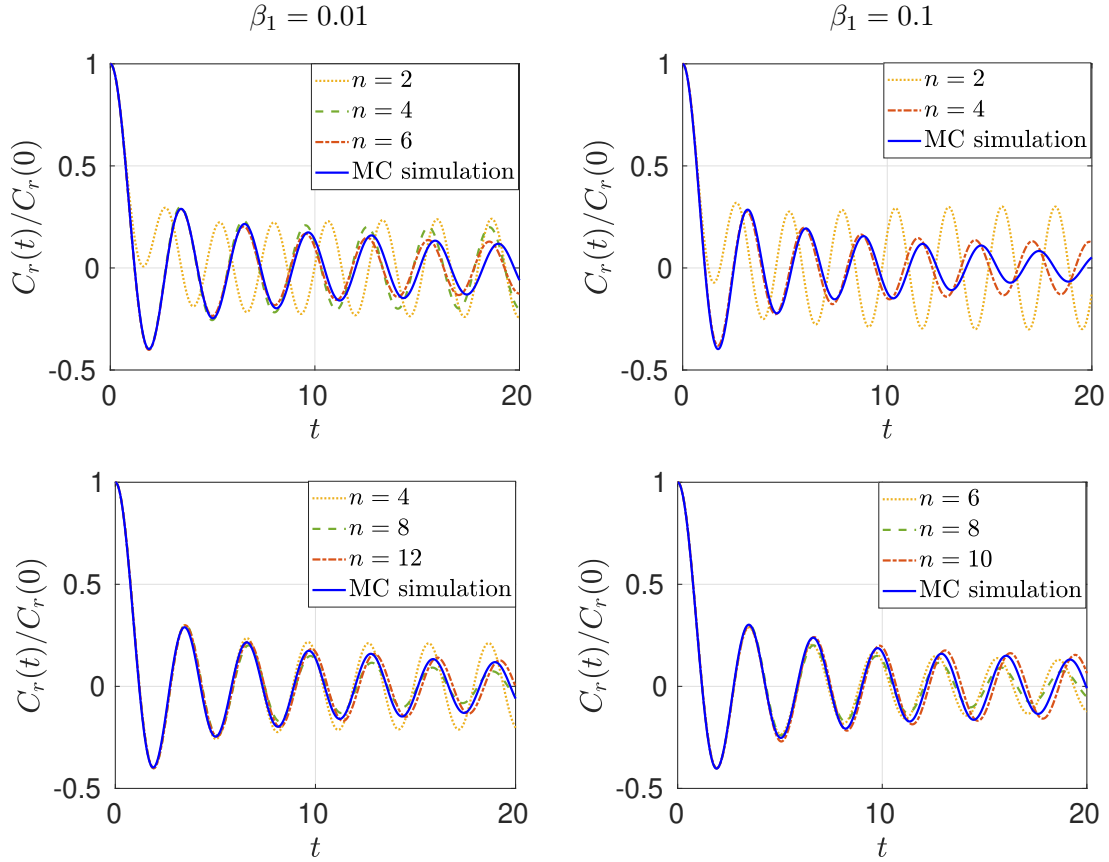


Figure 21: Nonlinear wave equation (363). Temporal auto-correlation function of the wave displacement $r_j(t)$ for different values of the nonlinear parameter β_1 . We compare results we obtained by calculating the MZ memory from first principles using n -th order Faber polynomials (Section 6.2) with results from Markov-Chain-Monte-Carlo (10^6 sample paths). The thermodynamic parameter γ is set to 1 (high-temperature) in the first row and to 40 (low-temperature) in the second row.

function of various polynomial observables of the nonlinear wave momentum and displacement at an arbitrary spatial point x_j . We compare results we obtained from Markov Chain Monte Carlo simulation (dashed line), with the MZ-KL expansion method based the first-principle memory calculation (continuous line). We also provide results we obtained by using KL expansions with covariance kernel estimated from data (dotted line).

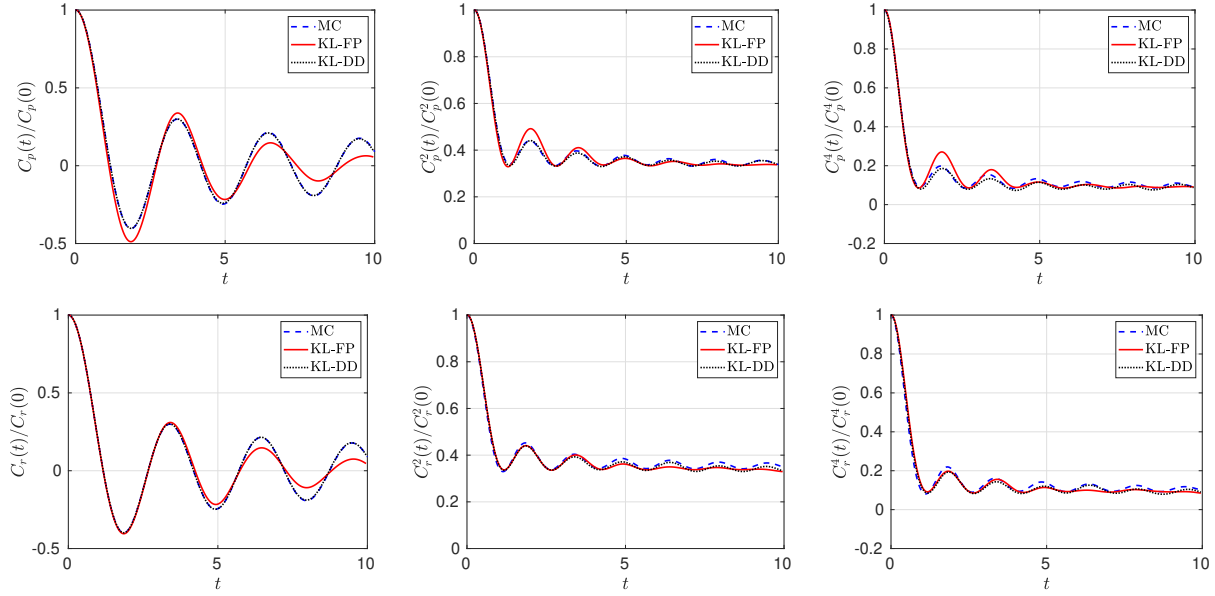


Figure 22: Nonlinear wave equation (363). Temporal auto-correlation function of polynomial observables $p_j^m(t)$ (first row) $r_j^m(t)$ (second row) with $m = 1, 2, 4$. We compare results from Markov-Chain-Monte-Carlo simulation (MC), KL expansion based on the first-principle MZ memory kernel calculation (359) (KL-FP), and KL expansion based on a data-driven estimate of the temporal auto-correlation function (KL-DD). The parameter γ appearing in (365) is set to 40, while $\alpha_1 = \beta_1 = 1$.

7 Publications during reporting period

1. Y. Zhu and D. Venturi, “Hypoellipticity and the Mori-Zwanzig formulation of stochastic differential equations”, *ArXiv*, 2001.04565, pp. 1-21, (2020).
2. Y. Zhu and D. Venturi, “Generalized Langevin equations for systems with local interactions”, *J. Stat. Phys.*, **178**, pp. 1217-1247, (2020).
3. A. Boelens, D. Venturi and D. Tartakovsky, “Parallel numerical tensor methods for high-dimensional PDEs”, *J. Comp. Phys.*, **375**, pp. 519-539, (2018).
4. Y. Zhu, J. Dominy and D. Venturi, “On the estimation of the Mori-Zwanzig memory integral”, *J. Math. Phys.*, **59**, pp. 103501(1-42), (2018).
5. C. Brennan and D. Venturi, “Data-driven closures for stochastic dynamical systems”, *J. Comp. Phys.*, **372**, pp. 281-298, (2018).
6. Y. Zhu and D. Venturi, “Faber approximation of the Mori-Zwanzig equation”, *J. Comp. Phys.*, **372**, pp. 694-718, (2018).
7. D. Venturi, “The numerical approximation of nonlinear functionals and functional differential equations”, *Physics Reports*, **732**, pp. 1-102, (2018).
8. H. Cho, D. Venturi and G. E. Karniadakis, “Numerical methods for high-dimensional kinetic equations”, in *Uncertainty quantification for kinetic and hyperbolic equations*, Springer, pp. 93-125, (2017).
9. J. Dominy and D. Venturi, “Duality and conditional expectations in the Nakajima-Mori-Zwanzig formulation”, *J. Math. Phys.*, **58**, pp. 103501(1-42), (2017)
10. D. Venturi, H. Cho and G. E. Karniadakis, “Mori-Zwanzig approach to uncertainty quantification”, in *Handbook of uncertainty quantification*, Springer, pp. 1-32, (2016).

References

- [1] J. Abate and W. Whitt. A unified framework for numerically inverting Laplace transforms. *INFORMS Journal of Computing*, 18(4):408–421, 2006.
- [2] B. J. Alder and T. E. Wainwright. Decay of the velocity autocorrelation function. *Phys. Rev. A*, 1(1):18, 1970.
- [3] G. Amati, H. Meyer, and T. Schilling. Memory effects in the Fermi–Pasta–Ulam model. *J. Stat. Phys.*, 174(1):219–257, 2019.
- [4] N. Aubry, R. Guyonnet, and R. Lima. Spatiotemporal analysis of complex signals: theory and applications. *J. Stat. Phys.*, 64:683–739, 1991.
- [5] N. Aubry and R. Lima. Spatiotemporal and statistical symmetries. *J. Stat. Phys.*, 81(3/4):793–828, 1995.
- [6] R. J. Baxter. *Exactly solved models in statistical mechanics*. Elsevier, 2016.
- [7] B. J. Berne and G. D. Harp. On the calculation of time correlation functions. *Advances in chemical physics*, pages 63–227, 1970.
- [8] N. Biggs. *Algebraic graph theory*. Cambridge University Press, 1993.
- [9] C. Brennan and D. Venturi. Data-driven closures for stochastic dynamical systems. *J. Comp. Phys.*, 372:281–298, 2018.
- [10] A. Budhiraja, P. Dupuis, and V. Maroulas. Large deviations for stochastic flows of diffeomorphisms. *Bernoulli*, 1:234–257, 2010.
- [11] M. Chen, X. Li, and C. Liu. Computation of the memory functions in the generalized langevin models for collective dynamics of macromolecules. *J. Chem. Phys.*, 141(6):064112, 2014.
- [12] A. Chertock, D. Gottlieb, and A. Solomonoff. Modified optimal prediction and its application to a particle-method problem. *J. Sci. Comput.*, 37(2):189–201, 2008.
- [13] H. Cho, D. Venturi, and G. E. Karniadakis. Karhunen-Loève expansion for multi-correlated stochastic processes. *Prob. Eng. Mech.*, 34:157–167, 2013.
- [14] H. Cho, D. Venturi, and G. E. Karniadakis. Statistical analysis and simulation of random shocks in Burgers equation. *Proc. R. Soc. A*, 2171(470):1–21, 2014.
- [15] A. J. Chorin, O. H. Hald, and R. Kupferman. Optimal prediction and the Mori-Zwanzig representation of irreversible processes. *Proc. Natl. Acad. Sci. USA*, 97(7):2968–2973, 2000.
- [16] A. J. Chorin, O. H. Hald, and R. Kupferman. Optimal prediction with memory. *Physica D*, 166(3-4):239–257, 2002.
- [17] A. J. Chorin, R. Kupferman, and D. Levy. Optimal prediction for Hamiltonian partial differential equations. *J. Comput. Phys.*, 162(1):267–297, 2000.
- [18] A. J. Chorin and P. Stinis. Problem reduction, renormalization and memory. *Comm. App. Math. and Comp. Sci.*, 1(1):1–27, 2006.

- [19] W. Chu and X. Li. The Mori-Zwanzig formalism for the derivation of a fluctuating heat conduction model from molecular dynamics. *arXiv:1709.05928*, 2017.
- [20] E. Darve, J. Solomon, and A. Kia. Computing generalized Langevin equations and generalized Fokker-Planck equations. *Proc. Natl. Acad. Sci. USA*, 106(27):10884–10889, 2009.
- [21] R. Dautray and J.-L. Lions. *Mathematical Analysis and Numerical Methods for Science and Technology: Vol. 3 Spectral Theory and Applications*. Springer Science & Business Media, 2012.
- [22] J. Dick, F. Y. Kuo, and I. H. Sloan. High-dimensional integration: the quasi-Monte Carlo way. *Acta Numerica*, 22:133–288, 2013.
- [23] J. M. Dominy and D. Venturi. Duality and conditional expectations in the Nakajima-Mori-Zwanzig formulation. *J. Math. Phys.*, 58(8):082701, 2017.
- [24] R. Donninger and B. Schörkhuber. Stable blow up dynamics for energy supercritical wave equations. *arXiv:1207.7046*, 2012.
- [25] J. P. Eckmann and M. Hairer. Non-equilibrium statistical mechanics of strongly anharmonic chains of oscillators. *Commun. Math. Phys.*, 212(1):105–164, 2000.
- [26] J. P. Eckmann and M. Hairer. Spectral properties of hypoelliptic operators. *Commun. Math. Phys.*, 235(2):233–253, 2003.
- [27] J. P. Eckmann, C. A. Pillet, and L. Rey-Bellet. Non-equilibrium statistical mechanics of anharmonic chains coupled to two heat baths at different temperatures. *Commun. Math. Phys.*, 201(3):657–697, 1999.
- [28] K.-J. Engel and R. Nagel. *One-parameter semigroups for linear evolution equations*, volume 194. Springer, 1999.
- [29] P. Español. Dissipative particle dynamics for a harmonic chain: A first-principles derivation. *Phys. Rev. E*, 53(2):1572, 1996.
- [30] G. W. Ford, M. Kac, and P. Mazur. Statistical mechanics of assemblies of coupled oscillators. *J. Math. Phys.*, 6(4):504–515, 1965.
- [31] R. F. Fox. Functional-calculus approach to stochastic differential equations. *Phys. Rev. A*, 33(1):467–476, 1986.
- [32] A. Gouasmi, E. J. Parish, and K. Duraisamy. A priori estimation of memory effects in reduced-order models of nonlinear systems using the Mori–Zwanzig formalism. *Proc. R. Soc. A*, 473:1–24, 2017.
- [33] G. D. Harp and B. J. Berne. Time-correlation functions, memory functions, and molecular dynamics. *Phys. Rev. A*, 2(3):975, 1970.
- [34] B. Helffer and F. Nier. *Hypoelliptic estimates and spectral theory for Fokker-Planck operators and Witten Laplacians*. Springer, 2005.
- [35] F. Hérau and F. Nier. Isotropic hypoellipticity and trend to equilibrium for the Fokker-Planck equation with a high-degree potential. *Arch. Ration. Mech. Anal.*, 171(2):151–218, 2004.
- [36] J. S. Hesthaven, S. Gottlieb, and D. Gottlieb. *Spectral methods for time-dependent problems*. Cambridge Univ. Press, 2007.

- [37] L. Hörmander. Hypocoelliptic second order differential equations. *Acta. Math*, 119(1):147–171, 1967.
- [38] W. Huisinga, P. Lorenzo, R. Kosloff, and P. Saalfrank. Faber and Newton polynomial integrators for open-system density matrix propagation. *J. Chem. Phys*, 110(12):5538–5547, 1999.
- [39] J. Florencio Jr and M. H. Lee. Exact time evolution of a classical harmonic-oscillator chain. *Phys. Rev. A*, 31(5):3231, 1985.
- [40] T. Karasudani, K. Nagano, H. Okamoto, and H. Mori. A new continued-fraction representation of the time-correlation functions of transport fluxes. *Progress of Theoretical Physics*, 61(3):850–863, 1982.
- [41] A. Karimi and M. R. Paul. Extensive chaos in the Lorenz-96 model. *Chaos*, 20(4):043105(1–11), 2010.
- [42] G. E. Karniadakis and S. Sherwin. *Spectral/hp element methods for computational fluid dynamics*. Oxford University Press, second edition, 2005.
- [43] T. Kato. *Perturbation theory for linear operators*. Springer-Verlag, fourth edition, 1995.
- [44] J. Kim and I. Sawada. Dynamics of a harmonic oscillator on the Bethe lattice. *Phys. Rev. E*, 61(3):R2172, 2000.
- [45] S. Klainerman. Global existence for nonlinear wave equations. *Commun. Pure Appl. Math.*, 33(1):43–101, 1980.
- [46] P. E. Kloeden and E. Platen. *Numerical solution of stochastic differential equations*, volume 23. Springer Science & Business Media, 2013.
- [47] V. I. Klyatskin. *Dynamics of stochastic systems*. Elsevier Publishing Company, 2005.
- [48] B. O. Koopman. Hamiltonian systems and transformation in Hilbert spaces. *Proc. Natl. Acad. Sci.*, 17(5):315–318, 1931.
- [49] R. Kubo. The fluctuation-dissipation theorem. *Reports on progress in physics*, 29(1):255, 1966.
- [50] H. Kunita. *Stochastic flows and stochastic differential equations*. Cambridge university press, 1997.
- [51] H. M. Lee. Derivation of the generalized Langevin equation by a method of recurrence relations. *J. Math. Phys.*, 24:2512–2514, 1983.
- [52] M. H. Lee. Solutions of the generalized langevin equation by a method of recurrence relations. *Phys. Rev. B*, 26(5):2547, 1982.
- [53] H. Lei, N.A. Baker, and X. Li. Data-driven parameterization of the generalized Langevin equation. *Proc. Natl. Acad. Sci.*, 113(50):14183–14188, 2016.
- [54] X. Li. A coarse-grained molecular dynamics model for crystalline solids. *Int. J. Numer. Meth. Engng.*, 83(8-9):986–997, 2010.
- [55] Z. Li, X. Bian, X. Li, and G. E. Karniadakis. Incorporation of memory effects in coarse-grained modeling via the Mori-Zwanzig formalism. *J. Chem. Phys*, 143:243128, 2015.
- [56] Z. Li, H. S. Lee, E. Darve, and G. E. Karniadakis. Computing the non-Markovian coarse-grained interactions derived from the Mori-Zwanzig formalism in molecular systems: Application to polymer melts. *J. Chem. Phys*, 146:014104, 2017.

- [57] E. N. Lorenz. Predictability - A problem partly solved. In *ECMWF seminar on predictability: Volume I*, pages 1–18, 1996.
- [58] A. M. Maiocchi, A. Carati, and A. Giorgilli. A series expansion for the time autocorrelation of dynamical variables. *Journal of Statistical Physics*, 148(6):1054–1071, 2012.
- [59] H. P. McKean and K. L. Vaninsky. Statistical mechanics of nonlinear wave equations. In *Trends and perspectives in applied mathematics*, pages 239–264. Springer, 1994.
- [60] C. B. Mendl and H. Spohn. Current fluctuations for anharmonic chains in thermal equilibrium. *J. Stat. Mech. Theory Exp.*, 2015(3):P03007, 2015.
- [61] C. Moler and C. Van Loan. Nineteen dubious ways to compute the exponential of a matrix. *SIAM review*, 20(4):801–836, 1978.
- [62] C. Moler and C. Van Loan. Nineteen dubious ways to compute the exponential of a matrix, twenty-five years later. *SIAM review*, 45(1):3–49, 2003.
- [63] I. Moret and P. Novati. The computation of functions of matrices by truncated faber series. *Numerical Functional Analysis and Optimization*, 22(5-6):697–719, 2001.
- [64] H. Mori. A continued-fraction representation of the time-correlation functions. *Prog. Theor. Phys*, 34(3):399–416, 1965.
- [65] F. Moss and P. V. E. McClintock, editors. *Noise in nonlinear dynamical systems. Volume 1: theory of continuous Fokker-Planck systems*. Cambridge Univ. Press, 1995.
- [66] P. Novati. Solving linear initial value problems by Faber polynomials. *Numerical linear algebra with applications*, 10(3):247–270, 2003.
- [67] S. A. Orszag and L. R. Bissonnette. Dynamical properties of truncated Wiener-Hermite expansions. *Phys. Fluids*, 10(12):2603–2613, 1967.
- [68] M. Ottobre, G. A. Pavliotis, and K. P. Starov. Exponential return to equilibrium for hypoelliptic quadratic systems. *arXiv preprint arXiv:1106.2326*, 2011.
- [69] E. J. Parish and K. Duraisamy. A dynamic subgrid scale model for large eddy simulations based on the Mori–Zwanzig formalism. *J. Comp. Phys.*, 349:154–175, 2017.
- [70] E. J. Parish and K. Duraisamy. Non-Markovian closure models for large eddy simulations using the Mori-Zwanzig formalism. *Phys. Rev. Fluids*, 2(1):014604, 2017.
- [71] G. Parisi. *Statistical field theory*. Addison-Wesley, 1988.
- [72] M. E. Peskin. *An introduction to quantum field theory*. CRC Press, 2018.
- [73] K.K. Phoon, H.W. Huang, and S.T. Quek. Simulation of strongly non-Gaussian processes using Karhunen-Loève expansion. *Prob. Eng. Mech.*, 20(2):188–198, 2005.
- [74] K.K. Phoon, S.P. Huang, and S.T. Quek. Simulation of second-order processes using Karhunen-Loève expansion. *Computers & structures*, 80(12):1049–1060, 2002.
- [75] G. Da Prato and J. Zabczyk. *Ergodicity for infinite dimensional systems*, volume 229. Cambridge University Press, 1996.

- [76] K. S. Singwi, , and A. Sjölander. Theory of atomic motions in simple classical liquids. *Phys. Rev.*, 167(1):152, 1968.
- [77] L. Sjogren. Numerical results on the velocity correlation function in liquid argon and rubidium. *Journal of Physics C: Solid State Physics*, 13(5):705, 1980.
- [78] L. Sjogren and A. Sjolander. Kinetic theory of self-motion in monatomic liquids. *Journal of Physics C: Solid State Physics*, 12(21):4369, 1979.
- [79] I. Snook. *The Langevin and generalised Langevin approach to the dynamics of atomic, polymeric and colloidal systems*. Elsevier, 2006.
- [80] P. Stinis. Stochastic optimal prediction for the Kuramoto–Sivashinsky equation. *Multiscale Modeling & Simulation*, 2(4):580–612, 2004.
- [81] P. Stinis. A comparative study of two stochastic model reduction methods. *Physica D*, 213:197–213, 2006.
- [82] P. Stinis. Higher order Mori-Zwanzig models for the Euler equations. *Multiscale Modeling & Simulation*, 6(3):741–760, 2007.
- [83] P. Stinis. Renormalized reduced models for singular PDEs. *Comm. Appl. Math. and Comput. Sci.*, 8(1):39–66, 2013.
- [84] P. Stinis. Renormalized Mori–Zwanzig-reduced models for systems without scale separation. *Proc. Royal Soc. A*, 471(2176):20140446, 2015.
- [85] D. Venturi. On proper orthogonal decomposition of randomly perturbed fields with applications to flow past a cylinder and natural convection over a horizontal plate. *J. Fluid Mech.*, 559:215–254, 2006.
- [86] D. Venturi. A fully symmetric nonlinear biorthogonal decomposition theory for random fields. *Physica D*, 240(4-5):415–425, 2011.
- [87] D. Venturi. The numerical approximation of nonlinear functionals and functional differential equations. *Physics Reports*, 732:1–102, 2018.
- [88] D. Venturi, H. Cho, and G. E. Karniadakis. The Mori-Zwanzig approach to uncertainty quantification. In R. Ghanem, D. Higdon, and H. Owhadi, editors, *Handbook of uncertainty quantification*. Springer, 2016.
- [89] D. Venturi and G. E. Karniadakis. Convolutionless Nakajima-Zwanzig equations for stochastic analysis in nonlinear dynamical systems. *Proc. R. Soc. A*, 470(2166):1–20, 2014.
- [90] D. Venturi, X. Wan, and G. E. Karniadakis. Stochastic low-dimensional modelling of a random laminar wake past a circular cylinder. *J. Fluid Mech.*, 606:339–367, 2008.
- [91] C. Villani. Hypocoercivity. *Memoirs of the American Mathematical Society*, 202(950), 2009.
- [92] X. Wan and G. E. Karniadakis. Multi-element generalized polynomial chaos for arbitrary probability measures. *SIAM J. Sci. Comput.*, 28(3):901–928, 2006.
- [93] S. Watanabe. *Lectures on Stochastic Differential Equations and Malliavin Calculus*. Lectures delivered at the Indian Institute of Science, Bangalore, 1984.

- [94] R. O. Watts and I. K. Snook. Perturbation theories in non-equilibrium statistical mechanics: II. methods based on memory function formalism. *Molecular Physics*, 33(2):443–452, 1977.
- [95] S. Wiggins. *Introduction to applied nonlinear dynamical systems and chaos*. Springer, 2003.
- [96] V. Wihstutz and MA. Pinsky. *Diffusion processes and related problems in analysis, volume II: Stochastic flows*, volume 27. Springer Science & Business Media, 2012.
- [97] C. H. Woo and H. Wen. Quantum statistical effects in the mass transport of interstitial solutes in a crystalline solid. *Phys. Rev. E*, 96(3):032133, 2017.
- [98] Y. Yoshimoto, I. Kinefuchi, T. Mima, A. Fukushima, T. Tokumasu, and S. Takagi. Bottom-up construction of interaction models of non-markovian dissipative particle dynamics. *Phys. Rev. E*, 88(4):043305, 2013.
- [99] Y. Zhu, J. M. Dominy, and D. Venturi. On the estimation of the Mori-Zwanzig memory integral. *J. Math. Phys.*, 59(10):103501, 2018.
- [100] Y. Zhu and D. Venturi. Faber approximation of the Mori-Zwanzig equation. *J. Comp. Phys.*, 372:694–718, 2018.
- [101] Y. Zhu and D. Venturi. Generalized Langevin equations for systems with local interactions. *arXiv:1906.04918*, 2019.
- [102] R. Zwanzig. Nonlinear generalized Langevin equations. *J. Stat. Phys.*, 9(3):215–220, 1973.